

REDACTOR-ŞEF: Prof. A. NEGUCIOIU

REDACTORI-ŞEFI ADJUNCTI: Prof. A. PĂL, conf. N. EDROIU, conf. L. GHERGARI

COMITETUL DE REDACŢIE CHIMIE: Prof. E. CHIFU, prof. I. HAIDUC (redactor responsabil), prof. L. KÉKEDY, prof. GH. MARCU, prof. L. ONICIU, conf. S. MAGER, conf. E. VARGHA (secretar de redacție)

TEHNOREDACTOR: C. Tomoaia-COTIŞEL

491170

STUDIA UNIVERSITATIS BABEŞ-BOLYAI

CHEMIA

2

Redacția: 3400 CLUJ-NAPOCA, str. M. Kogălniceanu, 1 ☎ Telefon 161 01

SUMAR - CONTENTS - SOMMAIRE - INHALT

ST. KREIBIK, P. PRUNEANU, E. HAUER, V. V. MORARIU, Filtration by Dielectrophoresis: PVC Particles in an Organic Solvent	3
I. NEACȘU, N. OIȚĂ, The Action of Some Diethylaminoethanol Derivatives on the Membrane Potential of the Striated Muscle Fibres	7
C. TARBA, Utilization of Model Bilayer Lipid Membranes to Characterize the Response Mechanism of Cyanine Dyes to Membrane Potentials	14
S. JITIAN, A. JITIAN, Study of the Oxidation Kinetics of Metals by Ellipsometry	21
L. GHIZDAVU, S. BARBU, GH. MARCU, Komplexverbindungen des Dihydralazinhydrazonbenzaldehyds mit Metall (II) Sulphaten ☉ Coordination Compounds of Dyhydralazinehydrazone-Benzaldehyde with Metal (II)-Sulphates	27
F. MÁNOK, E. KÓSZEGI, CS. VÁRHELYI, A. BENKŐ, Über Dioximinkomplexe der Übergangsmetalle LXXIII. Mitt. Polarographische Untersuchung über die Bildung und die Hydrolyse von 1,2-Cycloheptandion-Monoxim und 1,2-Cycloheptandiondioxim ☉ On the Dioximine Complexes of Transition Metals, Part LXXXIII	34
M. VAGAONESCU, L. GHIZDAVU, S. MAGER, L. STOICBESCU, I. CHIȘ, Molecular Complexes of N-Methylmorpholine	42
A. FODOR, S. LEOCA, E. CORDOȘ, Microprocessor Driven Prism Monochromator for Automated Spectrophotometry	49
M. TOMOAIÁ-COTIȘEL, J. ZSAKÓ, E. CHIFU, State Equations of Fatty Acid Monolayers	54
I. CRISTEA, Condensation des Pyrimidinyl-1-Pyrazolones-5 Avec des Aldehydes Aromatiques ☉ Condensation of the 1-(2-Pyrimidinyl)-5-Pyrazolones with the Aromatic Aldehydes.	61
T. KÉKÉDY, I. TEUCA, Investigation of Oxygen Permeability of Thin Protective Organic Liquid Layers Using a Membrane-Covered Polarographic Oxygen Sensor	65

144/1989

I. SIMINICEANU, I. TODEA, M. STANCA, AL. POP, Oxidation des Äthens mit Sauerstoff zu Äthylenoxyd, mit Silberkatalysatoren. I. Stöchiometrie des Vorgangs • Oxidation of Ethylene for Ethyleneoxide Using the Molecular Oxygen and a Silver Catalyst. I. The Stoichiometry of the Process	69
S. GOCAN, L. OLENIC, E. VARGHA, A Study on the Separation Optimization of Some Synthetical Amino Acid and Peptide Derivatives Through Thin Layer Chromatography	77
S. GOCAN, V. LITEANU, A Study on Some Performance Indices Used in Thin Layer Chromatography	82
L. ONICIU, D. A. LÓVY, M. JITARU, B. C. TOMA, Electrosynthesis of Propionitrile IV. Effect of the Cathode Crystalline Structure on the Faradaic Yield	87
M. ANTON, I. LEOCA, D. GHEȚE, F. PUSKAS, C. ROMAN, N. PRODAN, I. C. POPESCU, E. CORDOȘ, Semi-Conductor Gas Sensors I. Installation for Obtaining Gas Standards in the Air	92
I. TĂNĂSESCU, E. RAMONȚIAN, Condensation of 2,4-Dinitrobenzaldehyde with Naphthalene under the Action of Concentrated Sulphuric Acid	99

Recenzii Book Reviews Comptes Rendus Buchbesprechungen

Sydney Ross, Ian Douglas Morrison, Colloidal Systems and Interfaces (M, Tomoaia-Cotișel)	101
--	-----

Cronică — Chronicle — Cronik

Participări la manifestări științifice internaționale	102
Participări la manifestări științifice naționale	102
Vizite din străinătate	102
Publicări de tratate, cărți și cursuri universitare	102
Lucrări științifice apărute în reviste de specialitate din țară și străinătate	102
Brevete	104
Susțineri de teze de doctorat	104

FILTRATION BY DIELECTROPHORESIS: PVC PARTICLES IN AN ORGANIC SOLVENT

ST. KREIDIK*, P. PRUNEANU*, E. HAUER** and V. V. MORARIU*

Received: May 10, 1987

The dielectrophoretic separation of PVC particles from an organic solvent is investigated at 1 KHz frequency and various field intensities. Continuous recording of the separation process by using a photocell is described.

Dielectrophoresis is the motion of a particle in an electric field gradient. This phenomenon has been known for a long time [1] but it was largely neglected until recently [2]. A growing interest in this phenomenon is due to its numerous possible applications in separation processes [3].

The dielectrophoretic force is:

$$F_0 = \frac{1}{2} \alpha V \nabla (E^2)$$

where α is the polarisability, V the volume of the body and E the electric field intensity. For spheres the force is:

$$F_0 = 2\pi r^3 \frac{\epsilon_1(\epsilon_2 - \epsilon_1)}{\epsilon_2 + 2\epsilon_1} \nabla (E^2)$$

where r is the radius of the sphere and ϵ_1 and ϵ_2 are the absolute permittivities of the surrounding fluid medium and of the particle respectively. Obviously the force is independent of the electrode polarity and does not change direction under the influence of an AC field. Compared to electrophoresis it is a second-order force. However it offers the unique possibility of acting upon neutral bodies.

The main purpose of this work was to investigate the continuous recording of the separation process. The simplest dielectrophoretic cell is made of a cylinder, the outer electrode and an insulator-supported wire which is the inner electrode. The cell is filled with a suspension and the electrodes are connected to the high voltage. The solid particles are collected on the inner electrode by dielectrophoresis. The efficiency of dielectrophoresis is usually evaluated by measuring the content of solid particles before and after the process. This involves a tedious manipulation of the suspension. We have employed a photocell mounted on the dielectrophoretic cell and recorded the separation process. This offers the advantage of a rapid evaluation of the separation rate.

We have chosen for experiments powdered poly vinyl chloride (PVC) and as a suspending liquid, a mixture of carbon tetrachloride and benzene. This system was extensively investigated by Pohl [2].

* Institute of Isotopic and Molecular Technology, 3400 Cluj-Napoca POBox 700, Romania

** Faculty of Mathematics and Physics, University of Cluj-Napoca, 3400 Cluj-Napoca, Romania

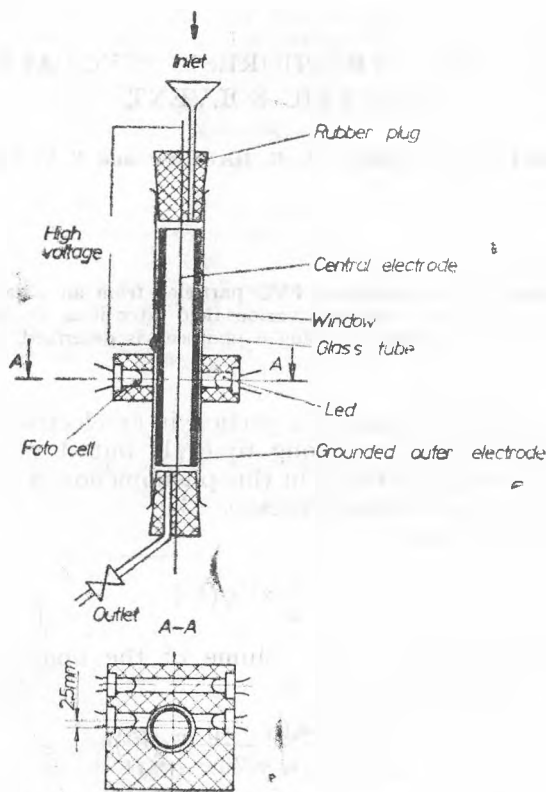


Fig. 1. Dielectrophoretic separator and an attached photocell device for rapid evaluation of the separation rate.

Materials and Method. PVC particles having a diameter between 32 and 71 μm were used throughout the experiment. The particles were suspended in a 1:1 V/V mixture of benzene and carbon tetrachloride, analytical grade. The suspension was obtained by mixing 1g of PVC particles with 200 g of solvent. The dielectric constant of PVC is 4.58 while for the fluid mixture is 2.26. Therefore, there is a significant difference among the dielectric constants of the two phases, and the two phases can be separated by dielectrophoresis.

The dielectrophoresis cell was constructed of a stainless steel tube, 8 mm diameter, covered by a glass tube and a rubber insulator supported the stainless steel wire of 0.25 mm diameter and 30.0 mm length (Fig. 1). A hole was worked up in the steel tube at 2.5mm distance from the central axis and a photocell was mounted on it, at about half the tube length. The photocell response is sensitive to temperature. Electric current flow during the experiment increases the temperature of the separation cell including the photocell altering its response. An electronic system was worked out to eliminate the thermal drift. The photo cell response was recorded on an Endim Y-t recorder. An AC field of 1 KHz was used throughout the experiment. The voltage from frequency generator was fed into a power amplifier.

Results and Discussion. The photocell response is shown in Fig. 2. After switching on the field, the particles are collected on the central electrode and the solvent becomes clear. The response of the cell, when the thermal drift is not

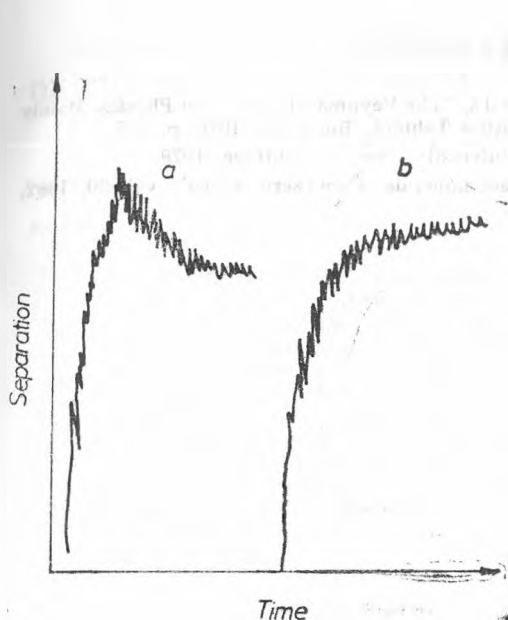


Fig. 2. The separation process as recorded by the photocell:
 a) thermally uncompensated system, and;
 b) thermally compensated system.

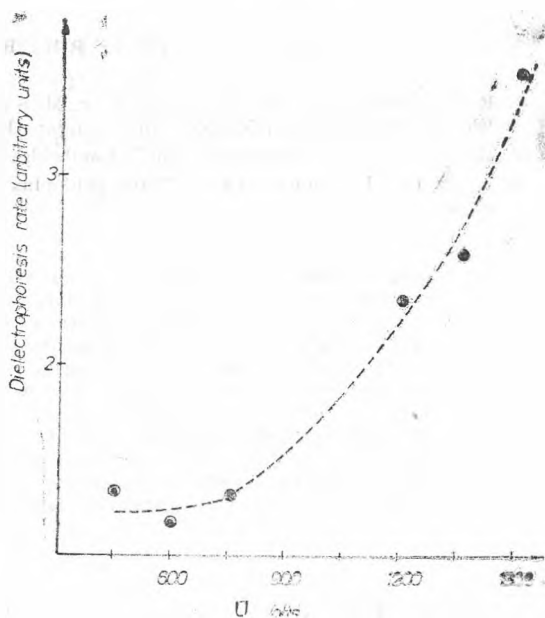


Fig. 3. The rate of the dielectrophoretic separation of PVC particles in a benzene-tetrachloride mixture, at various voltages. The frequency of the field is 1 KHz.

corrected, is shown in Fig. 2a whereas Fig. 2b shows the correct response. Complete separation is achieved in about two minutes.

The rate of separation can be evaluated from the initial slope of the recorded curves. The results are shown in Fig. 3. The dielectrophoretic separation is slow up to about 750 V and increases strongly at higher voltages.

As shown by Pohl [2], there is a critical voltage where further increase of the applied voltage does not increase the separation process. Here the material stuffs off the electrode. This critical voltage is nearly reached at about 1.5–2 KV. However, in our experiment there is no evidence for this limit at 1.5 KV where the curve is still rising steeply. This may reflect differences in the frequency of the field used in Pohl's experiment (60 Hz) and in ours (1 KHz). It is possible that the rate of separation is higher at higher frequencies, and this is a reasonable hypothesis; obviously optimum separation deserves investigation at fields of various frequencies.

In fine, the present work has shown that a rather simple device can be used to investigate the rate of the dielectrophoretic separation process.

REFERENCES

1. R. P. Feynman, R. B. Leighton, M. Sands, "The Feynman Lectures on Physics, Mainly Electromagnetism and Matter" (in romanian) Editura Tehnică, București, 1970, p. 200.
2. H. A. Pohl, "Dielectrophoresis", Cambridge University Press, Cambridge, 1978.
3. I. J. Lin, L. Benguigui, "Coal gold plus base minerals of southern Africa", vol. 30, 1982, p. 45.

THE ACTION OF SOME DIETHYLAMINOETHANOL DERIVATIVES ON THE MEMBRANE POTENTIAL OF THE STRIATED MUSCLE FIBRES

ION NEACȘU* and NICOLAE OITĂ**

Received: July 14, 1987

The influence of some new products derived from diethylaminosthanol, a procaine metabolite, (diethylaminoethanol glutamate, acetylglutamate, acetylglycinate, acethyl *para* aminobenzoate, as well as procaine glutamate) on the membrane potential of the frog (*Rana ridibunda*, Pall.) sartorius muscle fibres was investigated using the intracellular glass microelectrodes technique. These products have effects similar to those of procaine and diethylaminoethanol, determining a slight hyperpolarization of the membrane in a normal external medium, the inhibition of repolarization of the depolarized membrane by high external K^+ and the decreasing of the depolarization caused by the lack of the external calcium, revealing thus properties of membrane stabilizers. The data evidence the possibility of using these products as analogues of procaine in certain drugs.

Introduction. The action of procaine as a local anesthetic and membrane stabilizer or as a component of the „Gerovital” and „Aslavital” products showing its complex effects at different levels in the organism has been studied by many researchers [1–6]. It is also known that the procaine splits up in the organism, after a relatively short time, in *para* aminobenzoic acid (PABA) and diethylaminoethanol (DEAE), every metabolite having its own pharmacodynamical actions [3–7]. The action mechanism of the drug based on procaine is not known well enough [3, 6–8], and few researches on the procaine metabolites have been carried out [3, 7–9].

Since we have noticed that certain DEAE effects are similar to those of procaine [3, 8], in this paper we studied the action of some DEAE derivatives on the membrane potential under different conditions of extracellular medium in comparison with the action of procaine under the same conditions.

Experimental part. The experiments have been carried out on the membrane of the frog (*Rana ridibunda*, Pall.) sartorius muscle fibres using the intracellular glass microelectrodes technique. We have studied the bioelectric effects of some new products, diethylaminoethanol (DEAE) derivatives: diethylaminoethanol glutamate (DEAE GLU), acetylglutamate (DEAE A-GLU), acetylglycinate (DEAE A-GLY), *para*-acetylaminobenzoate (DEAE A-PAB) as well as procaine glutamate (PROC. GLU) in a 2.5 mM concentration, under the conditions of membrane depolarization determined by high external K^+ (30 mM) or in the absence of Ca^{2+} in the extracellular medium, in comparison with the procaine effects under similar conditions. The Ringer normal physiological solution (NR) with a pH=7.2 was administered in continuous current. The solutions with different agents were prepared by adding them to the NR solution. The solutions with high K^+ (30 mM) or Ca^{2+} -free (Ca-FREE R.) were prepared by the equimolar modification of the NaCl concentration from the NR. In each experiment we worked on five muscles from different animals at room temperature. The statistical data treatment was performed by the Student's test.

* Centre of Biological Research—Iasi, Calea 23 August 20 A, 6600 Iasi, Romania

** Military Hospital Iasi, Calea 23 August 6, 6600 Iasi, Romania

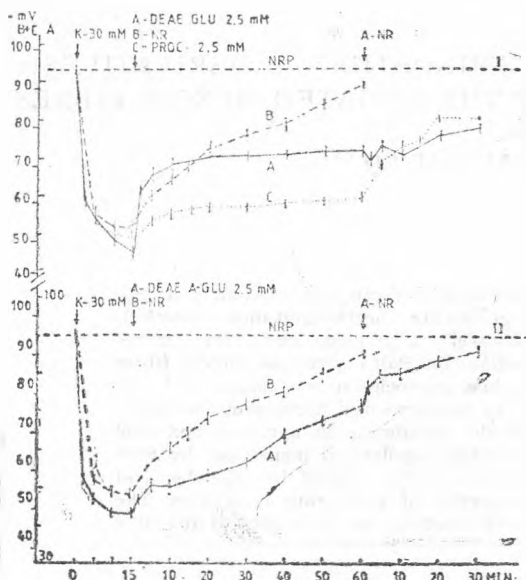


Fig. 1. The effect of 2.5 mM DEAE GLU (I-A) and 2.5 mM DEAE A-GLU (II-A) on the depolarized membrane by 30 mM K⁺ (B=NR; C=2.5 mM procaine).

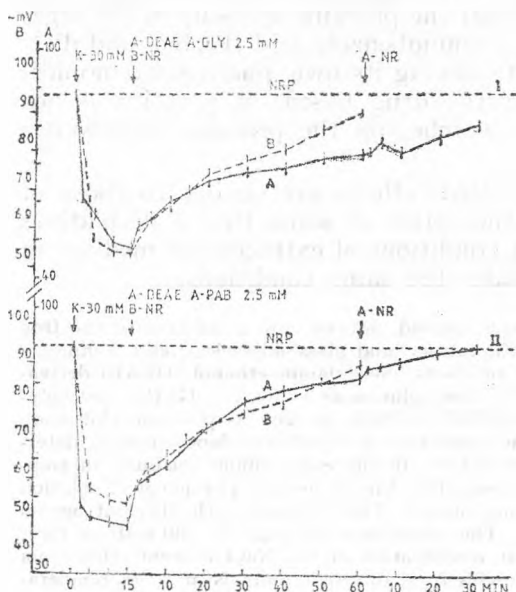


Fig. 2. The effect of 2.5 mM DEAE A-GLY (I-A) and 2.5 mM DEAE A-PAB (II-A) on the depolarized membrane by 30 mM K⁺ (B=NR).

Results and discussions. The normal resting potential (NRP) in our experiments had values between 88.55 mV and 95.30 mV (SE is about 0.75 mV) (Figs. 1–5).

When treating the muscle fibres with a 30 mM K⁺-Ringer solution a strong depolarization of the membrane can be seen, which after 15 minutes reaches an amplitude between 40.97 mV and 49.00 mV (Figs. 1–3). The washing of the depolarized fibres with a NR solution determines a slow re-establishment of the membrane potential, so that after 60 minutes a depolarization of only 4.30 mV (Figs. 1–3 B) is seen.

If the depolarized membranes by 30 mM K⁺ are treated with a NR solution containing 2.5 mM DEAE GLU (Fig. 1-I-A) a re-establishment of the membrane potential just for the first 10 minutes is recorded, when the depolarization amplitude diminishes from 49.00 mV to 24.66 mV, after which the blocking of the membrane repolarization takes place, so that after 60 minutes the depolarization amplitude becomes 21.25 mV. The NRP is not remade even after washing of membranes with NR without agent, so that after 30 minutes the depolarization amplitude is of 15.70 mV. This phenomenon is highly similar to that noticed at the 2.5 mM procaine action on the depolarized membranes by 30 mM K⁺ (Fig. 1-I-C), when, after 30 minutes of washing of the muscle fibres with NR a depolarization of 13.80 mV is noticed.

Similar effects are also observed when treating the depolarized membranes by 30 mM K⁺ with a 2.5 mM DEAE A-GLU solution (Fig. 1-II-A), but the braking of repolarization is less stressed than in the previous case. Thus, after 10 minutes, depolarization diminishes from 47.35 mV

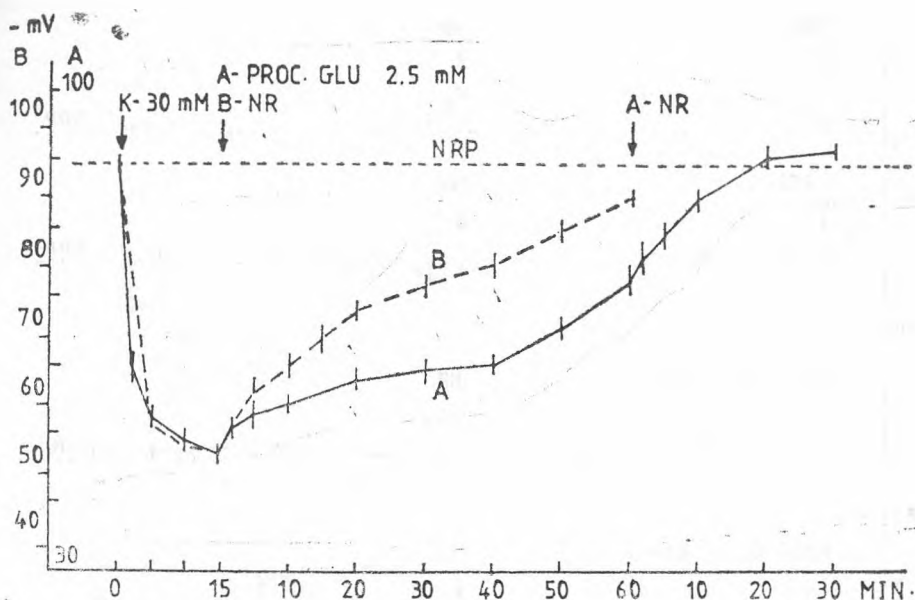


Fig. 3. The effect of 2.5 mM PROC.GLU on the depolarized membrane by 30 mM K^+ ($B=NR$).

to 40.02 mV and after 60 minutes to 18.02 mV. By washing the membranes with NR for 30 minutes the depolarization diminishes to only 4.44 mV.

DEAE A—GLY (2.5 mM) has an action similar to that of the DEAE GLU on the depolarized membranes by 30 mM K^+ (Fig. 2-I-A). After 10 minutes, the depolarization diminishes from 40.97 mV to 27.72 mV and after 60 minutes to 12.63 mV. When washing the membranes with NR this one reduces to 7.22 mV.

The influence of DEAE A—PAB (2.5 mM) on the repolarization of the depolarized membranes by 30 mM K^+ is weaker (Fig. 2-II—A), so that after 60 minutes of the action of the agent, the depolarization is reduced from 47.62 mV to 5.66 mV and after 30 minutes of washing the membranes with NR, a complete re-establishment of the NRP takes place.

But, the PROC.GLU (2.5 mM) has a strong braking action of the repolarization of depolarized membranes by high K^+ (Fig. 3—A), the depolarization decreasing from 42.47 mV to 34.97 mV in the first 10 minutes, to 29.80 mV after 30 minutes and to 12.56 mV after 60 minutes. But the washing of the membranes with a NR solution causes a fast NRP re-establishment and after 30 minutes there is a slight hyperpolarization of the membrane.

In fact, one can notice that even during the action on the normal membranes, 2.5 mM PROC.GLU (Fig. 4—C) has its characteristic effects, determining a slight depolarization (average amplitude of 0.56 mV). This action is stronger than those of DEAE—GLU, DEAE A—GLU, and DEAE A—PAB or of procaine (Fig. 4—A) in the same concentration which produce a hyperpolarization [3]. This effect is similar to that of higher procaine concentrations (over 3 mM)

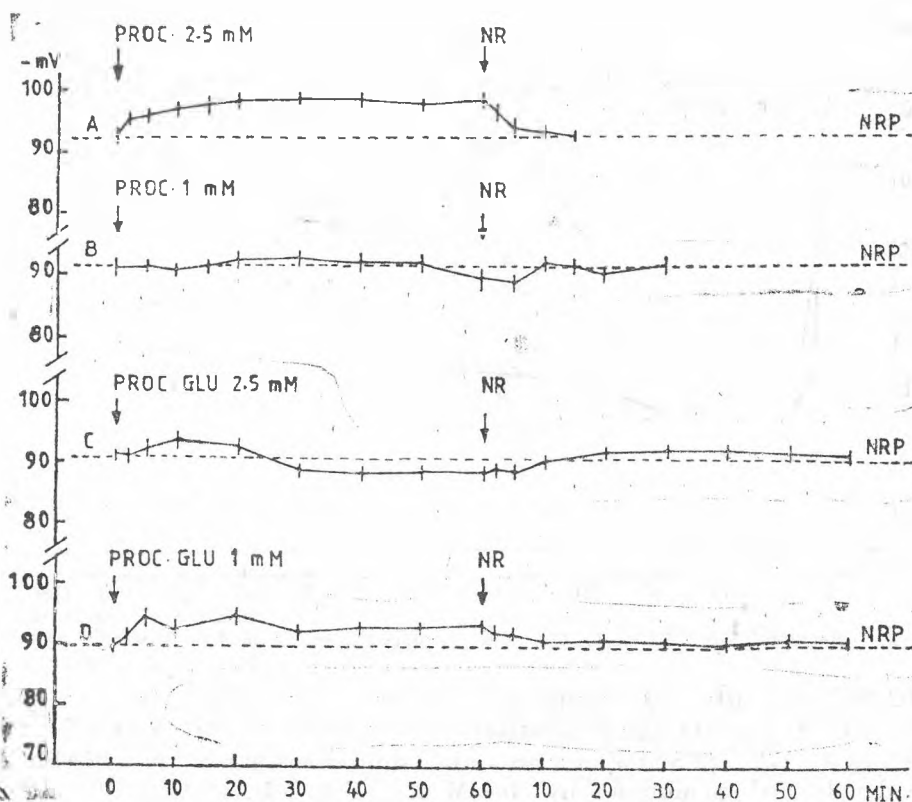


Fig. 4. The effect of 2.5 mM (A) and 1 mM (B) procaine and of 2.5 mM (C) and 1 mM (D) PROC. GLU on the membrane potential in a normal Ringer solution (NR).

which determine a „prelitic depolarization” [3]. But, in a 1 mM concentration, the PROC. GLU determines a hyperpolarization (average amplitude of 2.85 mV) of the membrane (Fig. 4—D) more prominent than that specific to a 1 mM procaine concentration (0.30 mV) (Fig. 4—B).

It is known that the $K^+ : Ca^{2+}$ ratio in the extracellular medium has a great influence on the membrane potential and when Ca^{2+} diminishes, a depolarization of the membrane takes place [3, 10]. In our experiments with Ca—FREE Ringer a depolarization with a 8.09 mV average amplitude (Fig. 5—A—2) easily reversible in NR was recorded.

By adding the DEAE derivatives in the Ca—FREE R. solution, we can notice a diminution of the depolarization determined by the lack of Ca^{2+} , the average amplitude of depolarization being of 4.92 mV for DEAE GLU, 4.80 mV for DEAE A—GLU, 2.93 mV for DEAE A—GLY, 2.08 mV for DEAE A—PAB and 4.16 mV for 2.5 mM PROC. GLU (Fig. 5 A—F). Thus, it can be estimated that these products imitate the role of Ca^{2+} at the level of the cellular membrane as the procaine does [2, 3].

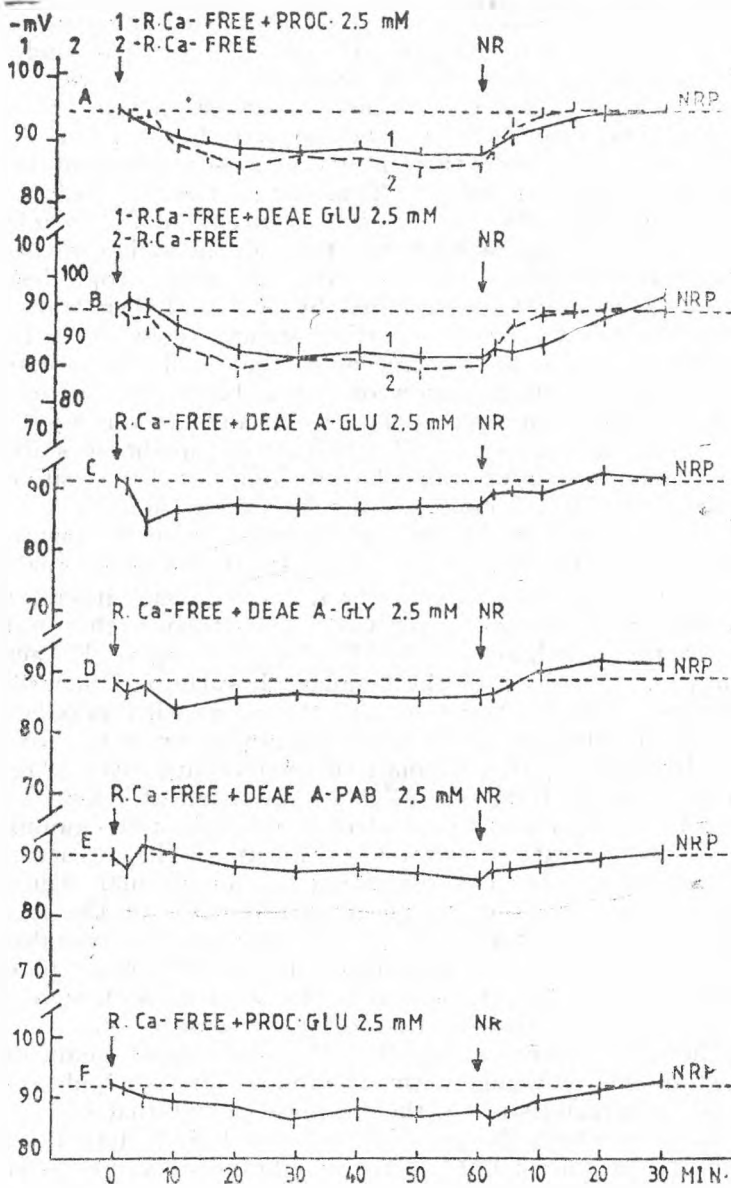


Fig. 5. The effect of 2.5 mM procaine (A-1), 2.5 mM DEAE GLU (B-1), 2.5 mM DEAE A-GLU (C), 2.5 mM DEAE A-GLY (D), 2.5 mM DEAE A-PAB (E) and 2.5 mM PROC. GLU (F) in a Ca^{2+} -FREE RINGER solution (A-2 and B-2: membrane potential in Ca^{2+} -FREE RINGER).

It was also shown that the bioelectric effect of procaine is based on its specific interactions with ions, with the structural phospholipids from the external layer of the cellular membrane and with the passive and active ionic transport [2, 3, 8]. But, procaine is DEAE derivative under the form of a PABA ester with this aminoalcohol. From the results shown, it comes out that the DEAE derivatives under the form of a salt, studied in this paper, have bioelectric effects similar to those of procaine and thus we can estimate that these effects derive from a series of their interactions with ions and the membrane structures similar to those of procaine. Thus, their effect of a slight membrane hyperpolarization according to the „2-MSI” concept on the membrane structure and functioning [11] can be explained through the action of these products on the globular phospholipidic micellae (with anionitic properties) from the external layer of the membrane, structured by K^+ and their transition to the laminar micellae (with cationitic properties) structured by Ca^{2+} . This leads to the increase of the degree of the packing up of the membrane structures and of that of stabilization, the modification of permeability, the increasing of the membrane electric charge (the hyperpolarization) and the raising of the excitation threshold. Such an action is similar to that of membrane stabilizers (procaine, Ca^{2+} etc.) and it derives from the possibility of the positive charge of the nitrogen from the DEAE molecule, depending on the pH.

This also accounts for the effects of these products on the membrane under the conditions of modifying the $K^+ : Ca^{2+}$ ratio from the external medium.

It is known that, when increasing the $K^+ : Ca^{2+}$ ratio either by increasing the K^+ concentration or decreasing the Ca^{2+} concentration, there takes place a depolarization of the membrane [3, 10, 12], due to a higher K^+ action, which determines the phase transition of the laminar phospholipidic micellae from the membrane external layer structured by Ca^{2+} to the globular micellae structured by K^+ . Thus, the depolarized membranes becomes richer in K^+ globular micellar structures. By treating the depolarized membranes with NR containing procaine or DEAE derivatives, the NRP re-establishment does not occur, because these agents hinder the coming out of the K^+ from the globular micellae and the Ca^{2+} rebinding with the re-establishment of the structure and the normal potential, determining a stabilization of the globular structure of the depolarized membrane, an effect which is characteristic of the local anesthetics and the membrane stabilizers [3]. The inhibition of the membrane repolarization by the anesthetics also takes place during the action potential [13]. Specific procaine and DEAE interactions with Ca^{2+} are also noticed in the case of the membrane hyperpolarization due to the decrease of the $K^+ : Ca^{2+}$ ratio by increasing the Ca^{2+} concentration [3, 8, 12] when these agents impede each other in respect of their binding to the membrane phospholipids, reducing the hyperpolarization characteristic to the increase of external Ca^{2+} .

These results show that the procaine and the DEAE derivatives have the capacity to imitate the role of Ca^{2+} at the membrane structures level, behaving as membrane stabilizers.

Taking into account the bioelectric effects of these DEAE derivatives, their interaction with the ions and the membrane structures, the complex role in the organism of the aminic acids and of the acetyl group from their molecule [14] as well as the positive effects of the DEAE and its derivatives on the cholesterol

deposited in the membrane structure [3, 8] there of re-establishing the normal functions of the hepatic cell [3, 15] and the DEAE distribution at different level in the organism [7], we estimate that these new products may be used as analogues of procaine, in certain drugs [16, 17] with stimulating, trophic, anti-atherosclerotic and hepatoprotective effects.

Conclusions. The DEAF derivatives have bioelectric effects similar to those of procaine and DEAE. These products determine a slight hyperpolarization of the cellular membrane, the inhibition of membrane repolarization depolarized by high K^+ and the decreasing of the depolarization of produced by the lack off he external Ca^{2+} , revealing the properties of the membrane stabilizers. Data show the possibility of using these derivatives as analogues of procaine in certain drugs.

REFERENCES

1. P. Seeman, *Pharmacol. Rev.*, **24**, 586 (1972).
2. Șt. Agrigoroaei, I. Neacșu, *Rev. Roum. Biol.-Biol. Anim.*, **24**, 155 (1977).
3. I. Neacșu, „Acțiunea unor ioni și a unor agenți organici asupra proprietăților electrice ale membranei celulare”, Thesis, Univ. „Al. I. Cuza” Iași (1984).
4. A. Aslan, *Viața medicală*, **XX**, **16**, 729 (1973).
5. A. Aslan, Al. Vrăbiescu, “Int. Symp. Gerontol.”, 26th–27th June, Bucharest, 1972, p. 35.
6. C. Vascan, V. Mihăilescu, Fl. Secardoțeanu, “Int. Symp. Gerontol.”, 26th–27th June, Bucharest, 1972, p. 505.
7. A. D. Abraham, M. Borșa, P. T. Frangopol, „Al II-lea Simpozion de chimia coloizilor și suprafețelor”, Rezumate, 8–10 sept. Cluj-Napoca, 1986, p. 73.
8. I. Neacșu, N. Oiță, *Rev. Roum. Biol.-Biol. Anim.*, **29**, 31 (1984).
9. M. S. Ionescu, „Al II-lea Simpozion de chimia coloizilor și suprafețelor”, Rezumate, 8–10 sept., Cluj-Napoca, 1986, p. 63.
10. I. Neacșu, Șt. Agrigoroaei, *Rev. Roum. Biol.-Biol. Anim.*, **23**, 133 (1978).
11. Șt. Agrigoroaei, *Rev. Roum. Biol.-Biol. Anim.*, **21**, 137 (1976).
12. I. Neacșu, Șt. Agrigoroaei, *Rev. Roum. Biol.-Biol. Anim.*, **25**, 39 (1980).
13. J. Etzensperger, *J. Physiol. (Paris)*, **62**, 299 (1970).
14. I. F. Dumitru, „Biochimie”, Ed. didactică și pedagogică, București, 1980.
15. Ch. Rouiller, ed., “The Liver. Morphology, Biochemistry, Physiology, vol. II, Acad. Press, New York and London, 1964.
16. N. Oiță, Z. Cojocaru, T. Sauciuc, O. C. Mungiu, I. Neacșu, „Medicamente trofice și procedeu de obținere”, Brevet R.S.R. 80.828 (1982).
17. Z. Cojocaru, G. Rusu, N. Oiță, T. Sauciuc, I. Neacșu, O. C. Mungiu, Brevet R.S.R. 83.820, 1982.

UTILIZATION OF MODEL BILAYER LIPID MEMBRANES TO CHARACTERIZE THE RESPONSE MECHANISM OF CYANINE DYES TO MEMBRANE POTENTIALS¹

CORNELIU TARBA*

Received: July 15, 1987

Using liposomes of different composition and electric charge, ion gradients and specific ionophores for the development of diffusion potentials it is shown that the mechanism of response of the cyanine dye diS-C₂-(5) (3,3'-diethylthiadicarbocyanine iodide) to membrane potentials depends mainly on the electric charge of the membrane phospholipids. With charged phospholipids, the mechanism of response consists basically in a potential-dependent monomer-dimer shift of the bound dye. In this case, the response is also sensitive to the low ionic strength of the medium, which (in the presence of a surface charge) gives rise to an external surface potential (double-ionic layer potential) that can obscure the effect of the diffusion potential. However, if these details of the mechanism are known, one can always select proper conditions for reliable measurements, the dye having a very high sensitivity ($\Delta A/A \geq 10^{-1}$, at micromolar concentrations) and relatively fast kinetics ($t_{1/2} < 10$ ms).

Introduction. Electric potential differences between the interior and the exterior of the cells or between different compartments of a cell represent an essential characteristic of the living matter. Traditionally, in the field of electrophysiology, membrane potential differences have been measured by means of microelectrodes, but in the field of bioenergetics (where usually small cells and organelles are employed) the use of microelectrodes is either inconvenient or even impossible. Therefore, in the past two decades, alternative, less invasive methods have been developed. One of these is the distribution of permeant ions, although it usually has the disadvantage of being a static (equilibrium) method that cannot be used for kinetic studies. However, certain molecular (ionic) probes with distinctive spectroscopic properties can be used to monitor relatively fast changes in membrane potential. The best known probes of this type are the oxonol, cyanine and merocyanine dyes, which exhibit a marked dependence of their spectra on the membrane potential. Their mechanism of response has been investigated by several groups [1-7] and also by the author of the present article, who studied extensively the response mechanism of the cyanine dye diS-C₂-(5) in liposomes, reconstituted system and mitochondria [8-10]. Bilayer lipid membranes, mostly liposomes, but, to some extent, also planar (black) lipid membranes have been essential in all these studies. In fact, bilayer lipid membranes constitute biophysico-chemical models of great importance for the general study of the structure, properties and functions of biological membranes. They are sufficiently complex to possess certain essential features

* University of Cluj-Napoca, Department of Biology, 3400 Cluj-Napoca, Romania

¹ The experimental part of this work was performed at Cornell University, Ithaca, N.Y., U.S.A., while the author was a graduate student in the laboratory of Dr. Peter C. Hinkle.

of the natural membranes (structural, electric and permeability properties), but simple enough to allow various manipulations, such as changes in lipid composition of the membrane and in the content of the two compartments separated by the membrane. As it shall become evident later, the simplicity of the system and the possibilities of manipulation mentioned above make the bilayer lipid membrane indispensable for an easy and complete study of the response mechanism of the membrane potential probes.

Although the general purpose of this article is to demonstrate the importance of lipid bilayer membranes in the characterization of the response mechanism of cyanine dyes to membrane potentials, considering the fact that it is not intended to be a review, it will do so by presenting the particular case of the liposomes and of the cyanine dye diS-C₂-(5). However, references to other cyanine dyes and in some instances to the use of black lipid membranes, as well as generalizing attempts will be frequently made.

Experimental part. *Liposomes* were prepared by sonicating 20–40 mg phospholipids in 1 ml buffer, as indicated in the figure legends, in a pyrex test tube held in a bath type sonicator (Lab. Supplies, Hicksville, N.Y., Model G80–80–1) until the emulsion cleared (20–30 min).

Spectral recordings were performed with an Aminco DW–2 differential spectrophotometer, which was also used for slow kinetic recordings. Fast kinetic recordings were performed with an Aminco–Morrow stopped-flow apparatus attached to a Beckmann DU spectrophotometer and a Tektronix 5103 oscilloscope.

Chemicals were all of analytical grade. Phospholipids and valinomycin were from Sigma and diS-C₂-(5) from Eastman–Kodak. 1799 (bis (hexafluoroacetyl)–acetone) was a gift of Dr. E. Racker (Cornell University).

Results and discussion. Fig. 1 presents the results obtained by the titration of a constant amount of dye with increasing amounts of liposomes prepared from a mixture of soybean phospholipids. This mixture, commercially known as azolectin, contains a certain percentage of negatively charged phospholipids (that bear a net negative charge at neutral pH). The dashed line (*a*) in the figure shows the dye spectrum in the buffer. Upon addition of a small amount of liposomes (0.04 mg phospholipid/ml) a spectacular shift occurs, both in the position and the magnitude of the two absorption maxima (trace *b*). Based upon studies on solvent dependency of the dye spectrum [8] and on the further behaviour of the dye (see Fig. 1) this shift can be ascribed to the binding of the dye to the lipid membrane. Indeed, further addition of liposomes does not appreciably alter the wavelength position of the new maxima but only their relative magnitudes (traces *c* to *e*), indicating a strong association of the dye with the bilayer. Moreover, the two isobestic points observed in the figure suggest the presence of two distinct optical forms. It has been shown by West and Pearce [11] that over a certain concentration range cyanine dyes dimerize in solution. Waggoner and Grinvald [4] have shown the same thing for merocyanine 540 in the presence of phosphatidyl choline vesicles. Therefore, we attribute the changes illustrated in Fig. 1 first to a monomer-dimer shift, as the dye concentrate on the liposome surface (higher order aggregates may form if the ratio dye/lipid is larger than 10^{-2} nmoles/cm²) and then to a dimer-monomer shift of the bound dye, as the lipid surface increases upon new addition of liposomes. In fact, using a modified procedure of West and Pearce [11] we were able to determine an association constant of about 1.5 cm²/nmole for the monomer-dimer aggrega-

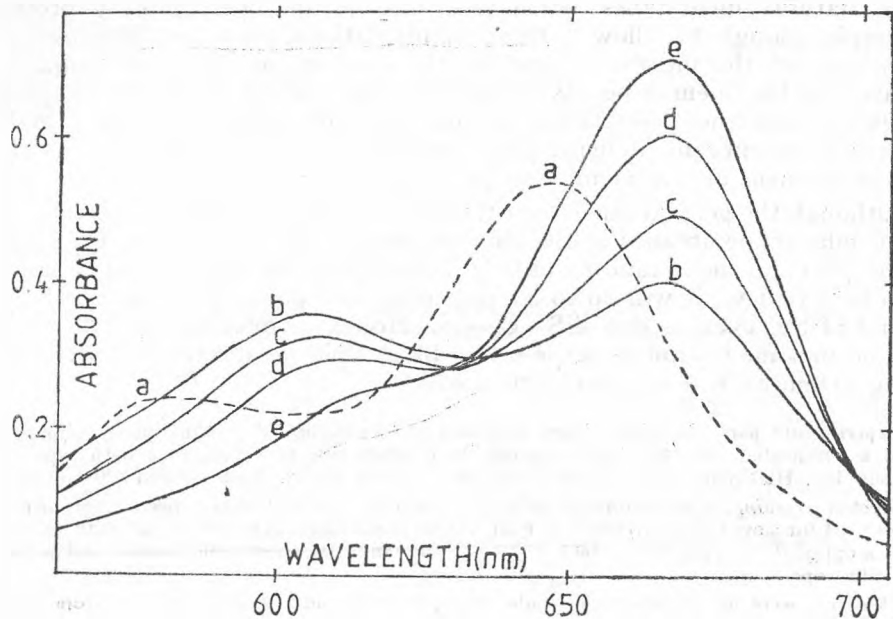


Fig. 1. Characteristics of diS-C₂-(5) spectrum in the presence of charged phospholipid liposomes. Different amounts of liposomes, sonicated in 50 mM KP_i (P_i = inorganic phosphate), pH 7.3, are suspended in 1 ml sonication medium in the presence of 5 μM dye: a — no phospholipid (PL); b — 0.04 mg PL; c — 0.08 mg PL; d — 0.02 mg PL; e — 2 mg PL.

tion [8], which compares very well with the surface density assumed by Waggoner and Grinvald for their dye [4]. More recently, Ivkov *et al.* [12] have proposed a model for the behaviour of the closely related dye diS-C₃-(5), supported by their own experiments [13], which is also compatible with our present interpretation.

A totally different picture is observed if the liposomes are composed of an electrically neutral phospholipid, such as (pure) phosphatidyl choline (Fig. 2). In this case the addition of liposomes results in a gradual shift of the main absorption maximum toward longer wavelengths and a much smaller increase of this maximum at a large liposomal surface. This behaviour can be interpreted as resulting from progressive association of the dye with the liposomes, *i.e.*, from an equilibrium between the free dye in solution and the bound dye (probably, mostly as monomers).

The pattern of response is correspondingly preserved when membrane potentials are elicited in liposomes of different composition. Fig. 3. represents the effect of a membrane potential created by facilitated diffusion of potassium ions from K⁺-loaded liposomes suspended in a low K⁺ medium in the presence of valinomycin (a specific K⁺ ionophore). It can be seen that the response is consistent with a monomer-dimer equilibrium („vertical” shift) if the phospholipids are negatively charged (Fig. 3A), whereas in the case of uncharged phospholipids the response of the dye is mainly a „horizontal” shift, indicative

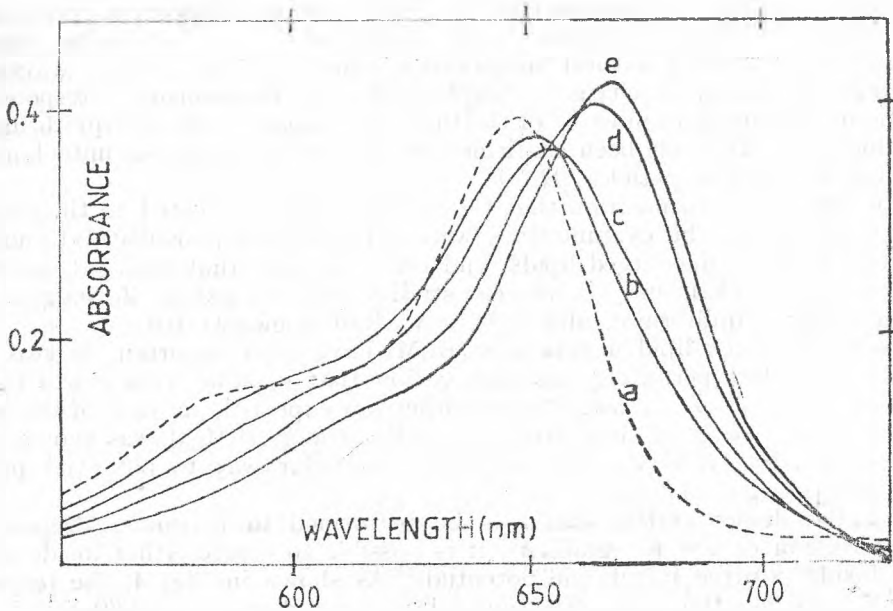


Fig. 2. Characteristics of $diS-C_2-(5)$ spectrum in the presence of uncharged phospholipid liposomes. Same conditions as in Fig. 1, but the phospholipid used is uncharged (phosphatidyl choline) and only $2.5 \mu M$ dye is present.

of an interplay between free and bound monomer, although a small quantity of bound dimer is also formed (Fig. 3B). The absorbance decrease in the region 660–670 nm is in both cases quite impressive ($>$ than 10% of the original absorbance).

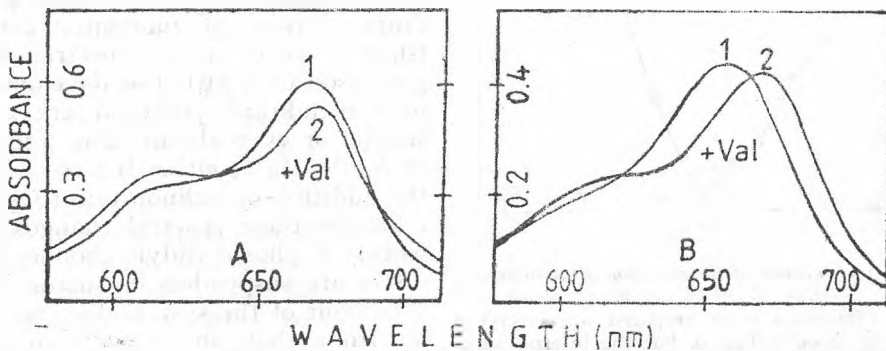


Fig. 3. Changes in absorption spectrum of $diS-C_2-(5)$ upon development of membrane potentials in charged (A) and uncharged phospholipid liposomes (B). Liposomes (0.4 mg PL) sonicated in 100 mM K_2SO_4 + 10 mM NaMOPS (4-morpholinopropane sulphonate), pH 7.3, are suspended in 1 ml buffer in which K^+ is replaced by Na^+ ; $3.5 \mu M$ dye (1) followed by 20 nM valinomycin (2).

It is clear from these results that the mechanism of response is very much dependent on the nature of the membranes and especially on their surface charge. It is also clear that in natural membranes, which usually possess a certain percentage of negatively charged phospholipids, the mechanism of response of the cationic cyanine dyes must be of the first type (monomer-dimer equilibrium of the bound dye). This has been confirmed by us also in studies on mitochondria and submitochondrial particles [8, 10].

It is instructive to mention that the initial studies dedicated to the mechanism of response of the cyanine dyes were performed in phosphatidyl choline-cholesterol vesicles (uncharged lipids) and the conclusion that emerged was that of an „on-off” mechanism [1], whereas studies made on axons [2] suggested a monomer-dimer equilibrium, although it was not demonstrated.

Studies on black lipid membranes (BLM) have been important in two respects. Firstly, they permitted the observation that cyanine dyes can actually cross the membrane [7], a fact which is otherwise expected, in view of the delocalized positive charge of these dyes. Secondly, using BLM, it was shown that the dyes (including diS-C₂-(5)) respond in a similar way to potential pulses of opposite polarity [3].

A similar demonstration can also be performed in liposomes. Depending on the direction of the K⁺ gradient, it is possible to create either inside-negative or inside positive membrane potentials. As shown in Fig. 4, the response of diS-C₂-(5) has the same direction (absorbance decrease at 660 nm) irres-

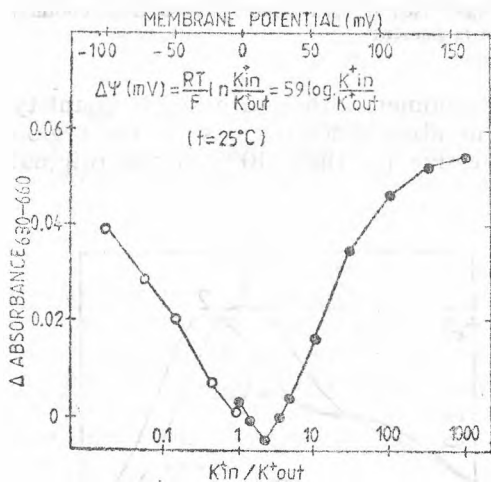


Fig. 4. Independence of the direction of absorbance change of diS-C₂-(5) on the sign of membrane potential. Liposomes were prepared and assayed similarly to those in Fig. 3, but the internal and external K⁺ content was selected such as to give the desired K⁺ in/K⁺ out ratio, the osmolarity, being maintained by different amounts of Na₂SO₄ + 10 mM NaF₃, pH 7.3; 0.2 mg soybean phospholipid, 2.5 μM dye and 20 nM valinomycin.

pective of the potential sign. This is to be expected, since the mechanism-proposed involves only the increase of the dye concentration on that side of the membrane which is negatively charged by the potential, the aggregation on either side being optically similar.

If liposomes composed of charged phospholipids are suspended in a medium devoid of inorganic cations (such as sucrose), the spectral changes associated with the development of a membrane potential are much smaller or even absent. The addition of 5 mM Mg²⁺, either before or after the addition of valinomycin (Fig. 5A) reinstalls these spectral changes. However, if phosphatidyl-choline liposomes are suspended in sucrose, the behaviour of the system does not differ from that in a salt medium (Fig. 5B). The most logical explanation is that of an external surface potential (double-ionic layer potential) which arises due to the surface charge

in conjunction with the lack of inorganic cations in the suspending medium. Indeed, this effect does not appear when the surface charge is absent or inorganic cations are present. Monovalent cations (such as Na^+ and K^+) are also capable of removing the effects of surface potential, but at much higher concentrations than the divalent cations. All these observations are perfectly consistent with the theory and practice of surface potentials (see, for example, [14]). A much more detailed account of this phenomenon is presented elsewhere [8].

The interference of surface potentials in the response of cyanine and oxonol dyes to transmembrane potentials was also observed in studies on sarcoplasmic reticulum [5]. In fact, certain discrepancies reported in the literature with regard to the magnitude of the membrane potential in natural systems may very easily be explained in terms of interference from surface potentials. A good example of this kind is the work of Walsh-Kinnally and Tedeschi on mitochondria [15].

Besides showing a high sensitivity and reliability, it is desired that a good potential probe have a reasonable fast response, in order to perform kinetic studies (with the intention of extending it to natural systems). Fig. 6 is the result of fast kinetic studies in liposomes, either by increasing the concentration of valinomycin or of the protonophore 1799. Since the rise time of the membrane potential was apparently a first order process,

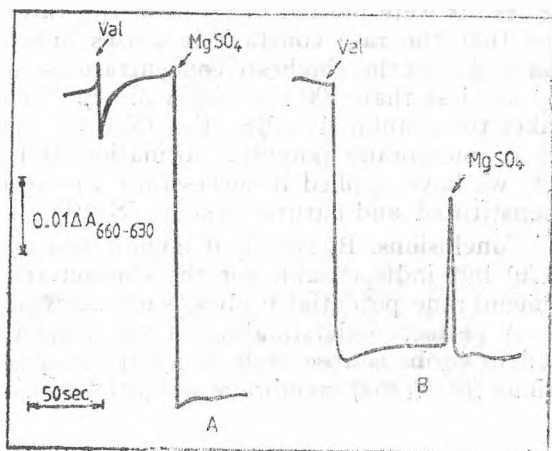


Fig. 5. Effect of ionic strength of the suspending medium on dye spectrum in charged (A) and uncharged phospholipid liposomes (B). Liposomes (0.2 mg PL) containing 50 mM K_2SO_4 + 10 mM NaMOPS, pH 7.3, are suspended in 150 mM sucrose + 5 mM NaMOPS, pH 7.3; 2.5 μM dye, 10 nM valinomycin and 5 mM MgSO_4 .

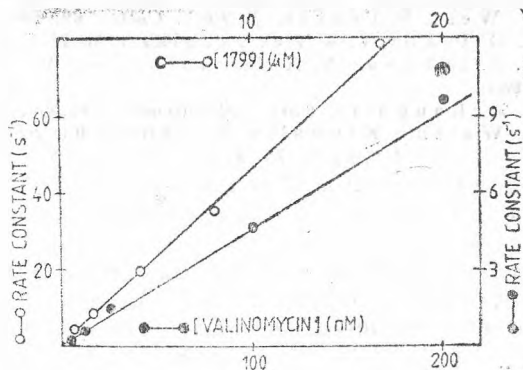


Fig. 6. Dependence of the rate constant of membrane potential formation on the ionophore concentration. Liposomes (0.2 mg PL) containing 50 mM KP_i , pH 7.4 ($\bullet-\bullet$) or 8.2 ($\circ-\circ$) are suspended in 50 mM NaP_i , either pH 7.4 ($\bullet-\bullet$) or 6.2 ($\circ-\circ$), with 2.5 μM dye and different amounts of ionophores, as shown.

the results were plotted in terms of the rate constant ($K = \ln 2/t_{1/2}$). It can be seen that the rate constant increases linearly with the ionophore concentration even at the highest concentrations used. The corresponding half times ($t_{1/2}$) are less than 100 ms with valinomycin and less than 10 ms with 1799. This makes the cyanine dye diS-C₂-(5) a very good candidate for measuring kinetics of membrane potential formation and dissipation in various systems. In fact, we have applied it successfully for spectral and kinetic measurements in reconstituted and natural systems [8, 10].

Conclusions. Bilayer lipid membranes and especially liposomes are not only useful but indispensable for the characterization of the mechanism of response of membrane potential probes, such as cyanine dyes.

A perfect understanding of the mechanism of response of a potential-dependent probe is absolutely necessary in order to avoid the use of improper conditions for (trans) membrane potential measurements.

REFERENCES

1. P. J. Sims, A. S. Waggoner, C. H. Wang, J. F. Hoffman, *Biochemistry*, **13**, 3315 (1974).
2. W. N. Ross, B. M. Salzberg, L. B. Cohen, H. V. Davila, *Biophys. J.*, **14**, 983 (1974).
3. A. S. Waggoner, C. H. Wang, R. L. Tolles, *J. Membrane Biol.*, **33**, 109 (1977).
4. A. S. Waggoner, A. Grinvald, *Ann. N.Y. Acad. Sci.*, **303**, 217 (1977).
5. T. J. Beeler, R. H. Farmen, A. N. Martonosi, *J. Membrane Biol.*, **62**, 113 (1981).
6. C. L. Bashford, B. Chance, J. C. Smith, T. Yoshida, *Biophys. J.*, **25**, 63 (1979).
7. S. Krasne, *Biophys. J.*, **30**, 441 (1980).
8. C. N. Tarba, "Membrane Potentials in Liposomes, Cytochrome Oxidase Vesicles and Other Biological Systems Estimated by Absorption Spectroscopy of a Cyanine Dye" (Ph. D. Thesis), Cornell University, Ithaca, N.Y., 1978.
9. C. Tarba, *Rev. Roum. Biochim.*, **20**, 51 (1983).
10. C. Tarba, *Rev. Roum. Biochim.*, **20**, 61 (1983).
11. W. West, S. Pearce, *J. Phys. Chem.*, **69**, 1894 (1965).
12. V. G. Ivkov, V. A. Pechatnikov, M. N. Ivkova, *Gen. Physiol. Biophys.*, **3**, 19 (1984).
13. M. N. Ivkova, V. A. Pechatnikov, V. G. Ivkov, *Gen. Physiol. Biophys.*, **3**, 97 (1984).
14. S. McLaughlin, *Curr Top. Membr. Transp.*, **9**, 71 (1977).
15. K. Walsh-Kinnally, H. Tedeschi, *FEBS Lett.*, **62**, 41 (1976).

STUDY OF THE OXIDATION KINETICS OF METALS BY ELLIPSOMETRY¹

SIMION JITIAN* and AURELIA JITIAN**

Received: September 8, 1986

Results obtained by ellipsometric measurements of steel, copper and nickel surfaces, maintained at the ambient pressure and humidity are presented. These measurements follow the time variation of the ellipsometric parameter Δ of the metallic surfaces during oxidation, and also of the thickness and the optical constants of the oxide films developed on freshly prepared metallic surfaces, assumed to lack surface films. The measured time-variation curves follow a logarithmic law.

Introduction. Metals, except gold, maintained in oxidizing ambient atmosphere are subjected to chemical corrosion. The manner of forming of oxide films is explained by different mechanisms in accordance with the type of the metal and with the characteristics of the film formed, obtaining different surface film forming kinetic laws. Knowledge of the chemical corrosion mechanism is very important in finding the ways to decrease its destructive effect.

In the case of oxide films forming with less than 40 Å thicknesses, the oxidation of metals is explained by the Mott and Cabrera's theory [1, 2]. Oxygen is adsorbed on the oxide film surface as negative ions. The necessary electrons to form the negative ions result from the metal and reach the surface across the film by tunnelling effect. The charging of the surface leads to the formation of a very strong electric field, able to pull out the metallic ions and to move them along the film. The oxide film thickness (d) is limited by the metallic ions pulling out rate at the metal-oxide interface and is given by a logarithmic law of the form:

$$d = A \ln (Ct + 1) + B \quad (1)$$

where t stands for the time and A , B , C are constants. A stands for the increase of the thickness of the film when $\ln(Ct + 1)$ is enhanced by a unit, and expresses the slope of the rights $d(f \ln t)$. B is the thickness of the film at the initial time $t = 0$.

Ellipsometry is one of the most accurate and sensitive methods of studying corrosion processes. One can detect by this method the monomolecular films of the species adsorbed or formed on different surfaces. Ellipsometry was successfully used to study the oxidation of surfaces [3, 4, 5].

The reflexion of a radiation on the interface of two different media is characterised in ellipsometry by the ellipsometric parameters Δ and ψ . These show the phase difference between the two components of the radiation (parallel to the

* "Traian Vuia" Polytechnic Institute - I.S. Hunedoara, 2750 Hunedoara, Romania

** Industrial High School 1, Hunedoara, 2750 Hunedoara, Romania

¹ This paper has been presented in the National Symposium of Surface and Colloid Chemistry, held in Cluj-Napoca, Romania, between September 8-10, 1986

plane of incidence and perpendicular to the plane of incidence) after reflexion, the ratio of their amplitudes, respectively. As a result of surface film formation by chemical corrosion, the optical constants of the surface and implicitly the ellipsometric parameters Δ and ψ are modified. The variation of the ellipsometric parameters Δ and ψ can be related to that of $\bar{\Delta}$ and $\bar{\psi}$ corresponding to the surface without film giving thus indications with respect to the oxidation of the surface.

In Drude approximation, valid for films less than 100 Å in thickness, the variations of the ellipsometric parameters are proportional with the film thickness [3, 6], according to the relations:

$$\delta\Delta = \bar{\Delta} - \Delta = \alpha d; \quad \delta\psi = \bar{\psi} - \psi = \beta d \quad (2)$$

In these relations α and β stand for constants of proportionality between the thickness of the surface film and the variations of the ellipsometric magnitudes Δ and ψ . Therefore, even the variations of the ellipsometric measurements only can be used in kinetic studies, avoiding thus complicated computations for the film thickness evaluation. Kinetic laws of the form:

$$\delta\Delta = A' \ln(C't + 1) + B' \quad (3)$$

are obtained.

A' stands for the increase of $\delta\Delta$ when $\ln(C't + 1)$ increases with unity: and, it expresses the slope of the rights $\delta\Delta = f(\ln t)$; B' is the value of $\delta\Delta$ at the initial moment $t = 0$.

With oxide films formed on metals, the thickness and the optical constants [7, 8] can be calculated using the ellipsometric parameters Δ and ψ measured on the oxidated surfaces, following the ellipsometry basic equation:

$$\tan \psi \cdot e^{i\Delta} = f(n_0, \varphi_0, \lambda, \bar{n}_1, \bar{n}_2, d) \quad (4)$$

where: n_0 is the refractive index of the ambient medium;

φ_0 is the incidence angle of radiation;

$\bar{n}_1 = \bar{n}_1 - i\bar{k}_1$ stands for the complex refractive index of the film, defined by means of the film optical constants \bar{n}_1 and \bar{k}_1 ;

$\bar{n}_2 = \bar{n}_2 - i\bar{k}_2$ stands for the complex refractive index defined by means of the metal optical constants \bar{n}_2 and \bar{k}_2 ;

d is the surface film thickness; and

λ is the radiation wavelength.

In the case of non-absorbing surface films ($\bar{k}_1 = 0$) the two parameters, \bar{n}_1 and d , can be obtained by one ellipsometric measurement only (Δ ; ψ), if the optical constants of the film lacking underlayer, \bar{n}_2 and \bar{k}_2 , are known. These are obtained by solving the ellipsometry fundamental equation for surfaces without films;

$$\tan \bar{\psi} e^{i\bar{\Delta}} = f(n_0, \varphi_0, n_2, k_2) \quad (5)$$

based on the ellipsometric parameters $\bar{\Delta}$ and $\bar{\psi}$.

For absorbing surface films ($k_1 \neq 0$) the thickness d and the optical constants \bar{n}_1 and \bar{k}_1 of the film are also obtained by solving the same equation (4) on the basis of minimum two ellipsometric measurements (Δ_1, ψ_1) and (Δ_2, ψ_2) made at two different incidence angles.

Experimental part. The metallic test samples of copper, nickel and steel OLC = 45 were cut from heavy metal lumps at the dimensions of $45 \times 22 \times 5$ (mm), then ground and polished with abrasive paper to the M12 grain-structure. Before measurements, the samples were polished with metallographic paper to the M14 grain-structure, then with metallographic aluminium oxide powder 2 "Presi" Italy. Further, the samples were washed with absolute ethanol.

The ellipsometric measurements were performed immediately after sample washing by an ellipsometer IFTAR—București, in PCSA arrangement using a radiation with the wavelength of $\lambda = 5625 \text{ \AA}$ at the incidence angle of 60° .

Results and discussions. For a complete ellipsometric measurement in all the four areas, which is necessary to correctly determine the ellipsometric parameters Δ and ψ , the needed working time is of about 15 min. The time is too long to follow up the progress of a surface process developing at a high speed. Because of this, for faster surface processes, ellipsometric measurements are made in one area only and the progress in time of the thus determined ellipsometric parameters Δ and ψ should be followed up. Although these ellipsometric parameters are not the right ones, as determinations were carried in one zone only, their progress in time may be successfully used for kinetic studies.

For the study of the chemical corrosion kinetics of copper, nickel and steel, time variation curves of the ellipsometric parameter $\delta\Delta$ have been plotted (Fig. 1) and they follow a logarithmic law given by relation (3). For the oxide films thicknesses of less than 40 \AA , the ellipsometric ψ parameter variation is too small (of 0.1° only) to be used in kinetic measurements.

The constants A' , B' and C' of relation (3) were obtained by processing the experimental curves on a computing programme of curvilinear correlation written in FORTRAN. To calculate these constants, we used the method of

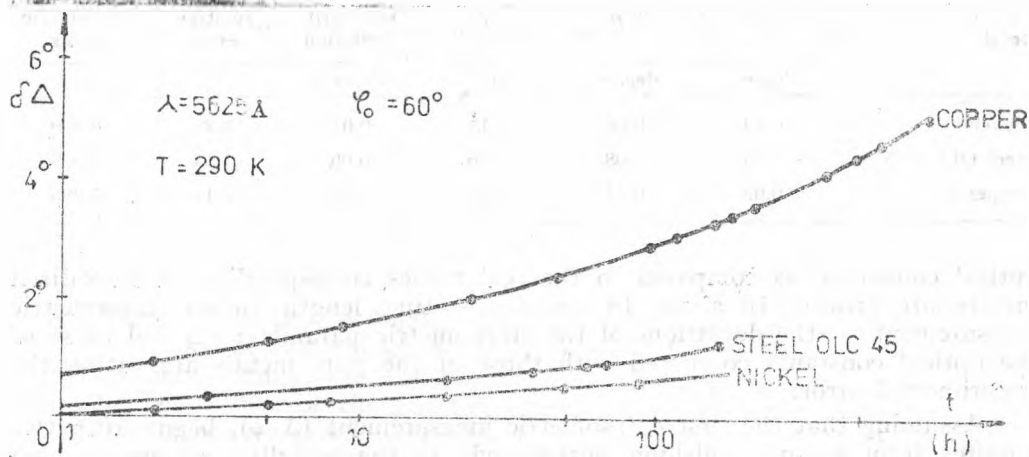


Fig. 1. Time variation of the ellipsometric parameter $\delta\Delta$ for metallic surfaces maintained in the ambient medium at $T = 290 \text{ K}$.

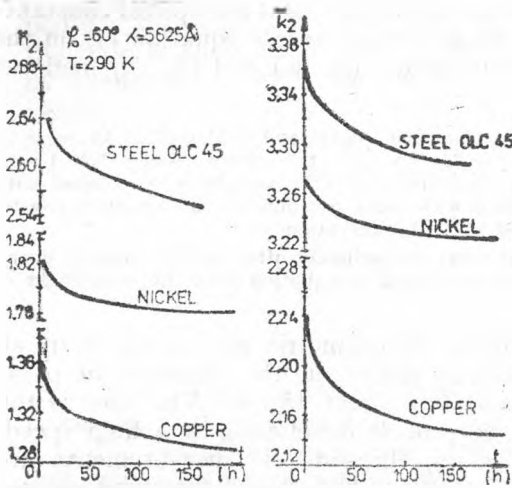


Fig. 2. Time variation of the optical constants of the metal-oxide system for the oxidation of metals in the ambient medium at $T = 290$ K.

Fig. 2. These curves show a decrease of the underlayer optical constants, \bar{n}_2 and \bar{k}_2 , towards constant values. As the metal oxidizes, the deviations of the

equidistant coordinates and the least square method [9]. Calculations have been improved by means of successive approximations. The relative error, the standard error and the correlation index of the experimental values versus the theoretical curve, calculated on the basis of constants A' , B' and C' previously obtained were also estimated. Table 1 gives results obtained by statistical processing of the experimental curves $\delta\Delta = f(t)$.

By computing the optical constants of the metal - oxide system with the aid of the computer routine elaborated by McCrackin [8], on the basis of the ellipsometric parameters Δ and ψ made at some intervals, time variation curves of the optical constants of the oxidizing metals have been obtained and plotted in

Table 1

Constant values from the kinetic law $\delta\Delta = A' \ln(C't + 1) + B'$, for copper, nickel and steel OLC-45 oxidizing in the ambient atmosphere at $T = 290$ K

Metal	A'	B'	C'	standard deviation	relative error	correlation index
	degrees	degrees	h^{-1}	degrees	%	—
Nickel	0.13	-0.06	2.13	0.01	1.38	0.999
Steel OLC-45	0.21	0.08	0.76	0.06	1.14	0.999
Copper	0.63	0.74	0.28	0.06	2.14	0.998

optical constants, as compared to the real values corresponding to unoxidized metals, are greater. In about 15 minutes — time length for an ellipsometric measurement — the deviations of the ellipsometric parameter $\delta\Delta$ and those of the optical constants compared with those of the pure metals are within the experimental error.

Assuming that the first ellipsometric measurement ($\bar{\Delta}, \bar{\psi}$), begun after two minutes from sample polishing, corresponds to the metallic surfaces without films, the thickness and the refractive index of the presumed non-absorbing oxide film ($\bar{k}_1 = 0$) were computed for the values Δ and ψ measured at different

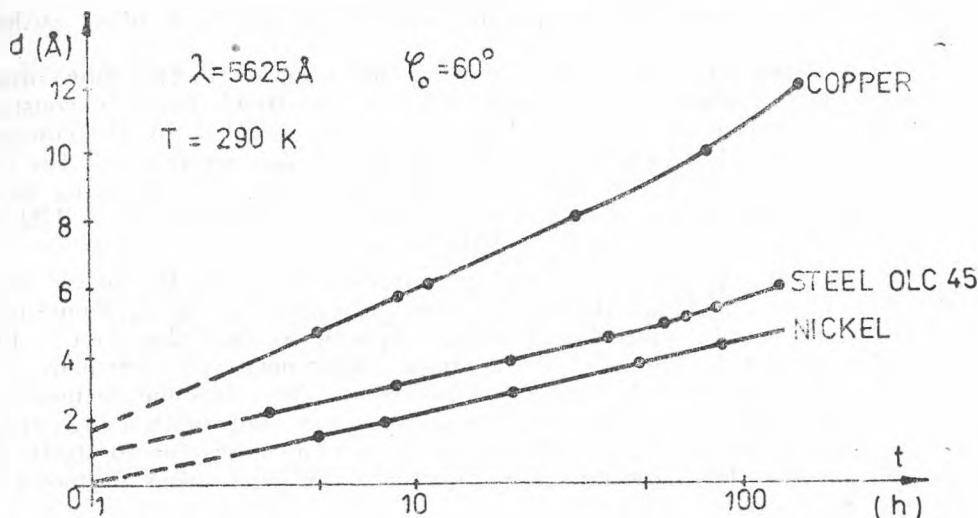


Fig. 3. Time variation of the oxide films thickness formed on metals maintained in the ambient medium at $T = 290\text{ K}$.

intervals. The computations were run on a FELIX C-256, on the basis of the computer routine elaborated by McCrackin in FORTRAN IV language. The variation curves of the film thickness versus time are presented in Fig. 3. These curves also describe a dependence of the film thickness on time, following a law given by relation (1). The constants of this kinetic law obtained from these curves are presented in Table 2.

Table 2

Constants from the kinetic law $d = A \ln(Ct + 1) + B$, for oxide films developed on copper, nickel and steel OLC-45 maintained in the ambient atmosphere at $T = 290\text{ K}$

Metal	A	B	C	Standard deviation	Relative error	Correlation index
	Å	Å	h^{-1}	Å	%	—
Nickel	0.9	-0.65	2.22	0.10	4.54	0.996
Steel OLC-45	1.03	-0.59	3.57	0.11	3.13	0.997
Copper	2.61	2.07	0.25	0.08	1.01	0.999

By means of the proportionality between the variation of the ellipsometric parameter Δ and the film thickness shown in Figs. 1 and 3, we calculated, for the metals under study, the constant α from the approximative relation of Drude (2). The values of the constant α have been obtained from the ratio A'/A of the constants given in Tables 1 and 2 corresponding to the kinetics laws $\delta\Delta = f(t)$ and $d = f(t)$, respectively. Consequently, for the constant α we have obtained the following values: 0.24 degree/Å for copper; 0.19 degree/Å for steel and 0.14 degree/Å for nickel.

The obtained results are comparable with those given by other authors [2, 3].

The calculated refractive indices of the oxide films on metals show rather large time and nonuniform variations, having a trend towards constant values. These nonuniform time variations can be entailed by the complex oxidation processes that take place at the interfaces, having as result the forming of some metal oxides in different oxidation states. The following mean values of the refractive index of the oxide films were obtained: $\bar{n}_1 = 3.32$ for steel, $\bar{n}_1 = 3.25$ for copper and $\bar{n}_1 = 2.78$ for nickel.

In calculating the thickness and the refractive index of the oxide films on metals, we presumed that the surface films were non-absorbent. Sometimes, the oxide films can be optically absorbing ($\bar{k}_1 \neq 0$) so that the three values \bar{n}_1 , \bar{k}_1 and d cannot be obtained by a single ellipsometric measurement, two ellipsometric measurements being at least necessary. Two ellipsometric measurements for each surfaces state are hard to perform, especially with a high speed oxidation reaction of the surface. Therefore, it is more advisable to study the time-variation of the ellipsometric parameter Δ for such films, in order to study the metals oxidation kinetics.

Conclusions. Ellipsometric measurements can be successfully employed in chemical corrosion studies on metal thanks to their uncommon accuracy and sensibility.

In the first 15 min from metallic sample polishing, both the ellipsometric parameter variation Δ and the variation of the constants of the surface as compared to the corresponding values of the non-oxidized metals are so small that they fall within the experimental error. Thus, it can be considered that the first ellipsometric measurement performed in the first 15 min. from the instance of sample polishing corresponds to non-oxidized metal. Thus measured ellipsometric parameters and $\bar{\Delta}$ allow us to calculate the metal optical constants [10].

With the optically absorbing oxide films developed on metals, the oxidation kinetics is better shown by the time variation of the ellipsometric parameter Δ .

REFERENCES

1. I. G. Murgulescu, S. Segal, T. Onicescu, „Introducere in chimia fizică, Cinetică chimică și cataliză”, vol. 2, Ed. Academiei, București, 1981, p. 720.
2. J. Mieluch, *Polish Journal of Chemistry*, **52**, 151 (1978).
3. R. J. Archer, "Manual on Ellipsometry", Gaertner Sci. Corp., Chicago, 1968, p. 26.
4. R. W. Stobie, M. J. Dignam, *Can. J. Chem.*, **56**, 1088 (1978).
5. R. M. A. Azzam, N. M. Bashara, "Ellipsometry and Polarized Light", North-Holland Pbl. Comp., Amsterdam, 1977.
6. D. Moisil, G. Moisil, „Teoria și practica elipsometriei”, Ed. Tehnică, București, 1973, p. 177.
7. F. L. McCrackin, E. Passaglia, R. Stromberg, H. L. Steinberg *J. Res. Nat. Bur. Stand.*, **67A**, 363 (1963).
8. F. L. McCrackin, *Natl. Bur. Std., Tech. Note 479*, U.S. Govn't Printing Office, Washington, 1969.
9. I. Todoran, „Tratarea matematică a datelor experimentale. Funcții empirice”, Ed. Academiei, București, 1976, p. 111.
10. S. Jitian, E. Chifu, *Stud. Univ. Babeș-Bolyai, Chem.*, **31(2)**, 69 (1986).

KOMPLEXVERBINDUNGEN DES DIHYDRALAZINHYDRAZONBENZALDEHYDS MIT METALL(II) SULPHATEN

LETIȚIA GHIZDAVU*, SILVIA BARBU* und GHEORGHE MARCU*

Eingegangen am 1 Dezember 1987

Coordination Compounds of Dihydralazinehydrazone-Benzaldehyde with Metal (II)-Sulphates. A number of coordination compounds of dihydralazinehydrazone benzaldehyde with bivalente transition metal sulphates were obtained in aqueous alcoholic solutions. Some structural and thermal stability problems were discussed on the basis of UV and IR spectra and by derivatographic measurements.

Einleitung. In vorhergehenden Arbeiten [1, 2] wurden neue Koordinationsverbindungen der Übergangsmetalle (I-ste Gruppe) mit Dihydralazinhydrazon (DHF) beschrieben und charakterisiert. Diese Hydrazon-derivate mit Metallen entstehen leicht, sind isolierbar in reinem Zustand und zeigen eine erhebliche biologische Aktivität [3–6]. Diese Erscheinung spricht für die Wichtigkeit der koordinationschemischen Forschung in dieser Richtung.

In dieser Arbeit wurden einige, neue Komplexverbindungen der Übergangsmetalle mit Dihydralazin-hydrazon-benzaldehyd (B–DHF) beschrieben und mit physikalisch-chemischen Methoden charakterisiert.

Experimenteller Teil. Herstellung des Ligandes (B–DHF). Dihydralazin-hydrazon-benzaldehyd (B–DHF) entsteht durch die Kondensation des Dihydralazino-phthalazins mit Benzaldehyd nach der Gleichung:



Eine wässrige Lösung von Dihydralazinophthalazin wird mit einer alkoholischen Lösung von Benzaldehyd (Molarverhältnis: 1: 2) auf dem Wasserbade 15 Minuten lang erwärmt. Nach Kühlung wird die Lösung mit viel Wasser verdünnt. Die ausgeschiedene Masse wird abfiltriert, mit verdünntem Alkohol (1: 1) gewaschen und aus heissem Alkohol umkristallisiert. Gelbe, mikrokristalline Masse, unlöslich im Wasser, löslich in Ethanol und in Aceton.

Analyse: gef. % N 23,19, C 72,21, H 4,95
aus B–DHF (C₂₂H₁₈N₆)

ber. % N 22,93, C 72,05, H 4,91

Darstellung der Komplexverbindungen vom Typ: ML(SO₄)·nH₂O. (M = Fe(II), Co(II), Ni(II), Cu(II), Zn(II), Cd(II), L = C₂₂H₁₈N₆, n = 2, 3, ...) Die Mischung einer methanolischen Lösung

* Universität Cluj-Napoca, Facultät für Chemische Technologie, 3400 Cluj-Napoca, Rumänien

von B-DHF und MSO_4 in verdünntem Alkohol (1:1) wird auf dem Wassebade 30 Minuten lang erwärmt. (Molarverhältnis: 1:1). Nach Abkühlung wird mit Wasser verdünnt und die ausgeschiedene kristalline Masse abfiltriert, mit Wasser gewaschen, aus heissem Alkohol umkristallisiert und bei Zimmertemperatur an der Luft getrocknet.

Die neuen Komplexverbindungen sind in der Tabelle 1 charakterisiert.

Tabelle 1

Neue Komplexverbindungen von Typ $\text{M(B-DHF)SO}_4 \cdot n\text{H}_2\text{O}$

Verbindung	Mol. Gew. ber.	Farbe	Analyse		
			Gef.	%	Ber.
$\text{Fe(B-DHF)SO}_4 \cdot 2\text{H}_2\text{O}$	554,3	dunkel-grün	Fe	9,75	10,07
			N	14,75	15,16
			S	5,08	5,57
$\text{Co(B-DHF)SO}_4 \cdot 3\text{H}_2\text{O}$	575,4	helle-grün	Co	9,68	10,24
			N	14,05	14,60
			S	5,08	5,57
$\text{Ni(B-DHF)SO}_4 \cdot 3\text{H}_2\text{O}$	575,2	dunkel-brown	Ni	9,31	10,20
			N	14,61	14,98
			S	5,85	5,57
$\text{Cu(B-DHF)SO}_4 \cdot 3\text{H}_2\text{O}$	580,1	helle-grün	Cu	11,21	10,95
			N	15,08	14,49
			S	4,62	5,52
$\text{Zn(B-DHF)SO}_4 \cdot 3\text{H}_2\text{O}$	581,8	gelb	Zn	10,58	11,21
			N	15,25	14,84
			S	4,62	5,52
$\text{Cd(B-DHF)SO}_4 \cdot 2\text{H}_2\text{O}$	610,9	gelb	Cd	17,78	18,40
			N	14,51	14,57
			S	4,32	5,24

Die Elektronenspektren der Komplexe wurden in Alkohol mit einem Spektrophotometer SPECORD UV-VISS aufgenommen.

Die UR-Spektren wurden in Kaliumbromid-Presslinge mit einem Spektrophotometer UR-20 (Carl-Zeiss) Jena aufgenommen. Das thermische Verhalten der Komplexe wurde mit einem Derivatograph vom Typ Paulik-Erdey OD-103 untersucht. Temperaturbereich: 293–1073 K, Heizungs geschwindigkeit: 15 K Min^{-1} , Gewicht der Proben: 20 mg.

Ergebnisse und Diskussion. Wie aus der Tabelle 1 ersichtlich, kristallisieren die Komplexverbindungen mit 2–3 mol. H_2O . Der Verhältnis der Komponente: $\text{M} : \text{B-DHF} : \text{SO}_4 = 1 : 1 : 1$. Die in Wasser unlösliche Komplexe sind sehr leicht löslich in basischen Lösungsmitteln. In dem Spektrum des freien Ligands (B-DHF) erscheinen die folgenden Bande: 48.400, 35.600 und 25.100 cm^{-1} . Einige Spektren der untersuchten Verbindungen sind in der Abb. 1. wiedergegeben.

Das bei 48.400 cm^{-1} auftretende, für das freie Ligand charakteristische Band verschiebt sich bei Komplexbildung (hypsochromische Verschiebung) und seine Intensität vermindert sich. Diese Erscheinung kann durch die Bildung der Koordinationsbindung mit dem Metall-ion erklärt werden.

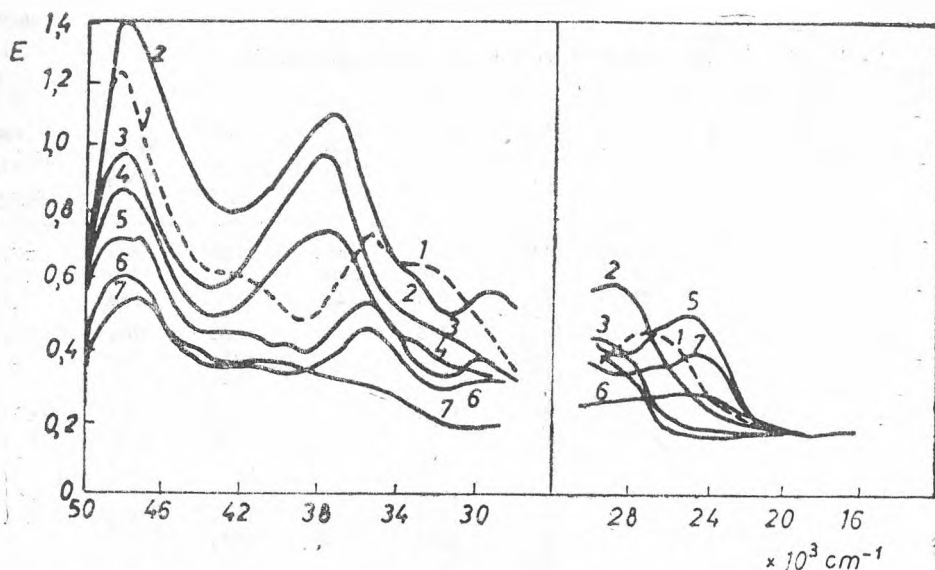


Abb. 2. Elektronische Spektren der Verbindungen: 1. B-DHF; 2. Co(B-DHF)SO₄ · 3H₂O; 3. Fe(B-DHF)SO₄ · 3H₂O; 4. Ni(B-DHF)SO₄ · 3H₂O; 5. Zn(B-DHF)SO₄ · 3H₂O; 6. Cd(B-DHF)SO₄ · 2H₂O; 7. Cu(B-DHF) · SO₄ · 3H₂O.

Das Band bei 35.600 cm⁻¹ zeigt eine hypsochromische Verschiebung mit annähernd 2.000 cm⁻¹ bei Komplexbildung. Im Bereiche 35.000–25.200 cm⁻¹ ist eine Überlagerung der $n \rightarrow \pi^*$ Bands, mit der Bande des freien Ligands erkennbar (um annähernd 29.800 cm⁻¹). Im Falle der Co(II)– und Ni(II)– Derivate tritt auch ein anderes Band um 33.000 cm⁻¹ auf, welches für die Verbindungen der Übergangsmetallionen mit ungefüllten d- Elektronenschalen charakteristisch ist [7, 8].

Die Ladungsüberführungsbande erscheinen im Bereiche 24.600–29.200 cm⁻¹.

Die UR-Spektren der Komplexverbindungen zeigen erhebliche Abweichungen im Wellenzahlbereichen von 1500–1700 cm⁻¹, bzw. 700–800 cm⁻¹, im Vergleich mit demjenigen des freien, nichtkoordinierten Ligands. Diese Erscheinung spricht für das Vorhandensein von starken kovalenten Metal-Ligand-Bindungen durch die Azomethin-Gruppe.

Das, im Spektrum des freien Ligands auftretende Band bei 1120 cm⁻¹ zerspaltet sich in mehreren Banden, in Spektren der Koordinationsverbindungen. Diese Zerspaltung ist ein direkter Beweis für die Koordination des Sulphat-anions und für M–O–S–O -Bindungen. Die Koordination der SO₄-Gruppe führt zur Bildung eines asymmetrischen Krystallfelds, bzw. zur Änderung der Symmetrie von T_d zu C_{3v}, C_{2v}, und zwar zu niedrigeren Symmetriegruppen.

Das thermische Verhalten der Komplexverbindungen vom Typ: ML(SO₄) · n H₂O ist in Abb. 2 und in der Tabelle 3 wiedergegeben.

Tabelle 2

IR — Spektral Data der Verbindungen (cm^{-1})

Verbindung	ν_{NH}	δ_{NN}	W_{NH}	δ_{NH}	δ_{CH}	$\nu_{\text{C}=\text{N}}$	W_{CH}
	ν_{CH}	$\nu_{\text{C}=\text{N}}$	$\nu_{\text{C}-\text{C}}$	$\nu_{\text{C}-\text{N}}$	ν_{CH}		W_{NH}
					$\nu_{\text{SO}_4^{2-}}$		$\delta_{\text{SO}_4^{2-}}$
B—DHF	3360	1640	1570	1360	1120	890	660
	3215		1480	1290		780	610
	3065		1400	1230	970	750	
$\text{Fe(B—DHF)SO}_4 \cdot 2\text{H}_2\text{O}$	3070	1640	1395		1120	760	690
		1580			1055	700	
		1570			1035		
$\text{Co(B—DHF)SO}_4 \cdot 3\text{H}_2\text{O}$	3070	1640	1395		1125	765	695
		1585			1060	760	
						700	
$\text{Ni(B—DHF)SO}_4 \cdot 3\text{H}_2\text{O}$	3070	1640					
	2380	1620	1480	1260	1120	765	695
		1590	1395	1205	1060	700	
		1570					
$\text{Cu(B—DHF)SO}_4 \cdot 3\text{H}_2\text{O}$	3070	1540	1410		1120	760	690
	2390				1060	700	
$\text{Zn(B—DHF)SO}_4 \cdot 3\text{H}_2\text{O}$	3080	1710	1400	1395	1290	880	620
	2375	1640	1450	1360	1205	770	
					1120	700	
					970		
$\text{Cd(B—DHF)SO}_4 \cdot 2\text{H}_2\text{O}$	3280	1640	1395	1295	1120	790	655
	3180	1590	1360	1260	1065	770	590
	3070	1565		1205	970	700	

Tabelle 3

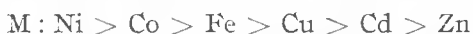
Dehydrations und thermische Zersetzungsprozesse der B—DHF—Derivate

Verbindung	Dehydrations-reaction		Zersetzungs-reaction		Rück-stand	
	T_{max}	Verlust	T_{max}	Verlust	Form	%
	K	%	K	%		
$\text{Fe(B—DHF)SO}_4 \cdot 2\text{H}_2\text{O}$	348	5,31	557;688;795	85,87	Fe	8,91
$\text{Co(B—DHF)SO}_4 \cdot 3\text{H}_2\text{O}$	340	10,58	561;669;819	76,40	CoO	13,02
$\text{Ni(B—DHF)SO}_4 \cdot 3\text{H}_2\text{O}$	341	9,27	563;676;793	81,83	Ni	8,90
$\text{Cu(B—DHF)SO}_4 \cdot 3\text{H}_2\text{O}$	366	9,31	543;663;790	79,78	Cu	10,91
$\text{Zn(B—DHF)SO}_4 \cdot 3\text{H}_2\text{O}$	380	10,86	518;643;803	77,83	Zn	11,31
$\text{Cd(B—DHF)SO}_4 \cdot 2\text{H}_2\text{O}$	363	6,25	521;648;799	72,73	CdO	21,02

Die untersuchten Substanzen sind Krystallohydrate. Der Krystalwasser-gehalt wird zwischen 340–362 K verlieren. Die entwässerten Komplexe sind bis 518–563 K beständig, wie durch die horizontalen Teilen der DTG-Kurven in diesem Temperaturbereiche angezeigt ist. (Abb. 2.1.). Über dieser Temperatur findet die Zersetzung der Substanz nach dem in unserer vorhergehenden Arbeit beschriebenen Schema statt. [2].

Die kinetische Erläuterung der Derivatogramme in Beziehung mit den elektronischen und UR-Spektren führte zur Bestimmung der Struktur der untersuchten Komplexverbindungen. Die kinetischen Parameter: die Aktivierungsenergie (E), die wahrscheinliche Reaktionsordnung (n), für die Dehydratation, bzw. für die erste Etappe der Zersetzung (Die Abspaltung der Hydrazon-Gruppe: $-N_4H_2$ mit dem Zerfall der $M-N$ -Bindung) wurden mit Hilfe der Freeman-Carroll'sche Methode berechnet [12]. (Tabelle 4).

Die scheinbaren Aktivierungsenergie-werten für die Dehydratation der Komplexe liegen zwischen 29,41 und 37,88 $\text{kJ} \cdot \text{Mol}^{-1}$ und die Reaktionsordnung: $n = 0,5-1$ entsprechend der niedrigen Temperaturbereiche dieses Prozesses: 340–362 K. Die erhaltenen Werte bestätigen die schwache Bindung der Wassermoleküle im Gitter der Komplexverbindungen. Die kinetischen Daten für die erste Etappe der Zersetzung des freien Ligands (B-DHF) und der Komplexverbindungen in der Tabelle 1 zeigen dass die Scheinbare Aktivierungsenergie, mit Ausnahme der Zn(II) - und Cd(II) -Derivate, annähernd gleiche Werte haben. (Abspaltung der Hydrazongruppen). Man kann annehmen, dass die Abspaltung der $M-N$ -Koordinationsbindung nur einen unerheblichen Einfluss auf die Zersetzungsenergie des freien Ligands ausüben kann. Die derivatographischen Untersuchungen zeigen dass die thermische Beständigkeit der Komplexverbindungen in der folgenden Richtung abnimmt.



(siehe Tabelle 3).

Die bestimmten niedrigen Aktivierungsenergie-werten stehen in Übereinstimmung mit den Literaturangaben [13, 14] für die Abspaltung der Hydrazon-

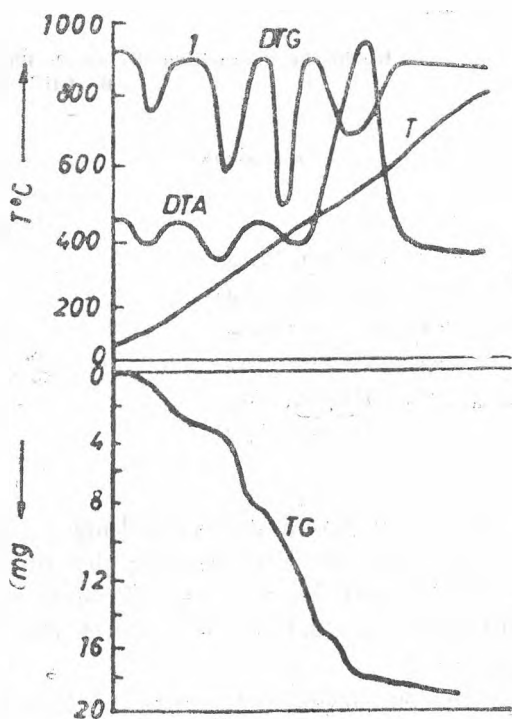


Abb. 1. Derivatogramm von $\text{Co(B-DHF)SO}_4 \cdot 3\text{H}_2\text{O}$.

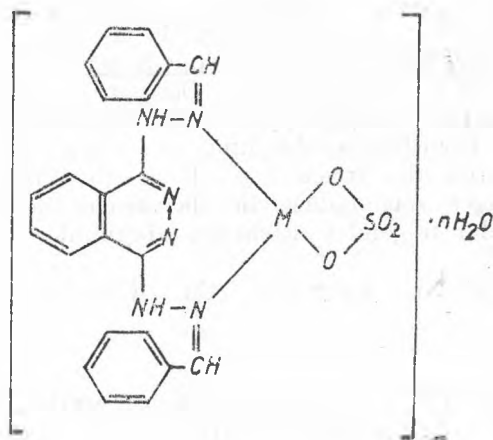
Kinetische Parametern der ersten Phase der thermischen Zersetzung der
B-DHF-Derivate

Verbindung	T_{\max} K	E $\text{kJ} \cdot \text{mol}^{-1}$	n
B-DHF	573	128,35	1,15
$\text{Fe}(\text{B-DHF})\text{SO}_4 \cdot 2\text{H}_2\text{O}$	557	110,13	1,58
$\text{Co}(\text{B-DHF})\text{SO}_4 \cdot 3\text{H}_2\text{O}$	561	118,92	1,94
$\text{Ni}(\text{B-DHF})\text{SO}_4 \cdot 3\text{H}_2\text{O}$	563	120,07	2,01
$\text{Cu}(\text{B-DHF})\text{SO}_4 \cdot 3\text{H}_2\text{O}$	543	107,22	1,35
$\text{Zn}(\text{B-DHF})\text{SO}_4 \cdot 3\text{H}_2\text{O}$	518	98,56	1,20
$\text{Cd}(\text{B-DHF})\text{SO}_4 \cdot 2\text{H}_2\text{O}$	521	96,71	1,27

gruppen aus Azomethin-Verbindungen. Die kleine Reaktionsordnungen (0,5–1) sprechen für die Überlagerung der obenerwähnten Zersetzungsreaktionen mit dem Transport der flüchtigen Produkte (Stickstoff und Ammoniak bei Disproportionierung des Hydrazins) durch dem Kristallgitter und mit ihrem Verdampfung.

In den folgenden Etappen der Zersetzung bei höherer Temperaturen findet auch die Abspaltung der M–O-Bindungen, wie aus den IR-Spektraldaten hervorgeht. Diese Erscheinung bestätigt das Teilnehmen der SO_4 -Gruppe in der Struktur der Komplexverbindungen.

Auf Grund der obenerwähnten experimentellen Daten kann man für die Komplexverbindungen die folgende Molekularstruktur annehmen:



L I T E R A T U R

1. Gh. Marcu, L. Ghizdavu, S. Barbu, *Congresul național de chimie, București, 11-14 sept. 1978*, p. 861.
2. L. Ghizdavu, S. Barbu, Gh. Marcu, *Stud. Univ. Babeș-Bolyai, Chem.* **30**, 73 (1985).
3. J. Druey, B. H. Ringier, *Helv. Chim. Acta*, **34**, 195 (1951).
4. B. Wesley — Hadzija, F. Adophy, *Croat. Chem. Acta*, **30**, 15 (1958).
5. P. Dehme, E. Goeres, C. Schwarz, G. Petsch, *Acta Biol. Med. Ger.*, **16**, 5, 546 (1966).
6. F. I. Khattab, *J. Thermal Anal.*, **21**, 2, 211 (1981).
7. A. B. Lever, "Inorganic Electronic Spectroscopy", Elsevier Publishing Company, Amsterdam — London — New-York, 1968.
8. I. Grecu, E. Curea, *Rev. Roumaine Chim.*, **6**, 781 (1968).
9. K. Nakamoto, "Infrared Spectra of Inorganic and Coordination Compounds", John Willey Company, 1962.
10. Mac Winnkie, *J. Inorg. Nucl. Chem.*, **26**, 21 (1964).
11. I. Haritonov, E. I. Deiciman, *Zhur. neorg. Khim.*, **10**, 853 (1965).
12. E. S. Freeman, B. Carroll, *J. Phys. Chem.*, **62**, 394 (1958).
13. P. B. Dervan, *J. Amer. Chem. Soc.*, **98**, 5, 1262 (1976).
14. B. V. Ioffe, M. A. Kuznetov, A. A. Potehin, "Himia organiceskih proizvodnih gidrazina", Izdatelstvo Himia, Leningrad, 1978, p. 78.

ÜBER DIOXIMINKOMPLEXE DER ÜBERGANGSMETALLE

LXXIII. Mitt. Polarographische Untersuchung über die Bildung und die Hydrolyse von 1,2-Cycloheptandion-monoxim und 1,2-Cycloheptandiondioxim

FERENC MÁYOK*, ENIKŐ KÖSZEGI*, CSABA VÁRHELYI* und ANDRÁS BENKŐ*

Eingegangen am 2. Dezember 1987

On the Dioximine Complexes of Transition Metals, Part LXXIII. Polarographic study on the formation and hydrolysis of 1,2-cycloheptanedione monoxime and 1,2-cycloheptanedione dioxime. In acidic medium an equilibrium between 1,2-cycloheptanedione dioxime and its hydrolysis products: 1,2-cycloheptanedione monoxime and 1,2-cycloheptanedione takes place. The apparent formation constants of the corresponding monoxime and dioxime from the 1,2-dione have been determined polarographically. These formation constants are influenced by the acidity of the solution. The acidity constants of both oximes have been also calculated.

Einleitung. Die α -Dioxime (Diox.H_2) stellen in wässrigen Lösungen sehr schwache, zweibasische Säuren dar.



Die Dissoziationskonstanten einer Reihe von aliphatischen, aromatischen und alicyclischen Dioximen wurden potentiometrisch und UV-spektrophotometrisch bestimmt [1–3]. Die erste Aciditätskonstante der α -Dioxime nimmt in folgender Reihe zu:



Die UV-spektroskopischen Messungen zeigen, daß in sauren Lösungen außer der Protonabspaltung auch andere chemische Vorgänge stattfinden. [4]. Bei einem Vergleich der UV-Spektren des 1,2-Cyclohexandiondioxims in neutralem Medium und in Anwesenheit von Mineralsäuren, gelangen Alibina und Mitarbeiter [5] zu der Schlußfolgerung, daß in sauren Lösungen eine teilweise Hydrolyse des Oxims, unter Rückbildung des entsprechenden Ketons stattfindet diese Beobachtungen besitzen zur einen qualitativen Charakter und wurden nicht quantitativ studiert.

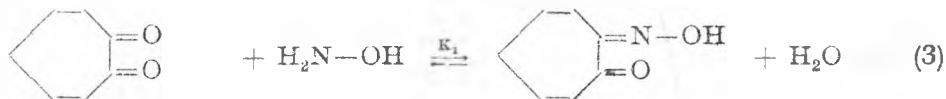
In einer früheren Arbeit [6] haben wir gezeigt, daß die polarographische Methode für die Untersuchung der Desoximierungsprozesse sehr geeignet ist.

* *Universităt Cluj-Napoca, Facultăt für Chemische Technologie, 3400 Cluj-Napoca, Rumänien*

In Fortsetzung dieser Arbeit haben wir die Bildungs- und Hydrolysereaktionen des 1,2-Cycloheptandiondioxims und 1,2-Cycloheptandionmonoxims mit Hilfe der obenerwähnten elektrochemischen Methode studiert.

Resultate und Diskussion. Die Bildung von 1,2-Cycloheptandiondioxim aus 1,2-Cycloheptandion und Hydroxylamin ist eine umkehrbare Reaktion.

Das 1,2-Cycloheptandionmonoxim tritt bei diesem Oximierungsprozess als Zwischenprodukt auf:



In einer Stammlösung von $\text{NaClO}_4 + \text{HClO}_4$ ($\text{HClO}_4 = 0,02-0,2$ Mol; Ionenstärke: 0,2 Mol) zeigt das Polarogramm von 1,2-Cycloheptandiondioxim (Heptoxim, Heptox.H₂) nur eine polarographische Stufe mit einem Halbstufenpotentialwert von $E_{1/2} = -740$ mV (gegen gesätt. Kalomelektrode). Die Form der Kurve spricht für einen komplizierten, nicht einheitlichen Prozess (Abb. 1.) Die experimentellen Daten zeigen jedoch, dass die Höhe dieser Welle der Konzentration des Heptoxims direkt proportional ist. Beim Stehenlassen tritt eine zweite Welle mit einem positiveren Halbstufenpotentialwert von $E_{1/2} = -390 - -410$ mV (gegen gesätt. Kalomelektrode) auf (Abb. 2.)

Die Höhe der letzten Welle nimmt mit der Zeit zu, und jene der vorhergehenden Stufe nimmt ab. Nach 4-5 tägigem Stehenlassen stellt sich ein Gleichgewicht ein. Die Welle „a“ entspricht wahrscheinlich der elektrochemischen Reduktion von 1,2-Cycloheptandionmonoxim, welches bei der Hydrolyse von Heptoxim entsteht.

Aus Mangel an reinem 1,2-Cycloheptandionmonoxim konnten wir keine direkte Beziehung zwischen der Höhe der polarographischen Stufe „a“ und der Konzentration des Monoxims erhalten.

Deshalb haben wir ein analoges System: Methyl-isopropyl-2,3-dion-monoxim und Methyl-isopropylglyoxim unter identischen experimentellen Bedingungen ($\text{HClO}_4 = 0,04-0,2$ M + NaClO_4 , Ionenstärke: 0,2 M) untersucht. Für die Halbstufenpotentiale wurden folgende Werte erhalten: $E_{1/2}^I = -400$ mV und $E_{1/2}^{II} = -750$ mV (gegen gesätt. Kalomelektrode).

Bei den letztgenannten Oximen verlaufen die Hydrolysevorgänge viel langsamer als im Falle des Cycloheptandionmonoxim.-Dioxim Systems und deshalb können die Stufenhöhe-Konzentration-Zusammenhänge in den frisch bereiteten sauren Lösungen bequem bestimmt werden. Die so bestimmte Verhältnisse zwischen der Höhe der ersten und zweiten Stufe wurden zur Berechnung der Konzentration von 1,2-Cycloheptandionmonoxim im Laufe des Hydrolysevorganges verwendet. Man kann annehmen, dass in beiden Systemen analoge Elektrodenprozesse verlaufen und nur die Diffusionskonstanten der Partikel einige

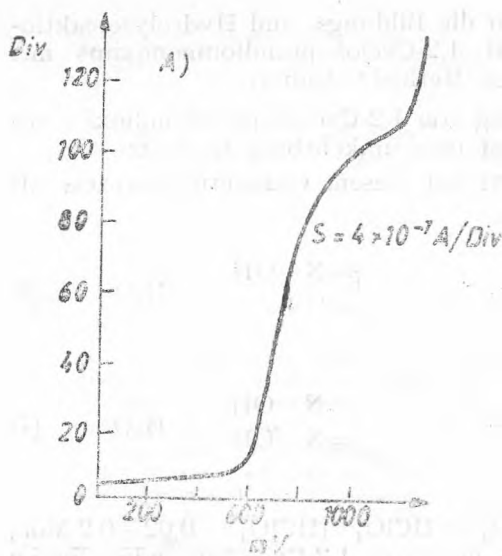


Abb. 1. Polarogramm des 1,2-Cycloheptandiondioxims $\text{HClO}_4 = 0,1 \text{ M l}^{-1}$; Ionenstärke: $0,2 \text{ M}$.

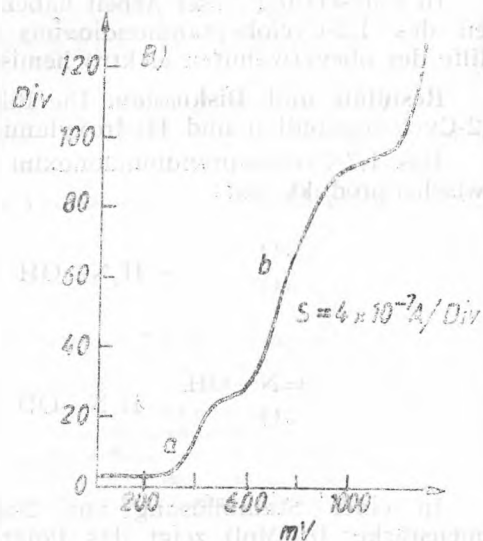


Abb. 2. Typisches Polarogramm für das 1,2-Cycloheptandion-monoxim – und ...-dioxim – System $\text{HClO}_4 = 0,1 \text{ M l}^{-1}$, Ionenstärke: $0,2 \text{ M}$, nach 60 Min. Stehenlassen.

Abweichungen zeigen können. Die Stufenhöhen sind proportionell der Konzentration der entsprechenden Oxime. Die Welle des Dioxims ist höher als diejenige des Monoxims.

Aus den polarographischen Messungen geht hervor, daß 1,2-Cycloheptandionmonoxim kein Endprodukt der Hydrolyse ist. Die Reaktion geht weiter zur Bildung des 1,2-Cycloheptandions. Die letzte Substanz wird an der Quecksilbertropfelektrode bis der Reduktion der Stammlösung nicht reduziert und kann deshalb nicht auf polarographischem Wege bestimmt werden.

Die Höhe der Stufe „a“ nimmt in Gegenwart von einem Überschuß von Hydroxylaminchlorhydrat ab und diejenige der Stufe „b“ wächst gleichzeitig. Unter solchen experimentellen Bedingungen (10–20-fache $\text{NH}_2\text{-OH}\cdot\text{HCl}$ -Menge gegen das Heptoxim) verläuft die entgegengesetzte Reaktion der Hydrolyse, d.h. die Rückbildung der Oxime.

Das Gleichgewicht in 1,2-Cycloheptandiondioxim-Lösung wurde bei verschiedenen Perchlorsäurekonzentrationen ($\text{HClO}_4: 0,04\text{--}0,2 \text{ M l}^{-1}$) untersucht. Die Messergebnisse sind in der Tabelle 1 wiedergegeben.

Auf Grund der Daten der Tabelle 1 wurden die globalen Gleichgewichtskonstanten der Bildungsreaktionen der Oxime aus 1,2-Cycloheptandion, bzw. aus 1,2-Cycloheptandionmonoxim berechnet. Für diese Gleichgewichtsreaktionen sind die folgenden Gleichungen gültig:

$$K_1 = \frac{[A^{\circ}]}{[B^{\circ}][D^{\circ}]} \quad (5); \quad K_2 = \frac{[B^{\circ}]}{[C][D^{\circ}]} \quad (6)$$

(siehe Tabelle 2)

Tabelle 1

Gleichgewichtskonzentrationen des Heptoxims und seiner Hydrolysenprodukte in sauren Lösungen

$[\text{HClO}_4]$ $M \cdot 1^{-1}$	Div <i>A</i>	$[A^\circ]$ $10^3 \cdot M \cdot 1^{-1}$	Div <i>B</i>	$[B^\circ]$ $10^3 \cdot M \cdot 1^{-1}$	$[C]$ $10^3 \cdot M \cdot 1^{-1}$	$[D^\circ]$ $10^3 \cdot M \cdot 1^{-1}$
0,04	40,1	0,80	28,4	0,96	0,24	1,44
0,06	31,8	0,63	31,9	1,08	0,29	1,66
0,08	26,2	0,52	34,1	1,15	0,33	1,81
0,10	22,8	0,45	35,4	1,20	0,35	1,90
0,12	19,8	0,40	36,4	1,23	0,37	1,97
0,16	15,0	0,30	38,6	1,30	0,40	2,10
0,20	12,5	0,25	39,7	1,34	0,41	2,16

 $[A^\circ] + [B^\circ] + [C] = 2 \cdot 10^{-3} M \cdot 1^{-1}$; $[D^\circ] = [B^\circ] + 2[C]$ $[A^\circ]$, $[B^\circ]$, $[C]$ und $[D^\circ]$ - Gesamtkonzentration des 1,2-Cycloheptandiondioxims, 1,2-Cycloheptandionmonoxims, 1,2-Cycloheptandions, bzw. des Hydroxylamins.

Tabelle 2

Globale Gleichgewichtskonstanten K_1 und K_2 in sauren Heptoxim-Lösungen

$[\text{HClO}_4]$ $M \cdot 1^{-1}$	$1/[\text{HClO}_4]$ $M^{-1} \cdot 1$	$10^{-3} \cdot K_1$	$10^{-3} \cdot K_2$
0,04	25	0,578	2,77
0,06	16,66	0,356	2,24
0,08	12,5	0,252	1,97
0,10	10	0,201	1,80
0,12	8,33	0,162	1,70
0,16	6,25	0,109	1,56
0,20	5,00	0,086	1,51

Natürlich sind die globalen Konstanten keine thermodynamische Konstanten, sondern nur scheinbare Gleichgewichtskonstanten, welche das untersuchte System bei einer bestimmten Acidität und Ionenstärke charakterisieren.

Die Änderung der globalen Gleichgewichtskonstanten mit der Acidität kann durch das Vorhandensein von verschiedenen neutralen und protonierten Formen der Oxime in den sauren Lösungen erklärt werden. Es wurden nur die monoprotonierten Formen der Oxime in Betracht gezogen. Nach unseren Berechnungen fehlen praktisch die protonierten 1,2-Cycloheptandionmoleküle unter den oben genannten experimentellen Bedingungen.

Die Protonierungsreaktionen können durch die Aciditätskonstanten der entsprechenden Oxime und des Hydroxylamins charakterisiert werden.

$$K_a = \frac{[A][H^+]}{[AH]} \quad (7); \quad K_a = \frac{[B][H^+]}{[BH]} \quad (8)$$

$$K_a'' = \frac{[D][H^+]}{[DH]} \quad (9)$$

Unter Berücksichtigung der folgenden Gleichungen:

$$[A_0] = [A] + [AH] \quad (10); \quad [B_0] = [B] + [BH] \quad (11);$$

$$[D_0] = [D] + [DH] \quad (12)$$

und Kombination der Gleichungen (5), (6), (7), (8) und (9), erhält man:

$$K_1 = \frac{[A] \frac{K_a + [H^+]}{K_a}}{[B] \frac{K'_a + [H^+]}{K'_a} [D] \frac{K''_a + [H^+]}{K''_a}} \quad (13)$$

und

$$K_2 = \frac{[B] \frac{K'_a + [H^+]}{K'_a}}{[C][D] \frac{K''_a + [H^+]}{K''_a}} \quad (14)$$

Nach Literaturangaben ist $K''_a \approx 10^{-6}$ und kann deshalb neben $[H^+]$ vernachlässigt werden.

Folglich gilt:

$$K_1 = K_{01} \frac{K + [H^+]}{(K'_a + [H^+]) \cdot [H^+]} \quad (15)$$

$$K_2 = K_{02} \frac{K'_a + [H^+]}{[H^+]} \quad (16)$$

wo

$$K_{01} = \frac{[A]}{[B][D]} \cdot \frac{K'_a \cdot K''_a}{K_a} \quad (17)$$

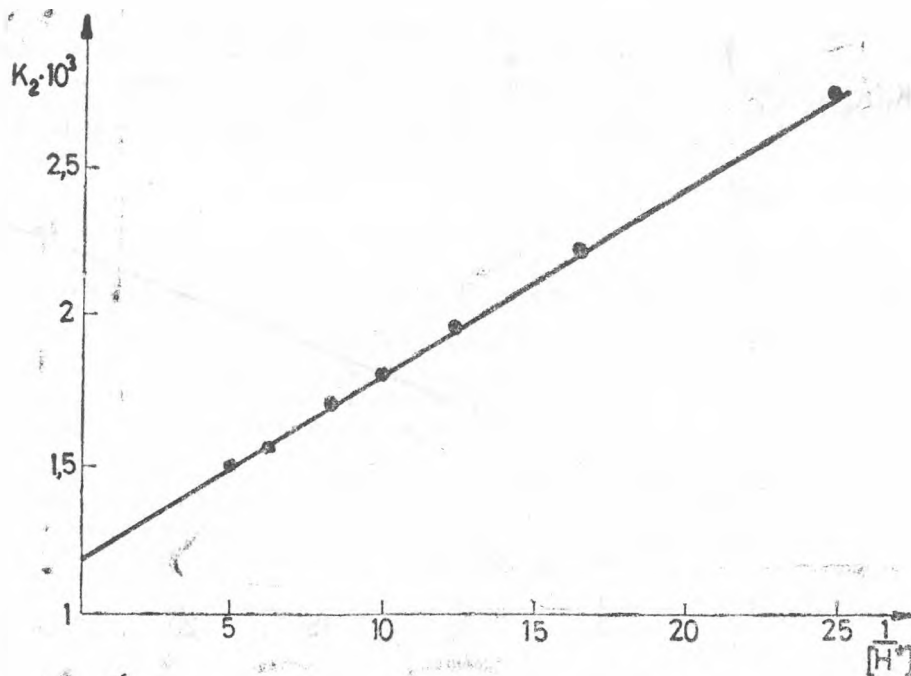
$$K_{02} = \frac{[B]}{[C][D]} \cdot \frac{K''_a}{K'} \quad (18)$$

Die Gleichgewichtskonstanten K_{01} und K_{02} sind unabhängig von der Acidität der Lösung.

Die graphische Darstellung von K_2 als Funktion der $1/[H^+]$ -Werte gibt eine Gerade. Diese Erscheinung unterstützt unsere Annahme über die Abhängigkeit der K_2 -Werte von der Acidität der Lösung.

Mit Hilfe des Anstiegs der Geraden und ihres Schnittpunktes mit der Ordinatenachse können die K_{02} und K'_a -Werte berechnet werden.

$$K'_a = 0,057; \quad K_{02} = 1,15 \cdot 10^3$$

Abb. 3. Abhängigkeit der K_2 -Werte von der Acidität

Die $K_1(K'_a + [H^+])$ - Werte bei verschiedenen $[H^+]$ sind in der Tabelle 3 zusammengestellt.

Die graphische Darstellung von $K_1(K'_a + [H^+])$ als Funktion von $1/[H^+]$ ist in Abb. 4. wiedergegeben.

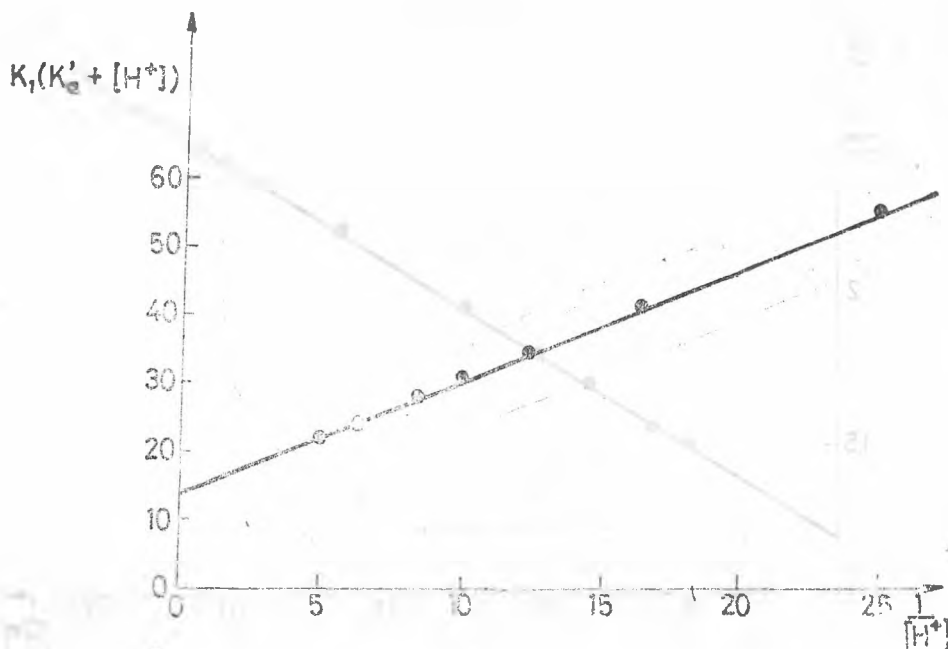
Es existiert ein direkter Zusammenhang zwischen den obigen Werten:

$$K_1(K'_a + [H^+]) = \frac{K_{01} \cdot K_a}{[H^+]} + K_{01} \quad (19)$$

Tabelle 3

$K_1(K'_a + H^+)$ bei verschiedenen Aciditäten

$1/\text{HClO}_4$ $M^{-1} \cdot l$	$K_1(K'_a + H^+)$
25,00	56,0
16,66	41,6
12,50	34,5
10,00	31,5
8,33	28,7
6,25	23,6
5,00	22,1



Ab b. 4. Graphische Darstellung von $K_1(K_a + [H^+])$ als Funktion der $1/[H^+]$ -Werte.

Mit Hilfe des Anstiegs dieser Geraden und ihres Schnittpunktes mit der Ordinatenachse wurden die K_{01} und K_a - Werte berechnet.

$$K_{01} = 14; K_a = 0,12$$

Diese Ergebnisse bestätigen die Annahme, daß die Protonisierung des 1,2-Cycloheptanons unter den oben genannten experimentellen Bedingungen vernachlässigbar ist. Die Konzentration der intermediär auftretender Additionsprodukte:



ist sehr klein und übt praktisch keinen Einfluss auf die Einstellung der Gleichgewichte aus.

Beschreibung der Versuche. *Darstellung von 1,2-Cycloheptandiondioxim.* Die Ausgangssubstanz, das Cycloheptanon wurde durch Ringerweiterung des Cyclohexanons mit Diazomethan, in Anwesenheit von wasserfreiem BF_3 , als Katalysator, in etherischer Lösung erhalten. Cycloheptanon wurde destilliert ($S \cdot p_{23}$: 55–60°C, n_D : 1,4600) und mit SeO_2 in siedendem wasserfreiem Äthanol zum 1,2-Cycloheptandion ($S \cdot p_{13}$: 100–110°C, n_D : 1,468) oxydiert [7–8].
Ausbeute: 70–75%.

Die Oximierung des 1,2-Dions erfolgt mit einem Überschuß von Hydroxylaminchlorhydrat und Kaliumhydroxid (Mol. verhältnis 1:1) in wässriger Lösung. (Ausbeute: 30–35%).

Die polarographischen Messungen wurden mit einem Polarograph Radelkis OH-102 (MOM – Budapest) mit Hilfe eines Adaptors Tast-Rapid OH 991 – durchgeführt. Die polarographische Zelle bestand aus einer Quecksilbertropfenelektrode und einer gesättigten Kalomelektrode. Tropfzeit: 0,3 Sek.

L I T E R A T U R

1. V. M. Peshkova, V. M. Savostina, E. K. Ivanova: Oksini", Izl. ut. Nauka, Moskva, 1977, S. 37–43
2. N. A. Plechanov, V. M. Peshkova, *Vestnik Moskov. Gos. Univ., Khimia*, **4**, 492 (1974).
3. C. V. Banks, A. B. Carlson, *Anal. Chim. Acta*, **7**, 291 (1952).
4. P. R. Ellefsen, L. Gordon, *Talanta*, **14**, 409 (1967).
5. A. N. Alibina, V. M. Peshkova, *Vestnik Moskov. Gos. Univ. Ser. II. Khimia*, **1**, 337 (1970).
6. F. Mánok, Cs. Várhelyi, A. Benkő, M. Tarsoly-Magyari, *Monatsh. Chem.*, **109**, 1329 (1978).
7. C. V. Banks, W. V. Haar, R. C. Voter, *J. Org. Chem.*, **14**, 836 (1949).
8. E. Müller, M. Bauer, *Liebigs Ann. Chem.*, **654**, 105 (1962).

MOLECULAR COMPLEXES OF N-METHYLMORPHOLINE

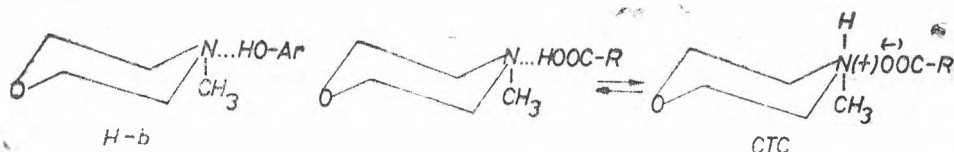
MARIA VAGAONESCU*, LETIȚIA GHIZDAVU*, SORIN MAGER*, LAURA STOICESCU** and IRINA CHIȘ*

Received: December 14, 1987

Molecular complexes of N-methylmorpholine with some acid compounds have been studied. The structure of complexes as well as their thermal behaviour has been determined by chemical, IR spectral and thermal analysis.

In a previous paper the synthesis of N-methylmorpholine and of N-cetyl-N-methylmorpholinium chloride has been studied [1]. According to the practical importance of N-methylmorpholine [2, 3] as well as of the complexes of amines, the present paper has as object molecular complexes of N-methylmorpholine. It is well known that molecular complexes of amines are important due to the fact that their preparation occurs easily and their splitting in to components may be practically quantitative [4].

In the present paper molecular complexes of N-methylmorpholine with some acid compounds as phenols and carboxylic acids, have been studied. N-methylmorpholine with phenols forms complexes through hydrogen bonds (H.b.) while with carboxylic acids it forms charge transfer complexes (C.T.C.) through proton transfer [5-8].



The preparation of these complexes occurs under mild reaction conditions, by mixing the respective components in ethanol under refluxing, for 30 minutes on the water bath. The obtained molecular complexes are solid substances, having different colours, deeper than the components, and clear melting points. (Table 1). Depending on the acid partner the molar ratios of components are 1:1 or 2:1. The structure of the prepared complexes, as well as the molar ratios between their components, has been proved by elemental microanalysis and by acid component determination, after splitting the complex. (Table 1, 2).

* University of Cluj-Napoca, Faculty of Chemical Technology, Department of Physical, Organic and Technologic Chemistry, 3400 Cluj-Napoca, Romania

** Polytechnic Institut, 3400 Cluj-Napoca, Romania

Table 1

Analytical data for complexes of *N*-methylmorpholine


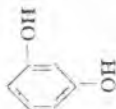

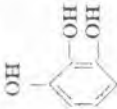

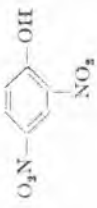
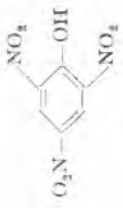

Nr.	Acid component of complex	Molecular formula	N% calc. found	<i>m.p.</i> °C	IR spectral bands, cm^{-1} ν_{OH} ν_{NH^+} ν_{COO^-} slim.	Molar ratio as.	Complex type
1	2	3	4	5	6	7	8
1		$\text{C}_{11}\text{H}_{17}\text{O}_3\text{N}$	6.63 6.54	71.5	3320-3570	1:1	H.b.
2		$\text{C}_{11}\text{H}_{17}\text{O}_3\text{N}$	6.63 6.24	79-80	3160-3260	1:1	H.b.
3		$\text{C}_{11}\text{H}_{17}\text{O}_3\text{N}$	6.63 6.28	154	3080-3280	1:1	H.b.
4		$\text{C}_{11}\text{H}_{17}\text{O}_3\text{N}$	6.16 5.99	75	3230	1:1	H.b.
5		$\text{C}_{11}\text{H}_{16}\text{O}_4\text{N}_2$	11.66 11.35	82	3220-3300	1:1	H.b.
6		$\text{C}_{11}\text{H}_{15}\text{O}_5\text{N}_3$	14.73 14.55	133-34	3200-3280	1:1	H.b.
7		$\text{C}_{11}\text{H}_{11}\text{O}_8\text{N}_4$	16.96 16.64	224	3200-3250	1:1	H.b.
8		$\text{C}_{11}\text{H}_{15}\text{O}_4\text{N}_2$	13.33 13.75	164	3300	1:1	H.b.

Table 1 (Continued)

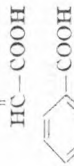
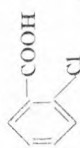


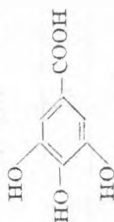
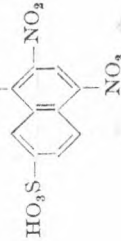
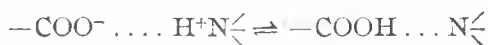
1	2	3	4	5	6	7	8	
9	$\begin{array}{c} \text{OH} \\ \\ \text{CH}_3 - \text{C} - \text{CH}_3 \\ \quad \\ \text{COOH} \quad \text{COOH} \quad \text{COOH} \end{array}$	$\text{C}_{14}\text{H}_{20}\text{O}_5\text{N}_2$	7.12 6.92 75	3300	2960	1330 1690	2:1	C.T.C.
10	$\begin{array}{c} \text{COOH} \\ \\ \text{COOH} \end{array}$	$\text{C}_{12}\text{H}_{14}\text{O}_4\text{N}_2$	9.58 9.99 188		3000	1350 1680	2:1	C.T.C.
11	$\begin{array}{c} \text{HOOC} - \text{CH} \\ \\ \text{HC} - \text{COOH} \\ \\ \text{COOH} \end{array}$	$\text{C}_{14}\text{H}_{16}\text{O}_5\text{N}_2$	8.80 8.53 125		2900	1350 1590	2:1	C.T.C.
12		$\text{C}_{12}\text{H}_{17}\text{O}_3\text{N}$	6.27 6.33 56		2950— 3060	1330 1620	1:1	C.T.C.
13		$\text{C}_{12}\text{H}_{16}\text{O}_3\text{NCl}$	5.43 5.25 62		2960— 3040	1330 1600	1:1	C.T.C.
14		$\text{C}_{12}\text{H}_{14}\text{O}_3\text{N}_2$	10.44 10.90 138		2860— 2700	1320 1610	1:1	C.T.C.
15		$\text{C}_{12}\text{H}_{15}\text{O}_4\text{N}_2$	13.41 13.50 167		3090	1350 1630	1:1	C.T.C.
16		$\text{C}_{17}\text{H}_{23}\text{O}_7\text{N}_2$	7.52 7.10 183— 84	3210—3320	2980— 2980	1330 1690	2:1	H.b., C.T.C.
17		$\text{C}_{20}\text{H}_{21}\text{O}_{10}\text{N}_4\text{S}$	10.84 10.79 164	3320—3340	2950— 3050	1350 1690	2:1	H.b., C.T.C.

Table 2

Splitting of N-methylmorpholine complexes

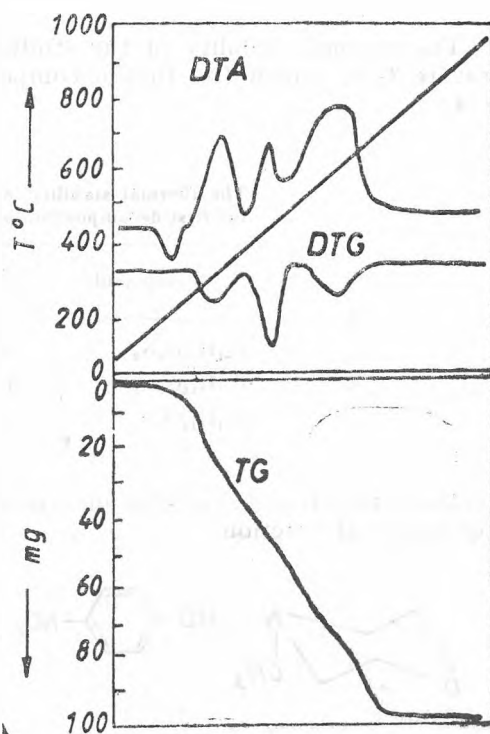
Acid component of complex	Complex g	Acid component (g) calc.	Acid component (g) found	molar ratio
4-nitrophenol	0,10	0,057	0,055	1 : 1
2,4-dinitrophenol	0,10	0,064	0,058	1 : 1
2,4,6-trinitrophenol	0,10	0,069	0,060	1 : 1
fumaric acid	0,10	0,037	0,035	1 : 1
benzoic acid	0,10	0,054	0,058	2 : 1
3-Cl-benzoic acid	0,10	0,060	0,058	1 : 1
4-nitrobenzoic acid	0,10	0,062	0,060	1 : 1
3,5-dinitrobenzoic acid	0,10	0,066	0,055	1 : 1
flavianic acid	0,10	0,060	0,058	2 : 1

The type of complex, H.b. or C.T.C., has been determined by IR spectral data, based on the ν_{OH} and ν_{NH^+} vibration modifications [6–9]. One can see that depending on the type of complex, in the IR spectra appear different frequency shifts as well as new frequencies [8]. The frequencies of these vibrations can be correlated with the type of the formed complex. (Table 1). Thus H.b. formation between the phenolic hydroxyl group and the nitrogen of amine, is evident in the IR spectra of complexes, through the pronounced shift of the ν_{OH} stretching vibration to lower frequencies. N-methylmorpholine with picric acid and carboxylic acids gives charge transfer complexes, in the spectra of which, typical bands can be seen at about 2900 cm^{-1} , which could be attributed to the stretching vibration ν_{NH^+} , due to ionic band formation:



including also H.b. formation [9]. It appears also the two stretching vibrations ν_{COO^-} at $1330\text{--}1350\text{ cm}^{-1}$ and at $1600\text{--}1690\text{ cm}^{-1}$.

In order to get more information concerning the structure of these complexes and their thermal behaviour, a thermal analysis for complexes and for their components has been carried out. The recorded thermal curves point out chemical modifications accompanied by weight loss

Fig. 1. Derivatogramme of $\text{C}_{11}\text{H}_{14}\text{O}_4\text{N}_4$.

in the TG and DTG curves, as well as physical transformations such as the melting and boiling points of the complexes and of the components. The recorded thermal curves of N-methylmorpholine complexes with: p-nitro-, 2,4-dinitro, and 2,4,6-trinitrophenol, show on the differential curves endothermic effects at 356 K, 406 K and at 497 K, corresponding to the melting of the studied compounds (Fig. 1), in good agreement with the literature data [10]. The melting process is followed by exothermic effects due to the thermal decomposition reactions of complexes into the components and to the final pyrolysis at 853–878 K (Table 3).

Table 3

Temperature K of DTA peaks and melting of the compounds

Sample	Melting temperature	Temperature of DTA exothermic peaks
$C_{11}H_{16}O_4N_2$	356	397; 588; 683; 853
$C_{11}H_{16}O_6N_3$	406	440; 598; 689; 878
$C_{11}H_{14}O_8N_4$	497	535; 703; 863

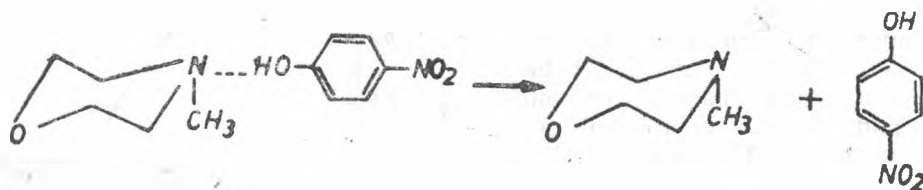
The thermal stability of the studied complexes, determined through temperature t_d at which the first decomposition reaction begins, is shown in Table 4.

Table 4

The thermal stability and kinetic parameters for first decomposition process of the compounds

Compound	t_d K	E_a kcal/mol	n
$C_{11}H_{16}O_4N_2$	380	9.81	1.10
$C_{11}H_{16}O_6N_3$	417	8.57	0.85
$C_{11}H_{14}O_8N_4$	509	13.23	0.88

Kinetic parameters have been determined for the first decomposition process, after chemical reaction:



using the Freeman-Carroll method [11].

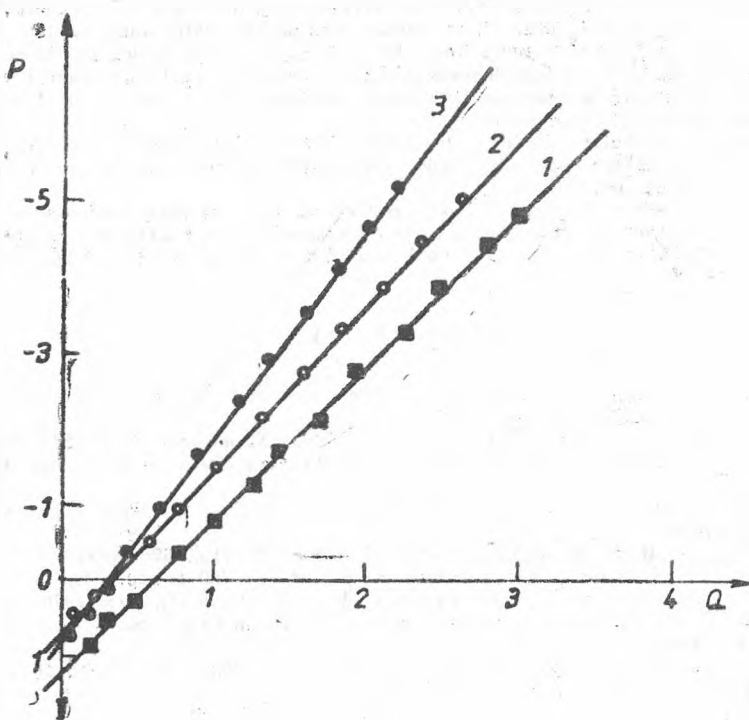


Fig. 2. Kinetic of thermal decomposition: 1 - $C_{11}H_{16}O_4N_2$; 2 - $C_{11}H_{15}O_6N_3$; 3 - $C_{11}H_{14}O_8N_4$.

From the Freeman-Carroll graphic representing $P = -\frac{\Delta \lg W_t}{\Delta \lg W_r}$ versus $Q = \frac{\Delta(T^{-3}) \cdot 10^3}{\Delta \lg W_r}$, where: W_t = weight loss at the t moment, W_r = the quantity of residual substance at the t moment, T = absolute temperature, have been determined activation energy, $E_a = 4,575 \cdot \text{tg } \alpha$ and n , which is the origin ordinate (Fig. 2).

The value of E for the complexes, of 8–14 kcal/mol is also a prove for the H.b. type [12–14]. It is to be mentioned that the heterogeneous kinetics is only a formal application of the homogeneous kinetics, namely E_a and n do not represent the real values which do characterise the thermal decomposition process.

Conclusions. 17 Molecular complexes of N-methylmorpholine with some phenols and carboxylic acids, unmentioned in the literature (excepting the picrate) have been prepared. The prepared complexes have been characterised by elemental, IR and thermal analyses. The type of complexes (H. b. and C.T.C.) has been established. Thermal analysis investigations of the complexes and of their components point out their thermal stability as well as their kinetic parameters.

Experimental. All the complexes have been prepared by heating 1 mole N-methylmorpholine with 1 mole acid component in ethanol, for 30 minutes on the water bath. Cooling the reaction mixture, the complex separates a precipitate, in most of the cases, which has been purified by crystallisation from ethanol. Some complexes which have remained in solution, have been separated by repeated extractions with solvents as benzene or acetone, followed by removal of the solvent and washing with diethylether (complexes 1-5, 9, 12).

The splitting of molecular complexes has been achieved with excess of 2N hydrochloric acid at room temperature, until the acid component precipitation. After cooling the acid component is filtered, than it is dried and weighted.

The IR spectra were recorded in KBr pellets with an UR-10 Zeiss spectrophotometer.

The thermal analysis of complexes has been followed with a MOM derivatograph of type OD-103, in the range of temperature 20-1000°C, with a warming velocity of 20°C/min.

REFERENCES

1. S. Mager, M. Vagaonescu, E. Hopirtean, L. Stoicescu, N. Cristea, *Stud. Univ. Babeş-Bolyai, Chem.*, **19**, 40 (1984).
2. V. Davidovitch, U. Ragnarsson, *Acta Chem. Scand. Ser. B* **33**, 311 (1979).
3. U. Oesch, D. Ammann, E. Pretsch, W. Simon, *Helv. Chim. Acta*, **62**, (7), 2073 (1979).
4. M. Vagaonescu, I. Cocrean, L. Ghizdavu, A. Tatar, *Stud. Univ. Babeş-Bolyai, Chem.*, **31**, 3 (1986).
5. P. Y. Krueger, B. H. Hawkins, *Can. J. Chem.*, **51** (19), 3250 (1973).
6. R. A. Kydd, P. Y. Krueger, *J. Chem. Phys.*, **72** (1), 280 (1980).
7. P. Y. Krueger, Y. Yan, H. Weiser, *J. Mol. Struct.*, **5** (5), 375 (1970).
8. M. Vagaonescu, L. Stoicescu, L. Aldea - Pomărac, *Stud. Univ. Babeş-Bolyai, Chem.*, **25**, 66 (1980).
9. M. Vagaonescu, S. Mager, L. Munteanu, *Rev. Roumaine Chim.*, **20**, 63 (1978).
10. V. K. Pogorelii, *Uspekhi Khim.*, (46), 602 (1977).
11. E. S. Freeman, B. Carroll, *J. Phys. Chem.*, **62**, 394 (1958).
12. A. Secară, E. Segal, *Rev. Roumaine Chim.*, **23**, 147 (1978).
13. K. Wojciechowski, J. Szadowski, *J. Thermal Anal.*, **31**, 297 (1986).
14. C. W. Fong, *Aust. J. Chem.*, **33**, 1285 (1980).

MICROPROCESSOR DRIVEN PRISM MONOCHROMATOR FOR
AUTOMATED SPECTROPHOTOMETRY

A. FODOR*, S. LECCA* and E. CORDOȘ*

Received: February 29, 1988

A prism monochromator is presented, in which the wavelength selection is accomplished by means of a microprocessor, using a data file containing the prism dispersion curve. The system is very simple, from mechanical point of view, having a very good reproductibility.

To achieve an accurate and/ or rapid selection of the working wavelength the modern automated optical instrumentation is equipped with monochromators driven by logic circuits or microcomputers. Most monochromators used for optical analysis in molecular absorption [1], inductively coupled plasma atomic emission [2] or atomic absorption and atomic emission [3] have a grating as a dispersion device. In this case the wavelength selection is facilitated by the linear relationship between the wavelength and the sinus of the angle of grating rotation.

In case of prism monochromators or the monochromators with a mixed dispersion device the automation of the wavelength selection is more difficult because of nonlinearity of prism dispersion and by its dependence on the prism material. To achieve the required linearisation, rather complex and high precision mechanical devices should be used.

The mechanical linearisation could be replaced by a soft driven operation using a simpler mechanical device. In this respect, in the present paper a microprocessor driven prism monochromator is presented in which the wavelength selection is implemented by means of software.

Experimental. The prism monochromator [4] from the SFV-03, visible spectrophotometer (Institute of Chemistry, Cluj-Napoca), has been modified by replacing the mechanism for wavelength selection with a micrometric screw linked to the lever of the M_2 mirror (Fig. 1). The micrometric

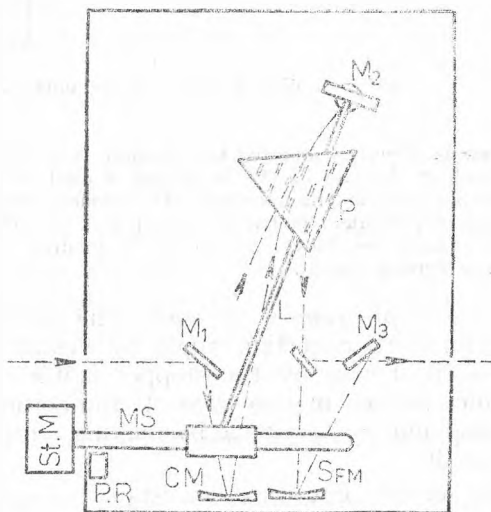


Fig. 1. The diagram of a modified SFV-03 monochromator operated by a microprocessor. M_1 , M_2 , M_3 — plane mirrors; CM — collimating mirror; FM — focal mirror; StM — stepper motor; MS — micrometric screw; L — lever.

* University of Cluj-Napoca, Faculty of Chemical Technology, 3400 Cluj-Napoca, Romania

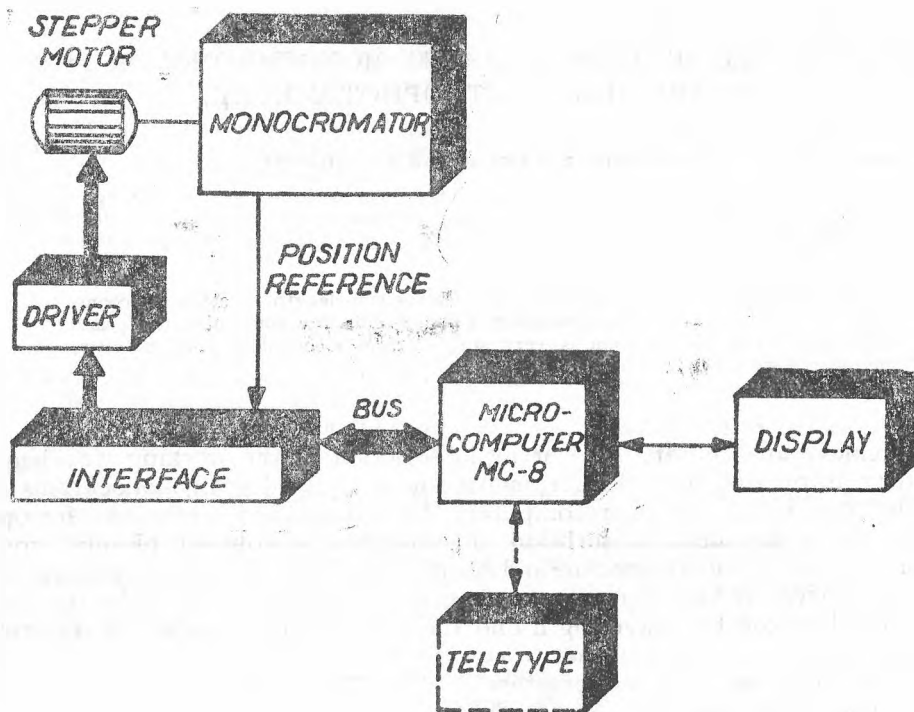


Fig. 2. Bloc diagram of the microprocessor driven prism monochromator.

screw is directly connected to the shaft of a stepper motor ($15^\circ/\text{step}$). An optoelectronic coupling, placed at the end of the lever run, is used as a reference position for a point in the low wavelength region of the spectrum. The monochromator has been driven by a MC-8 microcomputer (Computer Works, Bucharest) linked with a DAF-1001 display and keyboard (Fig. 2). An interface allows the data access to the computer bus line and provides the proper sequence for the motor driving circuit.

The programme structure. The wavelength is selected by rotating the M_2 mirror with a certain angle by means of the micrometric screw which, at its turn, is driven by the stepper motor. To get at the selected wavelength one could proceed in two ways. If the actual wavelength is known, for example λ_1 , movement to λ_2 is done by making a number of steps ΔS in the proper direction (Fig. 3).

The second procedure consists in bringing each time the monochromator at a reference position, preferably at the end of the working range, after that the required number of steps is implemented. The first procedure is recommended for spectra recording, when a spectrum is scanned by incrementing the wavelength with a constant value and the second, which is our case, for single wavelength measurements in routine quantitative determinations.

The number of steps made by the stepper motor in order to change the wavelength with $\Delta\lambda$ depends on the spectral range in which the instrument is actually

working. This number could be calculated on the basis of the prism dispersion equation:

$$n^2 = a + \frac{b}{\lambda^2} + \frac{c}{\lambda^4} + \frac{d}{\lambda^6}$$

where n is the refractive index of the prism and a , b , c and d , numerical coefficients specific for prism material. To use the above equation implies that the value of a , b , c and d is known which, in fact, means to plot the dispersion curve for each lot of prisms and sometimes for each individual prism. Calculation of the number of motor steps from the above equation calls for an appreciable number

of programming instructions which increases the execution time. Taking into account the memory capacity of the used computer a more practical solution was considered using a data file. The wavelength and the corresponding prism position are listed as pairs of data in the memory registers. The prism position is expressed by the number of steps of the stepper motor starting from the reference position. The working sequence of the monochromator is the following: after the desired wavelength is typed at the keyboard the computer starts the motor towards the reference position. At the moment the reference position is reached, the motor reverses its rotation and starts making the number of steps required to get at the wavelength typed at the keyboard. The flow chart of the programme is given in Fig. 4.

First, the working mode of the interface and the time increment for the motor are selected. A hexadecimal FE is displayed at the outport and then the system waits for the wavelength to be typed at the keyboard. After the wavelength is typed, it is read and compared with the highest and lowest wavelength between which the monochromator works. If the typed wavelength falls within the two limits the motor starts rotating towards the reference position (zero). Then the wavelength from the first address in the data file is compared with the typed wavelength. If they are not equal the number of steps from the corresponding address is implemented, the address is incremented by one unit and the comparison of wavelengths is repeated. If the new wavelength is lower than the one read from the keyboard the stepper motor is driven again to perform the number of steps from the address. The operations are repeated until the wavelength from the data file and that called at the keyboard are identical. Then, the end of the operation is signaled and the computer enters a waiting state.

The accuracy of wavelength selection by the prism monochromator is shown in Table 1.

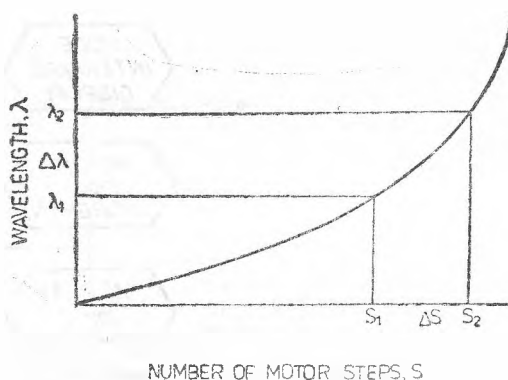


Fig. 3. Prism dispersion curve expressed by wavelength versus the number of steps of the stepper motor.



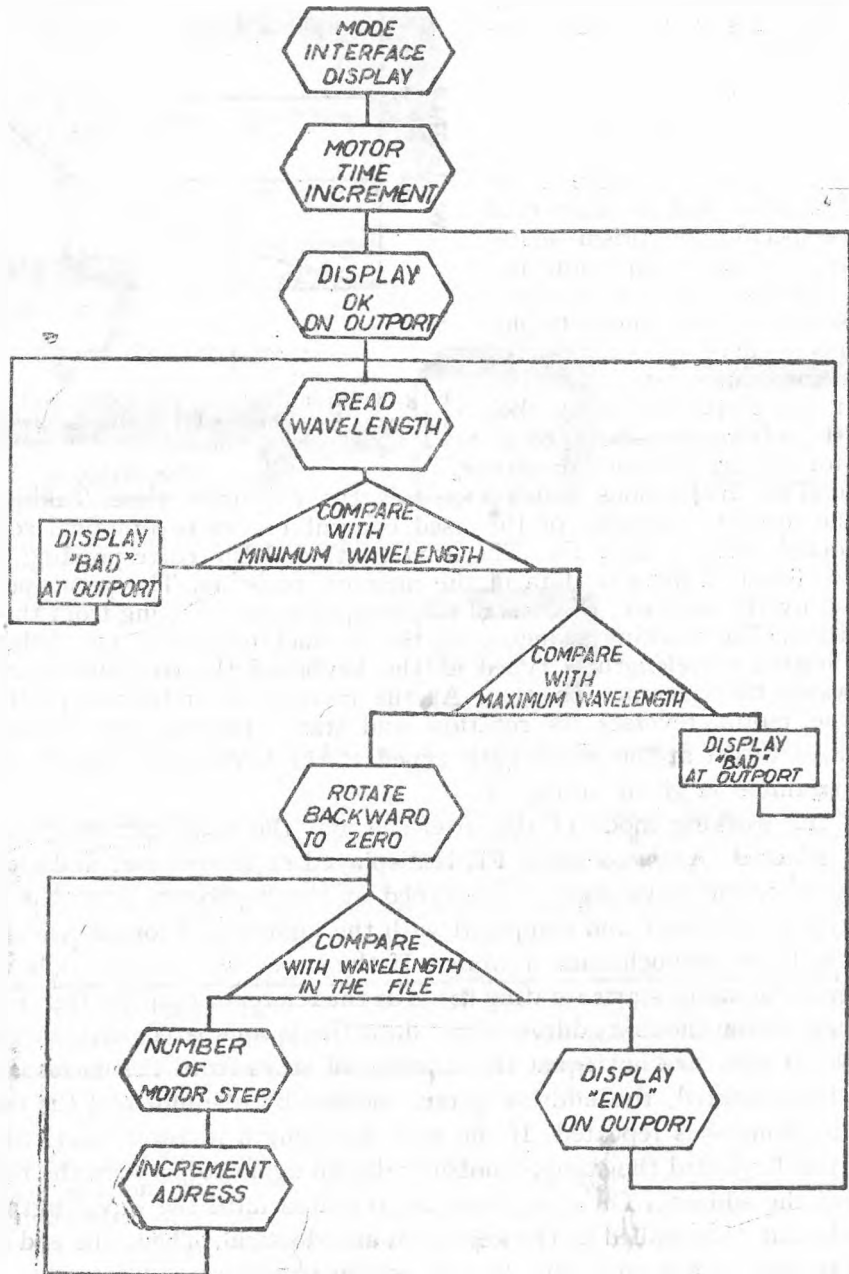


Fig. 4. Programme flow chart for prism monochromator driving.

Table 1

Accuracy of microprocessor driven monochromator

λ (nm)	steps/nm	$\Delta\lambda$ /step (nm)	E_r , calc (%)	E_r , exp (%)
410	9.0	0.11	0.024	0.022
450	5.4	0.18	0.040	0.043
500	3.6	0.27	0.054	0.061
550	2.6	0.38	0.069	0.066
600	2.0	0.50	0.083	0.088
650	1.4	0.71	0.110	0.112
700	1.0	1.00	0.140	0.136

The calculated errors (E_r , calc) were obtained considering that the stepper motor could be stopped with an error of ± 1 step. The experimental errors (E_r , exp), obtained by using a reference monochromator as a light source, fall in this range. The driving time of the monochromator for the complete spectral range is of 1 second.

REFERENCES

1. E. Cordoş, H. V. Malmstadt, *Analyt. Chem.*, **44**, 2407 (1972).
2. A. Zander, *Analyt. Chem.*, **58**, 1139 (1986).
3. E. Cordoş, C. Manoliu, „Spectrometria de absorbtie și fluorescență atomică”, Ed. Acad. R.S.R., 1984, p. 102.
4. E. Cordoş, I. Cățineanu, I. Savici, D. Pop, *Rev. Chim. (București)*, **34**, 1111 (1983).

STATE EQUATIONS OF FATTY ACID MONOLAYERS

MARIA TOMOAI-A-COTIȘEL*, JÁNOS ZSAKÓ* and EMIL CHIFU*

Received: February 29, 1988

By using the experimental surface pressure vs. mean molecular area curve of oleic acid monolayer spread at the air/water interface, a number of six state equations given in the literature are tested. Three new state equations, containing two adjustable parameters, are proposed for uncharged films and one of them is found to describe very well the experimental curve, the standard deviation being not larger than the experimental error in surface pressure measurements. Interaction parameters are derived for oleic and linoleic acids by means of this new state equation.

Introduction. The behaviour of insoluble monolayers of surfactants spread at the air/water interfaces is frequently studied by recording compression isotherms, i.e. surface pressure π vs. mean molecular area A curves. Mathematical modelling of these isotherms is performed by means of surface state equations. In the literature, a great variety of such equations have been proposed. The simplest of these two-dimensional state equations is analogous to the equation of perfect gases [1]:

$$\pi A = kT \quad (1)$$

where k stands for Boltzmann's constant and T for the absolute temperature.

Due to the finite dimensions of the surfactant molecules and to the intermolecular interactions in the monolayer, Eq. (1) is valid only at vanishingly low surface pressures.

In the Volmer-type state equation [2],

$$\pi (A - A_0) = kT \quad (2)$$

the mean molecular area is corrected for the co-area A_0 , theoretically related to the cross-section area of the surfactant molecules. Frequently, the experimental π values are lower than the theoretical ones, corresponding to Eq. (1), which in terms of Eq. (2) corresponds to negative A_0 values. Therefore, it seems more reasonable to correct π for the internal pressure π_0 , resulting from the intermolecular attractions, viz.

$$(\pi + \pi_0) A = kT \quad (3)$$

Langmuir's state equation

$$(\pi + \pi_0)(A - A_0) = kT \quad (4)$$

takes into account both effects mentioned above [3].

* University of Cluj-Napoca, Physical Chemistry Department, 3400 Cluj-Napoca, Romania

Since in the case of real gases, the internal tri-dimensional pressure is assumed to be inversely proportional to the volume square, in the case of monolayers, i.e. two-dimensional real gases, π_0 may be presumed to vary inversely proportional to the square of the molecular area. Consequently, the following van der Waals-type state equation has been proposed [4]:

$$(\pi + \alpha/A^2)(A - A_0) = kT \quad (5)$$

where α is a parameter characterizing the intermolecular interactions in the monolayer.

For cohering uncharged films a similar state equation has been derived [5], viz.

$$(\pi + \alpha/A^{3/2})(A - A_c) = kT \quad (6)$$

Eq. (6) was found to describe well the compression isotherms of the miscellaneous insoluble monolayers [6, 7].

The duplex film model [3] considers the monolayer to be theoretically formed of two parts, viz. a monolayer solution of the surfactant polar headgroups in water, covered by an oily monolayer consisting of the hydrocarbon chains of the surfactant molecules. By presuming that the monolayer solution is a regular one, being in thermodynamic equilibrium with the aqueous subphase, the following equation has been proposed [8]:

$$\pi + \pi_0 = -\frac{kT}{A_1} \ln x_1 - \frac{\beta_{12}}{A_1} x_2^2 \quad (7)$$

where (π_0) corresponds to the hypothetical spreading coefficient of the oily portion of the surfactant molecules, A_1 stands for the cross-section area of the water molecules, x_1 and x_2 represent the molar fractions of the water and of the surfactant headgroups in the monolayer solution, respectively, and β_{12} is a parameter characterizing the interactions between the polar headgroups and the water molecules in the monolayer.

In the present paper our experimental compression isotherms of oleic acid (OA) and of linoleic acid (LA) monolayers [9], recorded by means of the Wilhelmy method, have been used to test the validity of the above state equations.

Results and Discussion. In view of testing the state equations the OA monolayer has been chosen as model system. The compression isotherm recorded on a subphase with pH = 2 has been used since at this pH the protolytic equilibrium in the monolayer is shifted practically completely towards the neutral OA molecules [9]. The experimental π vs. A curve is given in Fig. 1 (curve 1). The theoretical curve, corresponding to Eq. (1) is visualized in the same figure (curve 2). As seen, at high A values important deviations from the perfect behaviour appear in the negative direction, indicating the role of the intermolecular attractive forces. On the contrary, at lower A values, the deviations become positive.

The other state equations contain a single (Eqs. (2) and (3)) or even two (Eqs. (4)–(7)) parameters to be derived from experimental data. Since a good mathematical description of the compression isotherms by means of state equa-

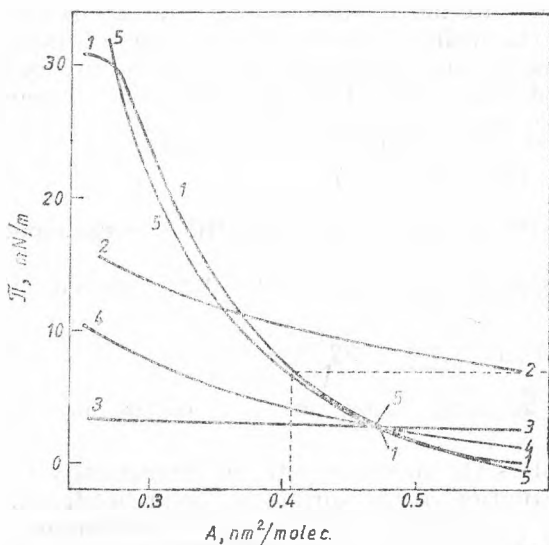


Fig. 1. π vs. A isotherms for OA monolayer. Experimental curve (1); theoretical curves (2)–(5) calculated by using parameters given in Table 1 and state equations: curve (2) – Eq. (1); (3) – Eq. (2); (4) – Eq. (3); (5) – Eq. (4).

lated (curves 3 and 4). As seen, Eq. (2) gives a rather unrealistic, negative A_0 value, while Eq. (3) yields a π_0 value corresponding to intermolecular attraction. Neither Eq. (2), nor Eq. (3) are able to give a good description of the experimental curve, the Δ_m value being rather high.

tions can be expected in the case of expanded films, i.e. at low surface pressures, the π range corresponding to $\pi \leq 7$ mN/m has been chosen. This domain is delimited in Fig. 1 by dashed straight lines, and we had in this region a number of 17 experimental points, i.e. $A_i - \pi_i$ pairs. These data were processed following a curve fitting method. For this purpose, the standard deviation Δ of the experimental points from the theoretical ones was calculated and minimized by performing a systematic variation of the parameter/parameters to be derived.

In the case of Eq. (2) and (3), by varying A_0 and π_0 , respectively, the minimum standard deviation, Δ_m , was determined, which is given in Table 1, together with the corresponding parameter value. By using the latter the theoretical ones, given in Fig. 1, were calculated

Table 1

Parameters of the state equation and standard deviations derived for OA monolayer ($\pi < 7$ mN/m)

Eq.	π_0 (mN/m)	A_0 (nm ² /molec.)	α^*	$\beta_{12} \times 10^{20}$ (Nm)	Δ^{**} (mN/m)
(1)	—	—	—	—	6.09
(2)	—	-1.123	—	—	1.95
(3)	6.0	—	—	—	1.19
(4)	10.5	0.169	—	—	0.29
(6)	—	0.268	5.69 ¹	—	0.17
(7)	10.46	—	—	-0.08	0.29
(9)	—	—	0.84 ²	-1.07	0.15
(10)	—	—	8.60 ³	-2.28	0.09
(11)	—	—	1.15 ³	-5.73	0.13

* Units: ¹) 10⁻³⁰ Nm²; ²) 10⁻²⁰ Nm; ³) 10⁻³⁸ Nm³; in all cases per molecule.

** It means Δ_m in the case of Eqs. (2) and (3), and $(\Delta_m)_m$ with Eqs. (4), (6), (7) and (9) – (11).

By using equations with two adjustable parameters, a double minimization of Δ is to be performed. To this end, one of the parameters is maintained at a constant value, and by varying the other one, the minimum of Δ , denoted as Δ_m is determined. The systematic variation of the first parameter allows us to determine the minimum of the Δ_m values, $(\Delta_m)_m$, indicating the best values of both parameters to be derived. These double minimum values of Δ are given in Table 1, and the theoretical curve calculated by means of Eq. (4), using π_0 and A_0 values given in Table 1, is also visualized in Fig. 1, curve (5). Obviously, the use of two adjustable parameters entails a spectacular improvement of the approximation.

As seen from Table 1, Eq. (6) gives better results than the others. As far as Eq. (7) is concerned, its use raises several problems, related to calculation of the molar fractions in the monolayer. The molar fraction of the surfactant can be calculated by means of the relation [8]:

$$x_2 = \frac{A_1}{A - A_2 + A_1} \quad (8)$$

where A_2 stands for the cross-section area of the polar headgroup of the surfactant and, obviously, $x_1 = 1 - x_2$. In our calculations, for the area necessity of the carboxyl group the approximate value of $A_2 = 0.20 \text{ nm}^2/\text{molecule}$ has been presumed, which is close to the collapse area of stearic acid. The cross-

section area of the water molecules has been approximated as $A_1 = \frac{V_{\text{H}_2\text{O}}^{2/3}}{N_A} \approx 0.10 \text{ nm}^2/\text{molecule}$, where $V_{\text{H}_2\text{O}}$ and N_A stand for the molar volume of liquid water and for Avogadro's constant, respectively. As seen, the use of Eq. (7) yields a minimum standard deviation equal to that given by Eq. (4).

In order to improve Eq. (7), we adopted a semiempirical method. If Eq. (7) is written for two neighbouring points of the experimental compression isotherm, corresponding to A_i and A_{i+1} , by eliminating β_{12} between them, the π_{0i} values can be obtained, which may be assigned to the arithmetical mean $A'_i = (A_i + A_{i+1})/2$ of the mean molecular areas. The plot of π_{0i} vs. A'_i is given in Fig. 2. As seen, in the expanded region of the isotherm, with increasing the A value, π_{0i} has at the beginning an almost constant value, and, further, it decreases systematically. This suggests the idea of substituting in Eq. (7) π_0 by a function of the type α/A^n . The simplest assumption, $n = 1$, yields:

$$\pi = - \left(\frac{\alpha}{A} + \frac{kT}{A_1} \ln x_1 + \frac{\beta_{12}}{A_1} x_2^2 \right) \quad (9)$$

By presuming $n = 3/2$, as in Eq. (6), one obtains:

$$\pi = - \left(\frac{\alpha}{A^{3/2}} + \frac{kT}{A_1} \ln x_1 + \frac{\beta_{12}}{A_1} x_2^2 \right) \quad (10)$$

By taking $n = 2$, as in the van der Waals-type Eq. (5), the following state equation results:

$$\pi = - \left(\frac{\alpha}{A^2} + \frac{kT}{A_1} \ln x_1 + \frac{\beta_{12}}{A_1} x_2^2 \right) \quad (11)$$

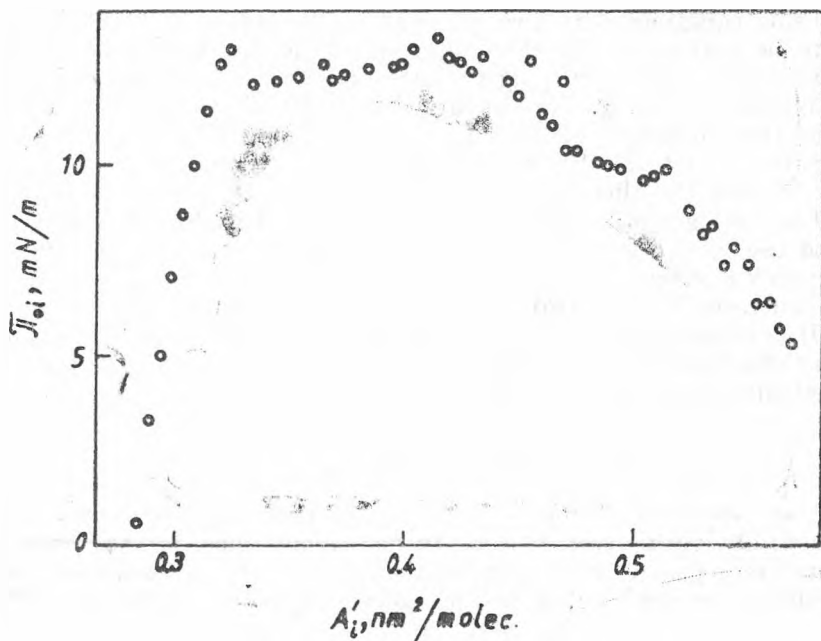


Fig. 2. π_{01} values obtained for OA by means of Eq. (7) from neighbouring points of the compression isotherm.

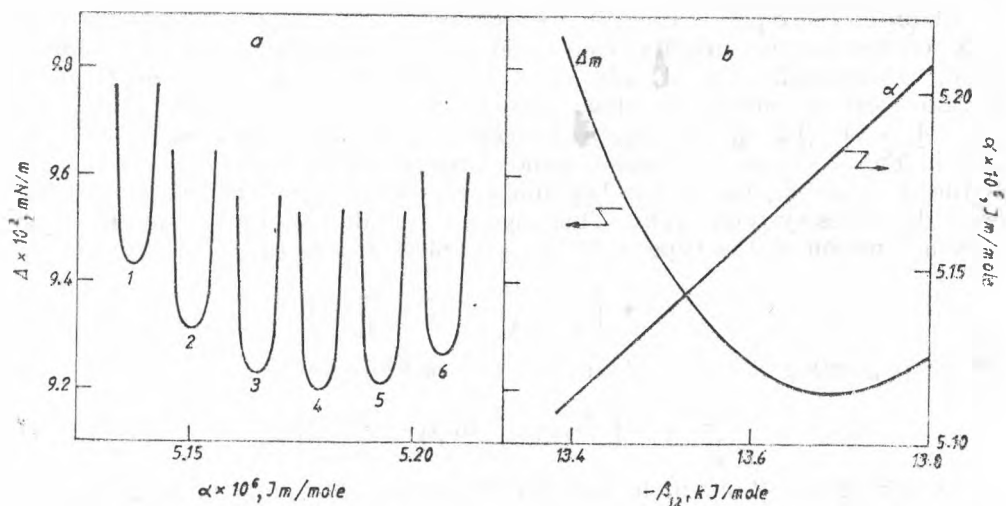


Fig. 3. Deriving of Δ_m for different β_{12} values presumed (a), and of $(\Delta_m)_m$ and interaction parameters (b), in the case of OA. ($-\beta_{12}$) in kJ/mole is: 13.50 (curve 1); 13.56 (2); 13.62 (3); 13.68 (4); 13.74 (5); 13.80 (6).

These new state equations (9)–(11) were also tested, and results are presented in the same Table 1. As seen, all Eqs. (9)–(11) give better description of the experimental compression isotherm as compared to those tested above. Especially Eq. (10) represents a very good approximation and the standard deviation does not exceed the experimental errors in surface pressure measurements.

Since Eq. (10) seems to be the most suitable from the tested ones, it was also used to derive interaction parameters from the compression isotherm of LA. Experimental data were processed up to $\pi = 7$ mN/m, as in the case of OA.

As an example, the double minimization procedure is illustrated by Figs. 3 and 4. In Fig. 3a the variation of Δ is visualized as function of α in the case of OA. The individual curves correspond to the presumed β_{12} value indicated in the legend of Fig. 3a. Fig. 3b gives the minimum standard deviation Δ_m derived from the above curves (Fig. 3a), as well as the corresponding α values as function of β_{12} . Fig. 3b allows us to derive the α and β_{12} values ensuring $(\Delta_m)_m$ and these values are given in Table 2, in this case α and β_{12} are molar

Table 2

Parameters of state equation (10) derived for the fatty acids studied ($\pi \leq 7$ mN/m)

Fatty acid	$\alpha \times 10^6$ (Jm/mole)	β_{12} (kJ/mole)	$(\Delta_m)_m$ (mN/m)
OA	5.18	-13.68	0.09
LA	5.20	-17.23	0.12

magnitudes. Fig. 4 shows the variation of Δ_m (obtained by varying β_{12} and by taking different constant α values), as function of α , for LA. The interaction parameters corresponding to $(\Delta_m)_m$ are given in the same Table 2.

As seen from Table 2, Eq. (10) describes almost as well the isotherm of LA as that of OA. It is interesting to remark that the derived α value is practically the same in both cases, but parameters β_{12} differ from each other. It is against the theoretical expectations since β_{12} was presumed to characterize the interactions between the carboxyl groups and water molecules, which must be the same with both fatty acids studied. Meanwhile, α had to be characteristic of the hydrocarbon chain interactions, which may be presumed to be different in the case of the two surfactants, since LA contains one more double bond as compared to OA. Therefore, one might expect the equality of the β_{12} parameters and a difference in the α ones [10]. Thus, α and β_{12} may be assumed as merely adjustable parameters characterizing in a certain way the cooperative interactions between the surfactant molecules, and between these and the water molecules, at different packing degrees, in the lattice of monolayers.

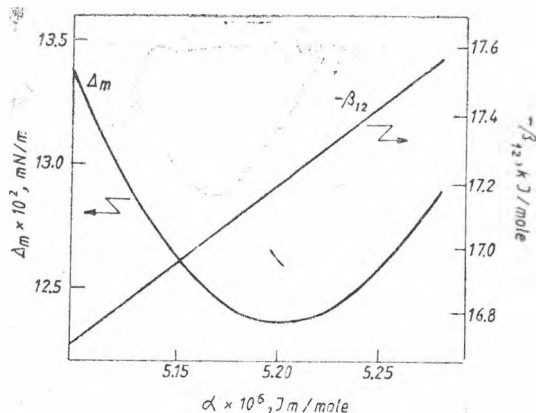


Fig. 4. Deriving of interaction parameters for LA.

REFERENCES

1. G. L. Gaines, Jr., "Insoluble Monolayers at Liquid - Gas Interfaces", Interscience, New York, 1966, p. 159.
2. M. Volmer, *Z. physik. Chem.*, **115**, 253 (1925).
3. I. Langmuir, *J. Chem. Phys.*, **1**, 756 (1933).
4. D. G. Hedge, *J. Colloid Sci.*, **12**, 417 (1957).
5. J. Guastalla, *Cahiers phys.*, **10**, 30 (1942); *J. Chim. Phys.*, **43**, 184 (1946).
6. I. Ter Minassian-Saraga, *J. Chim. Phys.*, **52**, 80 (1955).
7. E. Chifu, J. Zsako, M. Tomoai-a-Cotișel, *J. Colloid Interface Sci.*, **95**, 346 (1983).
8. Y. C. Lim, J. C. Berg, *J. Colloid Interface Sci.*, **51**, 162 (1975).
9. M. Tomoai-a-Cotișel, J. Zsako, A. Mocanu, M. Lupea, E. Chifu, *J. Colloid Interface Sci.*, **117**, 464 (1987).
10. E. Chifu, J. Zsako, M. Tomoai-a-Cotișel, A. Mocanu, *Studia Univ Babeș-Bolyai Chem.*, **34** (1), (1989) *in press*.

CONDENSATION DES PYRIMIDINYL-1-PYRAZOLONES-5 AVEC DES ALDEHYDES AROMATIQUES.

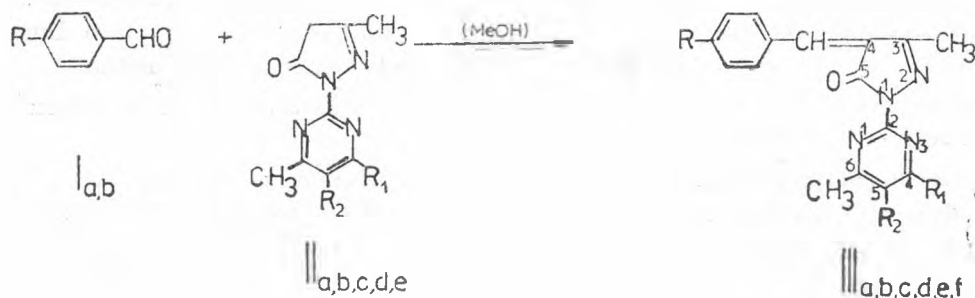
IOAN CRISTEA*

Reçu le 12 Avril 1988

Condensation of the 1-(2-Pyrimidinyl)-5-Pyrazolones with the Aromatic Aldehydes. By the condensation of the 1-(2-pyrimidinyl)-5-pyrazolones with the aromatic aldehydes some 4-benzylidene-1-(2-pyrimidinyl)-5-pyrazolones were obtained. The structure of the synthesized compounds was established by chemical methods and NMR spectroscopy.

Les pyrazolones, qui comportent un cas particulier de tautomérie, peuvent réagir avec des aldéhydes, en particulier aromatiques, soit en catalyse basique (pyridine, pipéridine, triéthylamine), soit en catalyse acide (AcOH, AC₂O) pour donner une classe importante de colorants pyrazoloniques [1, 2, 3]. La forme tautomère qui donne cette réaction de condensation, comporte un méthylène actif, activé par le groupement cétonique du noyau pyrazolonique. Ce méthylène est réactif vis à vis des aldéhydes, particulièrement aromatiques [3, 4, 5, 6], pour donner des colorants du type benzylidène-4 pyrazolones-5. D'après la littérature, on connaît une centaine de colorants benzylidène-4 pyrazolones-5, colorants employés pour teinter des tissus, des fibres synthétiques ou dans l'industrie photographique [1, 2, 4].

Résultats et Discussion. Nous avons soumis nos composés pyrimidinyl-1-pyrazolones-5 (II_{a,b,c,d,e}) [7, 8] à quelques réactions de condensation avec des aldéhydes aromatiques. Parmi les aldéhydes aromatiques étudiés le p-diméthyl-amino-benzaldéhyde (I_a) et p-méthoxy-benzaldéhyde (I_b) reagissent aisement pour engendrer des composés unitaires et colorés (III_{a,b,c,d,e,f}).



a: R=N(CH₃), R₁=OH, R₂=H
 b: R=N(CH₃), R₁=OH, R₂=CH₃
 c: R=N(CH₃), R₁=Cl, R₂=CH₃

d: R=N(CH₃), R₁=OCH₃, R₂=CH₃
 e: R=N(CH₃), R₁=OC₂H₅, R₂=CH₃
 f: R=OCH₃, R₁=OH, R₂=CH₃

* Universit  de Cluj-Napoca, Facult  de Chimie, 3400 Cluj-Napoca, Roumanie

Les autres aldéhydes aromatiques étudiés, ont donné des mélanges de produits de condensation bimoléculaire (du type benzylidénique) et trimoléculaire (du type triphénylméthanique) identifiés par chromatographie (CCM). Ces résultats seront l'objet d'une publication prochaine. Le but de notre recherche a été la synthèse de nouveaux colorants.

Les réactions avec le p-diméthylamino-benzaldéhyde ont été réalisées en milieu acid (AcOH) et avec le p-méthoxy-benzaldéhyde en milieu basique (pipéridine). Les composés ainsi obtenus ont été identifiés par l'analyse quantitative et par les méthodes spectrales.

Les résultats des nos recherche sont illustrés dans le tableau ci-dessous (Tableau 1).

Tableau 1

Caracteristiques physico-chimiques des composés obtenus

Composé obtenu	P.F. °C	Rend. %	Solvant recryst.	Analyse		UV-visible	
				calc.	exp.	λ_{\max}	ϵ
III _a	270	96	EtOH	20.77	20.6	500	39450
III _b	264	89	CHCl ₃	19.94	19.7	495	50200
III _c	250	83	MeOH	18.94	19.1	505	45200
III _d	228	77	MeOH	19.17	19.3	520	42250
III _e	234	76	EtOH	18.46	18.2	525	37135
III _f	256	68	DMFA	17.39	17.0	465	35460

Les composés obtenus présentent une bande d'absorption intense dans le domaine visible à $\lambda_{\max} = 460-520$ nm due à une transition $\pi - \pi^*$ du système conjugué. Dans le cas des composés III_{a,b,c,d,e} la bande est déplacée bathochrome avec 30-60 nm environ, par rapport au composé III_f. Le group diméthylamino exerce un effet bathochrome plus grande que le groupe méthoxy.

Les spectres UV-visible ont été enregistrés dans l'éthanol avec un spectrophotomètre „SPECORD UV-VIS”.

Avec le composé III_d nous avons enregistré le spectre dans l'éthanol (courbe 1) et également dans l'éthanol en présence d'acide (HCl) (courbe 2) Fig. 1

On observe en milieu acid un déplacement bathochrome due à la fixation du proton sur l'oxygène du noyau pyrazolonique, qui favorise la conjugaison du système.

La structure des composés obtenus a été également établis par RMN (Tableau 2). Les spectres ont été enregistrés avec un spectromètre RMN Tesla BS 487 C (80 MHz).

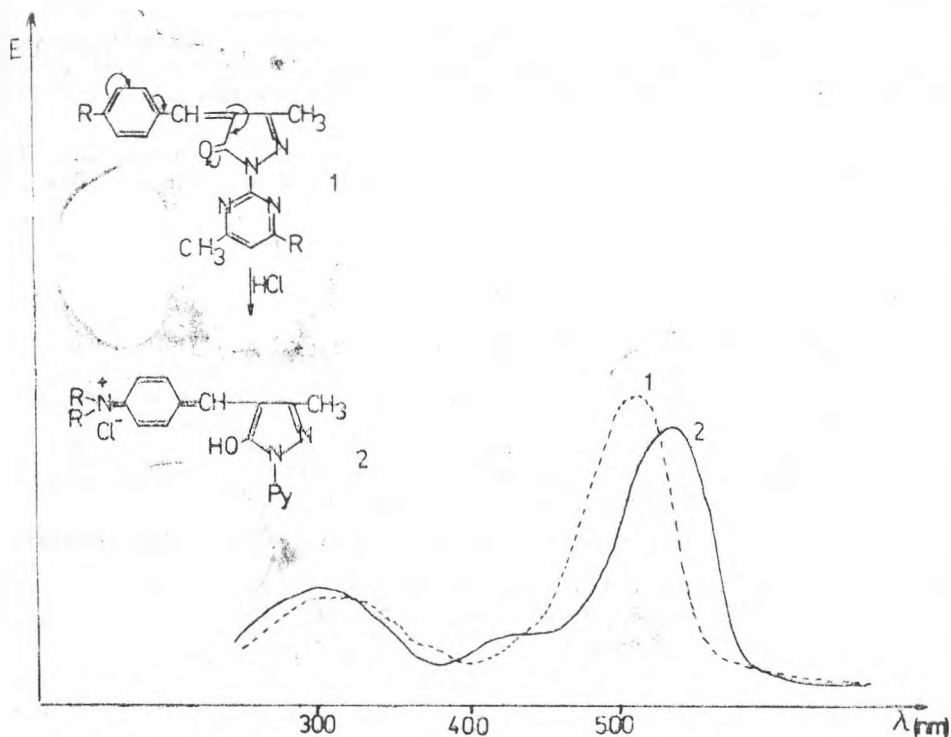


Fig 1. Spectre UV-visible du composé III dans l'éthanol (courbe 1) et dans l'éthanol + HCl (courbe 2).

Tableau 2

Les spectres de RMN des composés obtenus (solvant DMSO D₆)

Composé	Noyau pyrazolonique		Noyau pyrimidinique			Noyau benzenique		
	s CH ₃ (C ₈)	R ₁ (C ₄)	s R ₂ (C ₆)	s CH ₃ (C ₆)	s CH=	d H(C _{2,6})	d H(C _{3,5})	s R(C ₄)
III _a	2.10		6.10	2.40	7.10	6.48	8.42	2.95
III _b	2.11		2.23	2.34	7.10	6.45	8.45	2.85
III _c	1.98		2.20	2.30	7.15	6.95	8.40	2.85
III _d	2.05	4.0	2.23	2.40	7.08	6.65	8.50	2.96
III _e	2.08	4.46(q)	2.21	2.38	7.10	6.65	8.30	2.87
III _f	2.10	1.32(t)	2.27	2.45	7.71	6.93	8.31	3.78

s (singulet), d (doublet), t (triplet), q (quadruplet).
OH n'a pas été identifié.

Experimental. *Synthèse des composés III_{a,b,c,d,e}*. Un mélange de 0.01 mole pyrimidinyl-1-pyrazolones-5 (II), 0.01 mole p-diméthyl-amino-benzaldéhyde, 1ml AcOH dans 25-30 ml MeOH est porté au reflux pendant 2 h. D'après refroidissement, on filtre les colorants obtenus on lave avec MeOH et on les recristallise. Les résultats sont donnés dans le tableau 1.

Synthèse du composé III_f. Un mélange de 0.01 mole pyrimidinyl-1-pyrazolone-5 (II_b), 0.01 mole p-méthoxy-benzaldéhyde, 1ml pipéridine 30 ml EtOH est porté au reflux pendant 3h. On refroidit, on filtre et on le recristallise dans DMFA.

BIBLIOGRAFIE

1. M. Sugiyama, H. Sawaguchi, I. Nakamura, *Ger. Offen*, 2.582 (1976), *Chem. Abstr.*, **85**, 151747e (1976).
2. H. Curtis, L. Harris, W. Jannes, *Polaroid Corp., U.S.*, 3933798 (1976), *Chem. Abstr.*, **84**, 123427m (1976).
3. S. Nanda, D. Pati, A. S. Mitra, *J. Indian Chem. Soc.*, **40**, 833 (1983).
4. H. Bodo, F. Eckhord, *Ger. Offen*, 1800581 (1969), *Chem. Abstr.*, **72**, 80363v (1970).
5. S. Deniver, S. Daroga, *J. Chem. and Eng. Data*, **29**, 355 (1984).
6. *Oriental Photo Industrial Co. Ltd., Jpn. Kohai Tokyo Kaho*, 80155055 (1981), *Chem. Abstr.*, **94**, 176695k (1981).
7. I. Cristea, V. Fărcășan, I. Panea, *Brevet RSR*, 84355 (1984).
8. I. Cristea, V. Fărcășan, *Rev. Chim. (București)*, **33**, 674 (1987).

INVESTIGATION OF OXYGEN PERMEABILITY OF THIN PROTECTIVE ORGANIC LIQUID LAYERS USING A MEMBRANE-COVERED POLAROGRAPHIC OXYGEN SENSOR

LÁSZLÓ KÉKEDY* and ILEANA TEUCA**

Received April 12, 1988

The diffusion of air-oxygen through thin organic liquid layers used to protect oxidation-sensitive solutions in analytical practice was investigated with the help of an oxygen sensor. It has been stated that 2.5×10^{-7} moles of oxygen diffuse in 1000 s through a paraffin oil layer (thickness 3.96 mm, surface area 25.27 cm^2 , 20°C). The same value for a similar layer of pentane is 4.9×10^{-6} moles (10°C) significant only in trace analysis. Using Barrer's time-lag method diffusion coefficients of O_2 in the mentioned liquids have been estimated in good agreement with the calculated values via the Stock-Einstein equation.

Introduction. It is a general analytical practice to protect air-sensitive solutions against oxidation by covering them with a layer of water-immiscible organic liquid, e.g. with pentane. No exact data are available concerning the oxygen (air) permeability of such layers, their protective effect being known only from the practice. Literature data concerning the diffusion of oxygen through polymer membranes, [1-3] as well as the solubility of oxygen in organic liquids suggest that the respective layers are not perfect impermeable to oxygen. It is the aim of this paper to investigate quantitatively the oxygen (air) permeability of such protective organic liquid layers. For this purpose deaerated distilled water was covered with the organic layer, and after changing the inert atmosphere over the layer with air, the increase of oxygen concentration in the water was followed with a Clark-type oxygen sensor. Barrer's time-lag method [4] was used to calculate an apparent diffusion coefficient.

Experimental and Results. The apparatus used is shown in Fig. 1. 100 ml of distilled water was pipetted in the test cell of approximately 200 ml. Then the cell was closed with a thick rubber stopper in which a home-made Clark-type oxygen sensor and the gas inlet and outlet tubes, respectively, were fixed. The gas

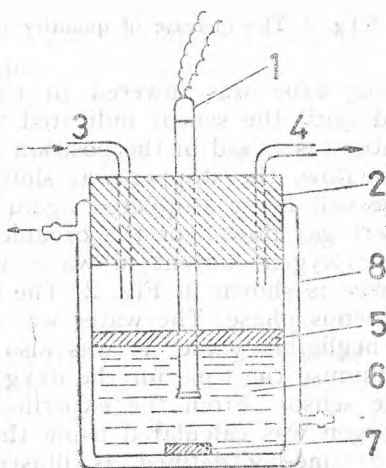


Fig. 1. The test cell: 1 - Clark-type oxygen sensor; 2 - stopper; 3 - gas inlet tube; 4 - gas outlet tube; 5 - organic liquid layer; 6 - distilled water; 7 - magnetic stirrer; 8 - thermostatic jacket.

* Faculty of Chemical Technology, Department of Inorganic and Analytical Chemistry, R-3400 Cluj-Napoca, Romania

** Institute of Chemistry, R-3400 Cluj-Napoca, Romania

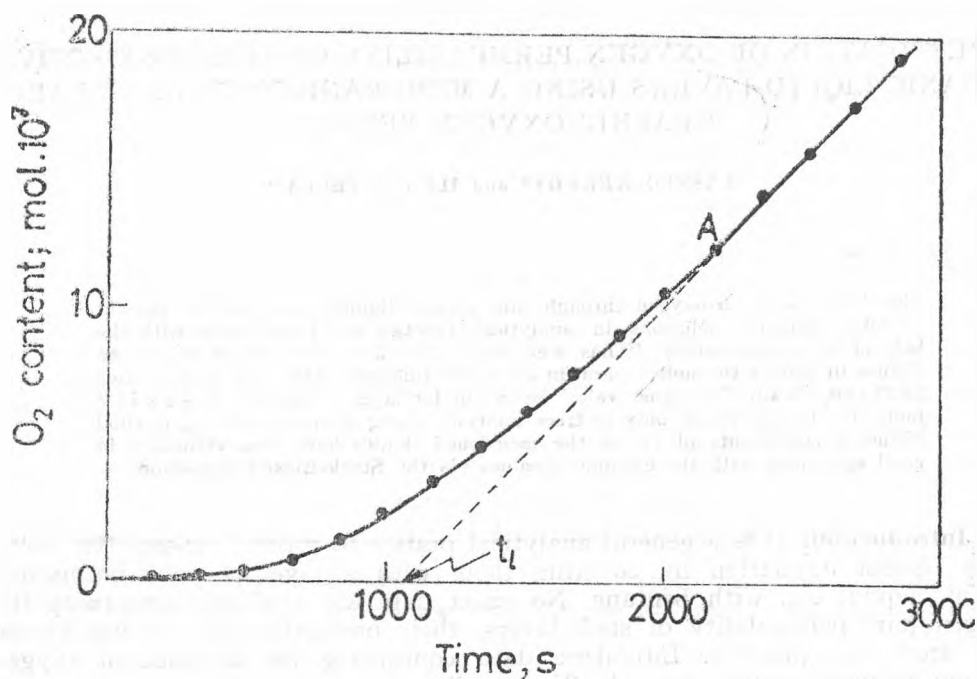


Fig. 2. The increase of quantity of oxygen in water as a function of time. t_L — time-lag

inlet tube was lowered in the water and oxygen-free argon was bubbled until the sensor indicated the absence of oxygen in water. Then the inlet tube was raised in the position shown in Fig. 1, and while continuing the inert gas flow, the stopper was slowly raised and the organic liquid was introduced, the cell being stoppered again. After the thermal equilibrium was set in, the inert gas flow over the organic layer was changed for air and the increase of the oxygen content in water was registered as a function of time. A typical curve is shown in Fig. 2. The oxygen sensor signal is sensitive to flow of the aqueous phase. The water was slowly stirred to reduce this flow sensitivity to a negligible value. It was also thought desirable to stir the aqueous layer to minimise the time for the oxygen diffusing through the organic liquid to reach the sensor. From the experimental data obtained, the diffusion coefficient of oxygen was calculated using the time-lag method. According to this procedure the time-lag defined as illustrated in Fig. 2 is correlated with the diffusion coefficient by the following equation:

$$D = \frac{l^2}{6t_L} \quad (1)$$

l being the thickness of the organic liquid layer. Our system is consistent with the model considered at the deduction of equation (1) (stationary conditions and zero partial pressure of the diffusing substance at one side of the membrane):

the concentration of oxygen in water (at the water-side of the organic layer) even after 1000 s of diffusion is of the order of tens of micromoles (see below), consequently the corresponding partial pressure can be considered as zero.

Before computing the corresponding D values we had to consider the time-lag caused by the diffusion of the oxygen through the polyethylene membrane of the oxygen sensor. For this purpose experiments were run as described above, but without organic layers, the observed time-lag (205 s) being subtracted from those observed in the presence of these layers. The thickness of the polyethylene membrane being known ($l = 0.036$ mm), the diffusion coefficient of oxygen in polyethylene could be calculated, obtaining $D = 1.06 \times 10^{-12}$ m² s⁻¹ in agreement with values ranging between 2.17×10^{-12} and 4.22×10^{-11} m² s⁻¹, respectively, reported in the literature [5, 6]. This confirms the correctness of our procedure. Our value for the diffusion coefficient of oxygen in polyethylene is about half the lowest value in the literature. This could be explained by the additional diffusion barrier of the layer of electrolyte between the membrane and electrode of a Clark-type sensor, and the time-lag for transport of the oxygen through the slowly stirred water layer.

Experiments were made with layers of paraffin oil (less volatile) and of pentane (often used in practice), respectively. 8, 9 and 10 ml of paraffin oil (or pentane) was pipetted into the cell so as to form layers with a thickness of 3.17 mm, 3.56 mm and 3.96 mm, respectively, the surface area being $S = 25.27$ cm². Curves like that in Fig. 2 were obtained. The region between O and A corresponds to the beginning of the oxygen passage through the organic layer, followed by the establishment of stationary conditions, when the concentration of oxygen in water increases linearly with time. Using corrected time-lag values, a mean value of $D = 2.61 \times 10^{-9}$ m² s⁻¹ has been obtained (paraffin oil, 20°C). Because of its high volatility, the pentane was studied only at 10°C, and only one thickness was studied (3.96 mm) giving a value for D of 3.48×10^{-8} m² s⁻¹.

Conclusion. Air-oxygen diffuses slowly through thin layers of paraffin oil or pentane, respectively. The apparent diffusion coefficient values obtained are: $D = 2.61 \times 10^{-9}$ m² s⁻¹ (paraffin oil, 20°C) and $D = 3.48 \times 10^{-8}$ m² s⁻¹ (pentane, 10°C). The theoretical D values can be calculated via the Stokes-Einstein equation:

$$D = kT/6\pi\eta a \quad (2)$$

where η is the viscosity (in kg m⁻¹ s⁻¹) and a the hydrodynamic radius of oxygen, 5.7×10^{-11} m. Now considering that η (paraffin oil 20°C) $\approx (25-55) \times 10^{-3}$ kg m⁻¹ s⁻¹, and η (pentane, 10°C) ≈ 0.25 kg m⁻¹ s⁻¹, the calculated D values for O₂ are: D (paraffin oil 20°C) = $(1.5-0.7) \times 10^{-11}$ m² s⁻¹ and D (pentane, 10°C) = 1.5×10^{-8} m² s⁻¹. Our D value in paraffin oil is greater with an order of magnitude than the calculated one. Though such differences are not uncommon in the literature, it is mainly due to the quality of the pharmaceutical oil used. Our D value in pentane compares well with the calculated one.

The amount of oxygen diffused is small, e.g. through a layer of paraffin oil ($l = 3.96$ mm, $S = 25.27$ cm²) in 1000 s diffuse only 2.5×10^{-7} moles of

oxygen (20°C), whereas through the same layer of pentane in the same time diffuse only 4.9×10^{-6} moles of oxygen (10°C). Thus if even the whole quantity of oxygen diffused were consumed to oxidize the air-sensitive compound being protected, this effect would be significant only in trace analysis.

REFERENCES

1. R. Houwink, A. J. Staverman „Chemie und Technologie der Kunststoffe”. Geerst und Portig, Leipzig, 1963.
2. B. H. Philipp, J. Purz, *Z. Chem.* **15**, 81 (1975).
3. D. F. Shriver, “The Manipulation of Air-Sensitive Compounds”, McGraw-Hill, New York, 1924.
4. R. M. Barrer: “Diffusion in and Through Solids”, Cambridge University Press, Cambridge, 1941.
5. J. Izidorczyk, J. Podkówa, J. Salwinski, *Roczniki Chem.*, **48**, 1341 (1974).
6. I. Jzydorczik, Z. Jodlowski, W. Miskiakewicz, K. Raszka, *Roczniki Chem.*, **50**, 281 (1976).

OXIDATION DES ÄTHENS MIT SAUERSTOFF ZU ÄTHYLENOXYD, MIT SILBERKATALYSATOREN

I. Stöchiometrie des Vorgangs

ILIE SIMINICEANU*, IOAN TODEA**, MARIA STANCA*** und ALEXANDRU POP***

Eingegangen am 21. November 1987

Oxidation of Ethylene for Ethyleneoxide Using the Molecular Oxygen and a Silver Catalyst. I. The Stoichiometry of the Process. The paper determines the independent stoichiometric equations, on the basis of which the mathematic model of mass balance, in a primary and secondary form, is drawn up for two variants: a) consecutive reactions; b) parallel reactions. The fact that for both variants taken into consideration we obtain the same secondary equations of balance prove that the balance of the process could be drawn up on the basis of any pair of the reactions that take place.

In den Industrieanlagen für Herstellung des Äthylenoxyds ist die katalytische Oxydation des Äthens mit Sauerstoff, der grundlegende chemische Vorgang.

Sogar in Anwesenheit von Silberkatalysatoren mit veränderlichen Mengen von Cadmium oder Cesium [1–3] aktiviert, deren Selektivität am grössten ist, wird ein Teil des Äthens durch Nebenreaktionen die zur Bildung von Kohlendioxyd und Wasser führen, verloren. Die Fertigung eines Massenbilanzes ist die erste Stufe für die mathematische Beschreibung eines chemischen Industrieprozesses. Für diesen Zweck muss man die algebraischen Gleichungen des Komponentenbilanzes feststellen um mit ihren Hilfe die numerische Werte zu bestimmen [4]. Für die Festlegung dieser Gleichungen und deren die die Zusammensetzung der Reaktionsmassen in jedem Moment, enschliesslich im Gleichgewicht, ausdrücken, kann man verschiedene Methoden anwenden [5–7].

Die vorliegende Arbeit versucht, durch die Beobachtung des Oxydationsprozesses des Äthens zu Äthylenoxyd, wobei die Konversionsmethode angewendet wird, eine allgemeine Methode zur Massenbilanzfertigung zu erhalten, die bei jedem Industriellen chemischen Vorgang angewendet werden kann. Es wird bewiesen das bei der Festlegung der algebraischen Gleichungen des Massenbilanzes nicht alle, sondern nur eine geringe Anzahl, der Reaktionen die im Betriebsreaktor stattfinden, in Betracht genommen werden müssen.

Die identische Form der sekundären Bilanzgleichungen, sowohl bei parallelen als auch bei nacheinander folgenden Reaktionen, zeigt die Möglichkeit des wahlens irgendwelcher Variante die zur Fertigung des mathematischen Modells des Materialienbilanzes, benützt werden kann.

* Polstechnische Institut Iași, 6600 Iași, Rumänien

** Chemische Lyceum Turda 3350 Turda, Rumänien

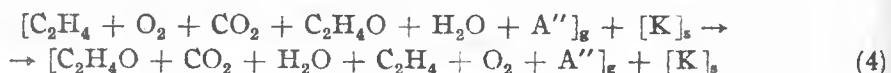
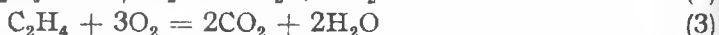
*** Universität Cluj-Napoca, Facultät für Chemische Technologie, 3400 Cluj-Napoca, Rumänien

Das, so bestimmte mathematische Modell des Massenbilanzes, erlaubt:

- die Bestimmung der Zusammensetzung der Reaktionsmasse, in jedem Moment, einschliesslich auch im Gleichgewicht (für umkehrbare Vorgänge);
- Vergleich der theoretischen und wirklichen Bilanzen die in Versuchs- oder Industriellen Anlagen, stattfinden;
- die richtige Bestimmung der Konversion und Selektivität des Katalysators, auf Grund geringer Anzahl von Konzentrationsmessungen, die direkt in Versuchs- oder Industrieanlagen durchgeführt werden können.

1. Die unabhängige stöchiometrische Gleichungen. Um ein mathematisches Modell des Massenbilanzes eines chemischen Vorgangs zu erhalten, ist notwendig in diesem Prozess enthaltene unabhängige stöchiometrische Gleichungen der Massenwandlungen zu kennen [4,8–10].

Wenn die Reaktionsmasse die Zusammensetzung der charakteristischen Gleichung (4) hat, finden im Oxydationsvorgang des Äthens die Reaktionen (1–3) statt.



Das Studium des Vorgangs im Gleichgewicht [11] ergibt die Beziehungen (5–7) die die Abhängigkeit der Gleichgewichtskonstanten von der Temperatur, darstellen.

$$\ln k_{p_1} = \frac{12.423,75}{T} + 0,833 \cdot \ln T - 0,0135 \cdot T + 8,845 \cdot 10^{-6} \cdot T^2 + 10,0329 \quad (5)$$

$$\ln k_{p_2} = \frac{110.248,11}{T} + 2,3946 \cdot \ln T + 0,0099036 \cdot T + 7,406 \cdot 10^{-6} \cdot T^2 + 81,217 \quad (6)$$

$$\ln k_{p_3} = \frac{158.878,1}{T} + 3,194 \cdot \ln T - 0,0033766 \cdot T + 0,4836 \cdot 10^{-6} \cdot T^2 + 49,94 \quad (7)$$

Die Prozessanalyse im Gleichgewicht führt zur Schlussfolgerung das alle in Betracht gezogene Reaktionen, thermodynamisch möglich sind, und in Temperaturbereichen die industriell wichtig sind, alle Gleichgewichtskonstanten sehr hohen Wert haben (wie auch aus Tabelle 1 hervorgeht).

Tabelle 1

Werte der Reaktionsgleichgewichtskonstanten

$\ln K_p$ \ T K	473	418	523	548	573
$\ln K_{p1}$	37,018	35,62	34,35	33,214	32,17
$\ln K_{p2}$	335,38	324,23	314,21	305,14	296,90
$\ln K_{p3}$	600,06	387,21	371,359	358,39	345,517

Für die Bestimmung der unabhängigen stöchiometrischen Gleichungen wird die Orthogonalisationsmethode benützt [4, 5, 8–10].

Die A_a Matrix der Elemente den Molekulararten der Reaktionsmasse in einem gewissen Moment, zugeordnet, hat die Form: (8)

$$\begin{array}{l} \text{C}_2\text{H}_4 \\ \text{C}_2\text{H}_4\text{O} \\ \text{O}_2 \\ \text{CO}_2 \\ \text{H}_2\text{O} \end{array} \begin{pmatrix} \text{C} & \text{O} & \text{H} \\ 2 & 0 & 4 \\ 2 & 1 & 4 \\ 0 & 2 & 0 \\ 1 & 2 & 0 \\ 0 & 1 & 2 \end{pmatrix} = A_a \quad (8)$$

Der Rang der Matrix A_a ist $R = 3$, folglich wenn man die Beziehung (9) anwendet erhält man die Anzahl der unabhängigen stöchiometrischen Gleichungen, L .

$$L = C - R = 2 \quad (9)$$

Auf Grund der Tabelle 2, kann man feststellen das jede der Reaktionen (1–3), die Unabhängigkeitsbedingung erfüllt (10)

$$A_{Ri}^T \cdot A_a = 0 \quad i = 1, 2, 3 - \quad (10)$$

Infolgedessen, für die stöchiometrische Beschreibung des Oxydationprozesses des Äthens, kann man irgendwelche der drei möglichen Reaktionspaare die aus den drei Reaktionen gebildet werden können, benützen:

In Folgenden werden zwei Varianten in Betracht gezogen:

Variante A: die unaunabhängigen Gleichungen (1) und (2);

Variante B: die unabhängigen Gleichungen (1) und (3).

In der A Variante finden die Reaktionen nacheinander, in der B Variante gleichzeitig, statt.

2. Mathematische Bilanzmodelle. Entsprechend der Variante A, bestimmt man die Konversionen η_{11} und η_{2} für die Gleichungen (11–12)

$$\eta_{11} = \eta_E = \frac{n_E^{01} - n_E^1}{n_E^{01}} = \frac{n_{O_2}^{01} - n_{O_2}^1}{\frac{1}{2} n_E^{01}} = \frac{n_{EO}^1 - n_{EO}^{01}}{n_E^{01}} \quad (11)$$

$$\eta_{2} = \eta_{EO} = \frac{n_{EO}^{02} - n_{EO}^2}{n_{EO}^{02}} = \frac{n_{O_2}^{02} - n_{O_2}^2}{5/2 n_{EO}^{02}} = \frac{n_{CO_2}^2 - n_{CO_2}^{02}}{2 n_{EO}^{02}} = \frac{n_{H_2O}^2 - n_{H_2O}^{02}}{2 n_{EO}^{02}} \quad (12)$$

Zieht man die charakteristische Gleichung (4) in Betracht und die Tatsache das die Reaktionen (1-2) nacheinander folgen, können die Konkretisationsgleichungen geschrieben werden (13),

$$\begin{array}{lll}
 n_{\text{EO}}^1 = n_{\text{EO}}^{02} & n_{\text{O}_2}^{01} = n_{\text{O}_2}^0 & n_{\text{H}_2\text{O}}^2 = n_{\text{H}_2\text{O}} \\
 n_{\text{EO}}^{01} = n_{\text{EO}}^0 & n_{\text{H}_2\text{O}}^{02} = n_{\text{H}_2\text{O}}^0 & n_{\text{A}''} = n_{\text{A}''}^0 \\
 n_{\text{CO}_2}^{02} = n_{\text{CO}_2}^0 & n_{\text{CO}_2}^2 = n_{\text{CO}_2} & n_{\text{O}_2}^2 = n_{\text{O}_2} \\
 n_{\text{E}}^1 = n_{\text{E}} & n_{\text{E}}^{01} = n_{\text{E}}^0 & n_{\text{EO}}^2 = n_{\text{EO}} \\
 & n_{\text{O}_2}^1 = n_{\text{O}_2}^{02} &
 \end{array} \quad (13)$$

mit deren Hilfe das mathematische Modell des Massenbilanzes in primärer Form (Tabelle 3) erhalten wird.

Tabelle 3

Algebraische Gleichungen des Massenbilanzes in primärer Form (A Variante)

Komp.	Massenbilanzgleichungen	
	mol.	molbrüche
CH	$n_{\text{E}} = n_{\text{E}}^0(1 - \alpha)$	$X_{\text{E}} = \frac{1 - \alpha}{A - \frac{1}{2}(\alpha - \beta)}$
C ₂ H ₄ O	$n_{\text{EO}} = n_{\text{E}}^0(\alpha - \beta) + n_{\text{EO}}^0$	$X_{\text{EO}} = \frac{1 + \alpha - \beta}{A - \frac{1}{2}(\alpha - \beta)}$
CO ₂	$n_{\text{CO}_2} = n_{\text{CO}_2}^0 + 2n_{\text{E}}^0 \cdot \beta$	$X_{\text{CO}_2} = \frac{\dot{X}_{\text{CO}_2}^0 + 2\beta}{A - \frac{1}{2}(\alpha - \beta)}$
H ₂ O	$n_{\text{H}_2\text{O}} = n_{\text{H}_2\text{O}}^0 + 2n_{\text{E}}^0 \cdot \beta$	$X_{\text{H}_2\text{O}} = \frac{\dot{X}_{\text{H}_2\text{O}}^0 + 2\beta}{A - \frac{1}{2}(\alpha - \beta)}$
O ₂	$n_{\text{O}_2} = n_{\text{O}_2}^0 - \frac{1}{2}n_{\text{E}}^0(\alpha + 5\beta)$	$X_{\text{O}_2} = \frac{\dot{X}_{\text{O}_2}^0 - \frac{1}{2}(\alpha + 5\beta)}{A - \frac{1}{2}(\alpha - \beta)}$
A''	$n_{\text{A}''} = n_{\text{A}''}^0$	$X_{\text{A}''} = \frac{\dot{X}_{\text{E}}^0}{A - \frac{1}{2}(\alpha - \beta)}$
Total	$n_{\text{T}} = n_{\text{T}}^0 \left[1 - \frac{1}{2} X_{\text{E}}^0(\alpha - \beta) \right]$	$\Sigma X_i = 1$

Weil man das Kohlendioxyd und Äthylenoxyd aus den Gasen die den Reaktor verlassen leicht bestimmen kann, verwendet man die Einsatzbeziehungen (14),

$$n_E^0 \cdot \beta = \frac{1}{2}(n_{CO_2} - n_{CO_2}^0)$$

$$n_E^0 \cdot \alpha = n_{EO} + \frac{1}{2}(n_{CO_2} - n_{CO_2}^0) \quad (14)$$

mit deren Hilfe die sekundäre Bilanzgleichungen der Tabelle 5 festgelegt werden.

Für die B Variante, definieren wir die Konversionen η_1' und η_2' :

$$\eta_1' = \frac{n_E^{01} - n_E^1}{n_E^{01}} = \frac{n_{O_2}^{01} - n_{O_2}^1}{\frac{1}{2} n_E^{01}} = \frac{n_{EO}^1 - n_{EO}^{01}}{n_E^{01}} \quad (15)$$

$$\eta_2' = \frac{n_E^{02} - n_E^2}{n_E^{02}} = \frac{n_{CO_2}^{02} - n_{CO_2}^2}{3n_E^{02}} = \frac{n_{CO_2}^2 - n_{CO_2}^{02}}{2n_E^{02}} = \frac{n_{H_2O}^2 - n_{H_2O}^{02}}{2n_E^{02}} \quad (16)$$

Tabelle 4

Algebraische Gleichungen des Massenbilanzes in sekundärer Form (A Variante)

Komp.	Massenbilanzgleichungen
C_2H_4	$n_E = n_E^0 - n_E^{01} \cdot \eta_1 - n_E^{02} \cdot \eta_2$
C_2H_4O	$n_{EO} = n_E^{01} \cdot \eta_1 + n_{EO}^0$
CO_2	$n_{CO_2} = n_{CO_2}^0 + 2n_E^{02} \cdot \eta_2$
H_2O	$n_{H_2O}^0 = n_{H_2O}^0 - 2n_{H_2O}^{02} \cdot \eta_2$
O_2	$n_{O_2} = n_{O_2}^0 - \frac{1}{2} n_E^{01} \cdot \eta_1 - 3n_E^{02} \cdot \eta_2$
A''	$n_{A''} = n_{A''}^0$
Total	$n_T = n_T^0 - \frac{1}{2} n_E^{01} \cdot \eta_1$

die mit den Konkretisationsbeziehungen (17) zu dem in der Tabelle 4 wieder-gegebene mathematische Massenbilanzmodell, führt.

$$\begin{array}{ll}
 n_E^0 = n_E^{01} + n_E^{02} & n_E = n_E^1 + n_E^2 \\
 n_{O_2}^0 = n_{O_2}^{01} + n_{O_2}^{02} & n_{O_2} = n_{O_2}^1 + n_{O_2}^2 \\
 n_{CO_2}^0 = n_{CO_2}^{01} & n_{EO} = n_{EO}^1 \\
 n_{H_2O}^0 = n_{H_2O}^{02} & n_{CO_2} = n_{CO_2}^2 \\
 & n_{H_2O} = n_{H_2O}^2 \\
 & n_{A''} = n_{A''}^0
 \end{array} \quad (17)$$

Zieht man in Betracht das wieder Kohlendioxyd und Äthylenoxyd die experimentell bestimmbare Komponente sind, erhält man die Einsatzgleichungen:

$$n_E^{02} \cdot \eta_2' = \frac{1}{2}(n_{CO_2} - n_{CO_2}^0) \quad (18)$$

$$n_E^{01} \cdot \eta_1' = n_{EO} - n_{EO}^0$$

Wendet man die Einsatzgleichungen (18) an so werden die sekundäre Bilanzgleichungen erhalten die mit denen aus der Tabelle 5 der A Variante identisch sind.

Die Tatsache, das beide Varianten zu den selben sekundären Gleichungen führen zeigt uns das das mathematische Modell des Massenbilanzes im Oxy-

Tabelle 5

Algebraische Gleichungen des Massenbilanzes in primärer Form (B Variant)

Komp.	Massenbilanzgleichungen
C_2H_4	$n_E = n_T^0 \left[\bar{X}_E^0 + \frac{1}{2} \bar{X}_{CO_2}^0 - \frac{1 - X_{EO}^0}{1 + \frac{1}{2} X_{EO}^0} \left(\bar{X}_{EO} + \frac{1}{2} \bar{X}_{CO_2} \right) \right]$
C_2H_4O	$n_{EO} = \frac{n_T^0 [(1 - X_{EO}^0)]}{1 + \frac{1}{2} X_{EO}^0} \cdot \bar{X}_{EO}$
CO_2	$n_{CO_2} = \frac{n_T^0 [(1 - X_{EO}^0)]}{1 + \frac{1}{2} X_{EO}^0} \cdot \bar{X}_{CO_2}$
H_2O	$n_{H_2O} = n_T^0 \left[X_{H_2O}^0 - \bar{X}_{CO_2} + X_{CO_2} \left(\frac{1 - X_{EO}^0}{1 + \frac{1}{2} X_{EO}^0} \right) \right]$
O_2	$n_{O_2} = n_T^0 \left[X_{O_2}^0 + \frac{3}{2} \bar{X}_{CO_2}^0 - \frac{1 - X_{EO}^0}{1 + \frac{1}{2} X_{EO}^0} \left(\frac{1}{2} \bar{X}_{EO} + \frac{3}{2} \bar{X}_{CO_2} \right) \right]$
A''	$n_{A''} = n_T^0 \cdot X_{A''}^0$
Total	$n_T = \frac{n_T^0 (1 - X_{EO}^0)}{1 + \frac{1}{2} X_{EO}^0}$

dationsprozess des Äthens zu Äthylenoxyd, auf Grund geringer Anzahl von stöchiometrischen Gleichungen und unabhängig davon ob die Reaktionen gleichzeitig oder nacheinander ablaufen, bestimmt werden kann.

3. Die experimentelle Prüfung des Bilanzmodells. Für die experimentelle Prüfung der Bilanzgleichungen wurden Messungen an einem industriellen Oxydationsreaktor des Äthens zu Äthylenoxyd durchgeführt. Die gemessene chemische Zusammensetzungen bei Eingang und Ausgang des Reaktors sind in Molbruchteilen ausgedrückt und in Tabelle 6 wiedergegeben.

Die gute Übereinstimmung der berechneten und der experimentell gemessenen Werte bestätigt die Richtigkeit des vorgeschlagenen mathematischen Bilanzmodells.

4. Berechnung der Katalysatorenspezifität. Obwohl für die erwünschte Reaktion ein Katalysator mit guter Selektivität benutzt wurde, ein Teil des Äthens verwandelt sich in Sekundärprodukte. Deshalb ist es sehr wichtig das

die Selektivität des Katalysators leicht und aus geringer Anzahl von messbaren Größen bestimmt werden kann.

Benützt man die Definitionsbeziehung der Selektivität, die in unserem Fall in der Gleichung (19) gegeben ist, so wie auch die Massenbilanzgleichungen der Tabelle 5, wird die Gleichung (20) erhalten.

$$S = \frac{n_E^0 \cdot \eta_1 - n_E^0 \cdot \eta_1 \cdot \eta_2}{n_E^0 \cdot \eta_1} = 1 - \eta_2 \quad (19)$$

Sie erlaubt die Selektivitätsbestimmung auf Grund zweier Konzentrationen (Kohlendioxyd und Äthylendioxyd),

$$S = 1 - \frac{0,5(\gamma \cdot X_{CO_2} - X_{CO_2}^0)}{\gamma(X_{EO} + 0,5X_{CO_2}) - 0,5X_{CO_2}^0 - X_{RO}^0}; \quad \gamma = \frac{1 + 0,5 X_{EO}^0}{1 + 0,5 X_{RO}^0} \quad (20)$$

die experimentell bestimmt werden können.

Enläuterung der Bezeichnungen

- A_n — Elementenmatrix;
- A_{Ri} — Reaktionsmatrix;
- A_{Ri}^T — Transponierte Reaktionsmatrix;
- C — Anzahl der Komponenten der Reaktionsmasse;
- i — Ordnungszahl der Reaktion, $i = 1, 2, 3$ —
- $[K]_s$ — die Masse des festen Katalysators;
- L — Anzahl der unabhängigen stöchiometrischen Gleichungen;
- n_j^{oi} — Anfangsmolzahl der Komponente j die bei der i Reaktion teilnimmt;
- n_T^0 — Molzahl der Anfangsreaktionsmasse;
- n_T — Gesamtmolzahl der Endreaktionsmasse;
- R — Rang der Elementenmatrix;
- X_j^0 — Anfangsmolarbruch der j Komponente;
- X_j — Endmolarbruch der j Komponente;
- α, β — Konversionen definiert durch die Beziehungen $\alpha = \eta_1$ und $\beta = \eta_1 \cdot \eta_2$
- η_1, η_2 — Konversionen des Äthens bzw. des Äthylendioxyds;
- η'_1, η'_2 — Konversionen des Äthens bei gleichzeitigen Reaktionen;
- $[]_g$ — untere Index für die Gasphase;
- EO — Äthylendioxyd;
- E — Äthen;
- A'' — Inerte;

Tabelle 6

Bilanz des Oxidationsreaktors des Äthens erhalten bei: $P = 22,5 \text{ ata.}; T = 483 \text{ K}$

Komp.	Zusammensetzung		
	Eingang gemessen	Ausgang	
		gemessen	berechnet
C_2H_4	0,15	0,1367	0,1367
O_2	0,47	0,0536	0,05359
C_2H_4O	50 p.p.m.	0,0103	0,0103
CO_2	0,1055	0,1137	0,1136
H_2O	0,0021	0,0098	0,0098
N_2	0,6742	0,6759	0,6760
Total	0,9999	1,0	0,9999

L I T E R A T U R

1. P. Krypillo, L. Mögling, D. Klosse, M. Süptitz, *Chem. Techn.* **34** (2), 85 (1982).
2. E. Alter, L. Bruns, W. Volprecht, *Pat. Germ. Offen D. E.* 3, 014, 091, *Chem. Abstr.* **96**, 12.100c 1982.
3. V. S. Sokolov, E. P. Otborkina, V. A. Davydov, B. B. Chesnokov, *Kinetika i Kataliz* **28** (2), 398 (1987).
4. C. Calistru, C. Leonte, „Tehnologia substanțelor anorganice”, Editura did. și ped., București, 1972.
5. B. Maydond, G. Hays, *Chem. Eng. Progr.* **45**, 452 (1949).
6. A. G. Leibuş, *Khim. Prom.*, **1960**, 213.
7. G. I. Projenik, A. I. Strejenski, *Khim. Prom.* **1969**, 39.
8. C. Calistru, I. Siminiceanu, C. Hagiu, C. Petrilă, *Rev. chim. (București)*, **24**, 880 (1973).
9. I. Siminiceanu, A. Pop, L. Cormoş, *Chem. Techn.*, **33** (2), 77 (1981).
10. I. Siminiceanu, C. Calistru, A. Pop, *Stud. Univ., Babeş-Bolyai, Chem.* **26** (1), 40 (1981).
11. M. H. Karapetiant, „Termodinamică chimică”, Editura Tehnică, București, 1956.

A STUDY ON THE SEPARATION OPTIMIZATION OF SOME SYNTHETICAL AMINO ACID AND PEPTIDE DERIVATIVES THROUGH THIN LAYER CHROMATOGRAPHY

SIMION GOCAN*, LILIANA OLENIC** and EUGEN VARGHA*

Received: June 17, 1988

This paper presents the results concerning the optimization of some eluent systems for the thin layer chromatography of silica gel of an activity degree of 0.45 of some amino acid and peptide derivatives. In the case of the amino acid derivatives the best results have been obtained with the following eluent: ethyl acetate/2-propanol/chloroform/petroleum ether (1:1:1:1.29, v/v); and in the case of peptide and amino acid derivatives with the following eluent: ethyl acetate/2-propanol/chloroform (7:1:2, v/v).

A central problem of chromatography is that of the optimization of eluent systems for the separation of mixtures of given samples. An analyst is evidently interested in obtaining the desired result by a minimum number of experiments. As to this respect Snyder's writings [1, 2] were really helpful because he gives a classification of a great number of solvents into eight groups according to their capacity of being proton donors or proton acceptors and strong dipole interactors.

In order to study the separation optimization through thin layer chromatography of some synthetical amino acid and peptide derivatives we choose the following seven solvents belonging to different groups: diethyl ether (I; 2.8), 2-propanol (II; 3.9), acetic acid (IV; 6.0), methylene chloride (V; 3.1), ethyl acetate (VII; 4.4), benzene (VIII; 2.7) and chloroform (VIII; 4.1). The Raman figures point to the group to which they belong while the Arabic ones indicate the Solvent strength: P' . The solvent strength of a mixture will be obtained through the following relation $P' = \sum f_i P_i$, where f_i is the volume fraction of the solvent i in the mixture, while P' is its strength; in the case of the petroleum ether P' was considered equal to zero [1, 2]. Then a separation was performed on each of these solvents in order to choose those that give best separations. Thus, three solvents were chosen: ethyl acetate, chloroform and 2-propanol. Using these solvents, a series of mixtures were made. This method is similar to that suggested by Nyiredy et al. [3-6] and is known as the „Prisma” model. Using this method, they achieved optimization of some eluent systems for the separation by thin layer chromatography of some synthetical amino acid and peptide derivatives in a very short time and by very few experiments.

Evaluation of the separations was made according to a criterion suggested by Gocan and Liteanu [7], which involves the calculation of an index I_p which

* University of Cluj-Napoca, Faculty of Chemical Technology, 3400 Cluj-Napoca Romania
** Chemistry Institute of Cluj-Napoca, 3400 Cluj-Napoca, Romania

measures the deviation from a separation which we consider ideal. This index is given by the following relation :

$$I_P = \sqrt{\sum (\Delta \bar{h}R_f - \Delta hR_{f,i})^2 / N(N+1)}$$

where N is the number of samples from the mixture to be separated, $\Delta \bar{h}R_f = 100/(N+1)$ is the "ideal medium interval" when all the N samples would be distributed on a chromatogram at an equal distance without occupying the starting and the front line, $\Delta hR_{f,i} = hR_{f,i+1} - hR_{f,i}$ are the intervals obtained experimentally between 0 and 100, once the hR_f values were arranged in an increasing order. The lower the value of the I_P , the better the separation.

Experimental. Ready-made R-silica gel plates produced by the Chemistry Institute in Cluj-Napoca were used. The activity degree of the silica gel layer was determined experimentally and was found to be: $\alpha = 0.49$. The determination was made with the following test dyes (p-aminazobenzene, Sudan red and Sudan yellow), using benzene as an eluent [8].

The development was performed in saturated N-chromatographic chambers. The eluents which were used are given in Tables 1 and 2. They were made at "Reactivul"—Bucharest.

The samples to be analysed were synthetical amino acid and peptide derivatives [9]. The detection was made with iodine vapours.

Table 1

The hR_f and I_P values of amino acid derivatives

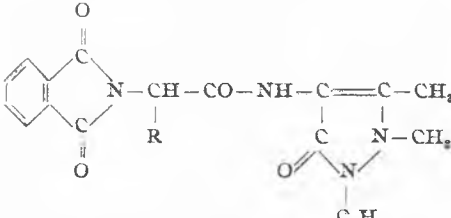
Eluent	P'					I_P
		-H	$-(CH_2)_2SCH_3$	$-R$ $-CH_2C_6H_5$	$-(CH_2)_2CO_2H$	
Ethyl ether	2.8	8	19	24	0	14.12
2-Propanol	3.9	81	85	84	10	12.99
Acetic acid	6.0	100	100	100	100	20.00
Methylen chloride	3.1	0	0	0	0	20.00
Ethyl acetate	4.4	30	66	84	3	5.54
Benzene	2.7	0	0	0	0	20.00
Chloroform	4.1	78	80	82	18	10.62
Ethyl acetate/ 2-Propanol/ $CHCl_3$:						
(1: 1: 1, v/v)	3.99	93	95	95	7	17.04
(7: 1: 2, v/v)	4.29	66	83	81	3	11.17
(2: 1: 7, v/v)	4.14	76	88	88	3	13.46
(2: 7: 1, v/v)	4.02	86	92	91	8	14.56
(1: 7: 2, v/v)	3.99	93	98	99	9	16.07
Ethyl acetate/ 2-Propanol/ $CHCl_3$ / Petroleum ether:						
(1: 1: 1: 1, 29 v/v)	2.89	76	88	88	3	13.46
(1: 1: 1: 2.45, v/v)	2.27	66	85	89	0	11.95
(7: 1: 2: 2.45, v/v)	1.32	22	48	55	0	7.85
(1: 2: 7: 2.45, v/v)	3.27	64	83	89	4	10.33
(1: 7: 2: 2.45, v/v)	3.19	77	88	82	4	13.32

Table 2

The R_f and I_P values of peptide and amino acid derivatives

Eluent	$ \begin{array}{c} H_3C-CHCO-NHCHCO-NHC_6H_4OCH_3 \\ \quad \\ H_2C \quad NH \\ \diagdown \quad / \\ \quad C \\ \quad \\ \quad O \end{array} $						$ \begin{array}{c} R_2-CH-CO-NH-C(=O)-CH_3 \\ \\ R_1 \end{array} $						$ \begin{array}{c} O=C \\ \\ N-CH_3 \\ \\ N \\ \\ C_6H_5 \end{array} $					
	P^r	R	R_1/R_2	R_1/R_3	R_1/R_3	I_P	P^r	R	R_1/R_2	R_1/R_3	R_1/R_3	I_P						
Ethyl ether	2.8	10	3	4	4	0	-H	-CH(CH ₃) ₂	-C ₆ H ₅	-H	14.70							
2-Propanol	3.9	91	84	76	86	33	91	84	76	80	8.27							
Acetic acid	6.0	100	100	100	100	100	100	100	100	100	5.35							
Methylen chloride	9.1	0	0	0	0	0	0	0	0	0	6.08							
Ethyl acetate	4.4	35	23	11	25	2	4.4	35	11	2	16.67							
Benzene	2.7	0	0	0	0	0	0	0	0	0	9.82							
Chloroform	4.1	63	63	58	63	27	63	58	58	27	16.67							
Ethyl acetate/2-Propanol/(CHCl ₃):																		
(1:1:1, v/v)	3.99	93	88	80	91	27	93	88	80	27	8.27							
(7:1:2, v/v)	4.29	76	60	47	67	7	76	60	47	7	5.35							
(2:1:7, v/v)	4.14	79	65	67	69	25	79	65	67	25	6.08							
(2:7:1, v/v)	4.02	93	84	84	91	31	93	84	84	31	8.58							
(1:7:2, v/v)	3.99	95	89	89	96	41	95	89	89	41	8.89							
Ethyl acetate/2-Propanol/(CHCl ₃)/ petroleum ether																		
(1:1:1:1.29, v/v)	2.89	79	74	69	76	14	79	74	69	14	8.23							
(1:1:1:2.45, v/v)	2.27	82	66	62	69	10	82	66	62	10	7.43							
(7:1:2:2.45, v/v)	1.32	39	17	11	21	2	39	17	11	2	9.16							
(1:7:2:2.45, v/v)	3.19	91	75	73	80	17	91	75	73	17	8.14							

Results and discussion. The experimental results obtained are given in Tables 1 and 2.

In the case of the amino acid derivatives given in Table 1, the best separations were obtained with the following mono-component elements: ethyl acetate, chloroform, 2-propanol and diethyl ether. A series of mixtures were obtained with the first three. The best result ($I_P = 11,17$) was obtained with the mixture in which the ethyl acetate has the highest concentration. To these ternary mixture, petroleum ether was added in order to diminish the strength of the eluent and to lower the hR_f values. Evidently, in this case too, the best result ($I_P = 7,85$) was given by the eluent which contained the most amount of ethyl acetate.

According to their basic structure the three derivatives behave as expected from a chromatographic point of view. The $R = -(\text{CH}_2)_2 - \text{COOH}$ derivative, being most polar, will have the lowest hR_f values. On the contrary the $R = -(\text{CH}_2)_2 - \text{S} - \text{CH}_3$ derivatives will have weaker interactions with the $-\text{OH}$ groups of the silica gel than the basic $R = -\text{H}$ derivative, but stronger than those of the highest hR_f values being the least polar.

In the case of the amino acid and peptide derivatives given in Table 2, the best results were obtained with the same solvents. The best separation ($I_P = 5,35$) was obtained with the eluent formed by: ethyl acetate/2-propanol/chloroform (7:1:2, v/v).

By adding petroleum ether we succeeded in bringing all the hR values of all the constituents to lower values without obtaining better separations. The selectivity of the separation is embettered by the growth of the proportion in the ethyl acetate.

As to the chromatographic behaviour of the first derivatives from Table 2, we came to the conclusion that when using the ethyl acetate as an eluent, the $R = -\text{C}_6\text{H}_5$ derivative has the hR_f value of 25 compared to the $R = -\text{H}$ derivative which has the hR_f value of 35. In the first case the peptide derivative gives a stronger interaction with the stationary phase than the other derivative, as it results from their chromatographic behaviour.

In the case of the last two derivatives from Table 2 the $R_1 = -\text{NH}_2$ and $R_2 = -\text{CH}_2 - \text{C}_6\text{H}_5$ groups give a more polar character to the respective derivative than the $R_1 = -\text{H}$ and $R_2 = -\text{NH}-\text{CO}_2-\text{CH}_2-\text{C}_6\text{H}_5$ groups, a fact confirmed by their chromatographic behaviour.

REFERENCES

1. L. R. Snyder, *J. Chromatog.*, **92**, 223 (1974).
2. L. R. Snyder, *J. Chromatog. Sci.*, **16**, 223 (1978).
3. Sz. Nyiredy, B. Meier, C. A. J. Erdelmeier, O. Sticher, *J. High Resolut. Chromatog., Chromatogr. Commun.*, **8**, 186 (1985).

4. Sz. Nyiredy, C. A. J. Erdelmeier, B. Meier, O. Sticher, in E. Tyihák (Editor), "Proceedings on TLC with Special Emphasis on OPLC, Labor MIM Comp.," Budapest, 1986, p. 222.
5. Sz. Nyiredy, C. A. J. Erdelmeier, B. Meier, O. Sticher, *GIT Suppl. Chromatog.*, **4**, 24 (1985).
6. K. Dallenbach-Toelke, Sz. Nyiredy, B. Meier, O. Sticher, *J. Chromatog.*, **365**, 63 (1986).
7. S. Gocan, V. Litranu, *Stud. Univ. Babeş-Bolyai, Chem.*, **33** (2), 82 (1988).
8. G. Vernin, "La France et ses Parfums", no 64, 205.
9. E. Vargha, D. Breazu, E. Szántai, L. Moraru, *Stud. Univ. Babeş-Bolyai, Chem.*, **27**, 64 (1982).

A STUDY ON SOME PERFORMANCE INDICES USED IN THIN LAYER CHROMATOGRAPHY

SIMION GOCAN* and VICTOR LITEANU*

Received: June 18, 1988

The present paper offers a computer compared of two quality indices of separation in TLC: the former is of information type, the latter, the proposed one, concerns the distribution of the chromatogram, in relation to that considered ideal. The advantage of using the second index may be noticed. The proposed quality index can be used in optimizing chromatographic separation.

The criteria derived from the information theory [1-4] have been found to be the most adequate of all the criteria used in considering the quality of thin layer chromatographic separations. The fact that results obtained in separations in thin layer chromatography are mainly presented in the form of tables by R_f or hR_f values accounts for this. However, there are few cases in which the result of separation is presented in the form of some registered densitograms (each spot corresponds to a peak shaped curve) or under the form of some values that are in accordance with the resolution between two adjacent peaks.

On the other hand it concerns informational criteria inconveniences, which arise from their being derived into classes. First, the number of classes is to be the same, in order to allow for a comparison of the amounts of information. Secondly, two values of neighbouring classes may be closer to each other than two values belonging to the same class.

This study aims at suggesting a new performance index I_p , that measures the deviation in case of an ideally considered separation.

Experimental. Thin layer polyamide 11 F₂₅₄ (Merck) chromatographic plates (0,15 mm) have been employed in order to separate a mixture of polyphenols. The developings have been performed in saturated N-chambers, by testing a number of 12 eluent systems, whose composition is shown in Table 1. The detection of components has been performed by spraying first with diazotized p-nitroaniline, and then with a 10% NaOH solution [5].

Layers of microcrystalline cellulose have been used in order to separate the amino acids. The developings have occurred in saturated N-chambers. The classic method (with ninhydrin) has been used for the detection. Table 2 shows the eluent-systems that have been used.

Results and discussion. A computer study of the amount of information, in accordance with the number of classes has been employed, in an initial stage.

The amount of information accompanying each separation has been computed by means of Shannon's well-known relation:

$$I \cong - \sum_{i=1}^N f_i \log_2 f_i \cong -1.443 \sum_{i=1}^N f_i \ln f_i \quad (\text{bits}) \quad (1)$$

* University of Cluj-Napoca, Faculty of Chemical Technology, Department of Inorganic and Analytical Chemistry, 3400 Cluj-Napoca, Romania

The hR_f values of polyphenols

Set	Eluent	Phenol	Pyrocatechol	Hydroquinone	Resorcinol	Pyrogallol	Phloroglucinol
1	I	72	52	42	41	31	16
2	II	77	56	49	45	36	22
3	III	73	58	51	48	40	25
4	IV	70	56	51	49	42	28
5	V	72	48	34	32	23	10
6	VI	79	26	21	13	0	0
7	VII	49	14	10	7	0	0
8	VIII	30	4	2	2	3	4
9	IX	41	12	4	3	3	0
10	X	50	16	6	5	3	4
11	XI	69	47	36	33	27	12
12	XII	65	40	26	23	17	6

Eluent:	I	-	Buthyl acetate/benzene/acetic acid/methanol (11:34:4:8, v/v);
	II	-	" " " " (22.5:22.5:4:8, v/v);
	III	-	" " " " (34:11:4:8, v/v);
	IV	-	Buthyl acetate/acetic acid/methanol (45:4:8, v/v);
	V	-	Benzene/acetic acid/methanol (45:4:8, v/v);
	VI	-	Ethyl acetate/benzene (2:1, v/v);
	VII	-	Buthyl acetate/benzene (2:1, v/v);
	VIII	-	Benzene/acetic acid/water (45:4:8, v/v);
	IX	-	" " " " (6:3:1, v/v);
	X	-	" " " " (4:2:1, v/v);
	XI	-	Buthyl acetate/benzene/acetic acid/water (2:2:2:1, v/v);
	XII	-	" " " " (2:2:1:2, v/v).

in which $f_i = N_i/N$ are relative frequencies, N_i — the number of hR_f values within a class and N — the total number of spots.

Tables 1 and 2 show the results obtained with the two sets of experimental data. They have been further processed by using a Fortran 77 programme. The amount of information I is obviously an index for the efficiency of separation, the higher the value of I the better the separation.

Table 3 shows the correspondence between the number of classes and I . Generally, an increase in the number of classes, brings about the expected increase in the amount of information. However, with several eluents the value of I oscillates (as apparent in Table 3).

An examination of the values of relative frequencies f_i on the computer listing reveals that the oscillations of I result precisely from changes f_i .

The changes f_i arise from their dependence on the number of classes. Consequently, we find it necessary that the number of classes should be specified when the efficiency of a thin layer separation is presented by means of the amount of information I .

Further on, we suggest a performance index, I_p , to, measure the deviation from a supposedly ideal separation. In this respect, we consider the thin layer chromatography separation of a mixture of N components. All the N components are totally separated as well as distributed on the whole extend of the cro-

Table 2

The hR_f Values of amino acids

Set	Eluent	L-IHS HCl	L(+)-LYS HCl	L(-)-ARG HCl	D,L-SER	L(+)-ASP	GLY	D,L-THR	L-GLU	D,L-ALA	L(-)-PRO	L(-)-TYR	D,L-MET	D,L-VAL	L-LEU
13	I	16	17	21	21	22	23	26	27	31	36	46	49	50	65
14	II	3	3	5	9	7	9	14	12	20	24	25	37	42	57
15	III	26	28	31	34	34	38	41	45	52	53	57	64	67	77
16	IV	12	12	16	17	17	20	20	24	25	27	36	41	43	57
17	V	7	7	8	9	10	12	18	16	20	25	35	41	39	53
18	VI	11	11	14	17	16	18	25	26	32	36	46	52	51	65
19	VII	9	11	14	20	22	23	29	19	35	41	47	55	57	72
20	VIII	12	6	6	15	8	16	24	9	23	32	34	46	48	63
21	IX	69	72	60	72	73	76	76	74	78	76	73	78	80	84

Eluent: I - Butanol/acetic acid/water (12:3:5, v/v);
 II - " " " (8:2:1, v/v);
 III - " " " (2:1:1, v/v);
 IV - " " " (4:1:5, v/v);
 V - Butanol/acetone/acetic acid/water (35:35:7:23, v/v);
 VI - " " " " (35:35:10:20, v/v);
 VII - Butanol/formic acid 80%/water (15:3:2, v/v);
 VIII - γ -propanol/water (4:1, v/v);
 IX - Chloroform/methanol/ NH_4OH 35% (9:8:4, v/v).

matogram. The first component should not be placed on the starting line and neither should the last one be on the line of the eluent. $N - 1$ intervals exist between the N components. Besides, the two marginal intervals are considered. Therefore, there are $N + 1$ intervals. In the case of an ideal separation, the value of the theoretical interval between two adjacent components will be:

$$\Delta h\overline{R}_f = 100/(N + 1) \quad (2)$$

The experimental values hR_f are arranged in an ascending scale and the experimental intervals are calculated:

$$\Delta R_{f,1} = hR_{f,1} - 0 = hR_{f,1}$$

$$\Delta hR_{f,i} = hR_{f,i} - hR_{f,i-1}, \quad i = 2, \overline{N} \quad (3)$$

$$\Delta hR_{f,N+1} = 100 - hR_{f,N}$$

Table 3

The I and I_P values vs. the number of classes

Set	I bits											I_P			
	10	15	16	17	18	19	20	21	22	23	24		25		
1	2.76	2.25	2.25	2.68	2.25	2.25	2.25	2.25	2.25	2.25	2.25	2.25	2.58	2.25	4.96
2	2.25	2.28	2.25	2.58	2.25	2.58	2.25	2.58	2.58	2.58	2.58	2.58	2.58	2.58	4.42
3	1.92	2.25	2.58	2.25	2.58	2.25	2.58	2.25	2.58	2.25	2.58	2.25	2.58	2.58	5.03
4	1.92	2.25	2.25	2.25	2.58	2.25	2.58	2.25	2.58	2.25	2.58	2.25	2.58	2.25	5.73
5	2.25	2.58	2.25	2.25	2.58	2.25	2.25	2.58	2.25	2.58	2.25	2.25	2.58	2.25	5.06
6	1.92	1.92	2.25	2.25	2.25	2.25	2.25	2.25	2.25	2.25	2.25	2.25	2.25	2.25	7.68
7	1.46	1.92	1.92	1.92	1.92	1.92	1.92	1.92	1.92	1.92	1.92	1.92	1.92	1.92	9.42
8	0.65	0.65	0.65	0.65	0.65	0.65	0.65	0.65	0.65	0.65	0.65	0.65	0.65	0.65	11.90
9	1.25	1.25	1.25	1.25	1.25	1.25	1.25	1.25	1.25	1.25	1.25	1.25	1.25	1.25	10.29
10	1.25	1.25	1.25	1.79	1.79	1.79	1.92	1.92	1.92	1.92	1.92	1.92	1.92	1.92	9.21
11	2.25	2.25	2.25	2.58	2.58	2.25	2.58	2.58	2.25	2.58	2.25	2.58	2.58	2.58	5.42
12	2.25	2.25	2.58	2.58	2.25	2.25	2.58	2.58	2.25	2.25	2.25	2.25	2.58	2.58	6.20
13	2.27	2.55	2.61	2.81	2.75	2.61	2.81	2.81	2.84	2.81	2.84	3.04	2.95	2.81	2.80
14	2.22	2.55	2.75	2.84	2.84	2.70	2.81	2.81	2.95	2.81	2.95	3.04	3.18	3.09	3.23
15	2.47	3.04	2.90	3.04	3.18	3.09	3.18	3.18	3.09	3.18	3.09	3.47	3.24	3.24	2.28
16	2.00	2.61	2.70	2.35	2.41	2.69	2.70	2.84	2.70	2.84	2.70	2.90	2.95	2.70	3.24
17	2.38	2.27	2.41	2.55	2.55	2.50	2.81	2.81	2.95	2.81	2.95	2.84	2.84	3.18	3.44
18	2.27	2.81	2.66	3.04	3.09	2.70	2.84	2.84	2.66	2.84	2.66	3.04	3.09	3.18	2.68
19	2.61	3.04	3.09	2.95	3.32	3.24	3.18	3.18	3.32	3.18	3.32	3.38	3.24	3.24	2.19
20	2.47	3.04	2.75	2.75	2.61	2.81	2.66	3.09	2.66	3.09	2.66	2.90	2.90	2.90	2.85
21	1.15	1.73	1.59	1.75	2.02	1.73	2.01	1.75	2.02	1.75	2.02	2.13	2.15	2.15	4.06

The performance index I_p is calculated by means of the relation :

$$I_p = \sqrt{\frac{\sum_{i=1}^N (\Delta h R_{f,i} - \Delta h \bar{R}_f)^2}{N(N+1)}} \quad (4)$$

I_p represents the average square deviation of the mean of the selection, of the values of experimental intervals $\Delta h R_{f,i}$, as compared to the theoretical one $\Delta h \bar{R}_f$.

The computed I_p values are shown in Table 3. A separation will be considered to be more successful if the obtained value I_p is lower.

Unlike I , I_p itself, taking into account the distributions of the values $h R_f$ the chromatogram, is not influenced by the class division. This index measures any deviation from a supposedly ideal separation.

A comparison of the resulting values (Table 3) reveals the existence of a parallelism for the data sets for which I is minimum; I_p , as expected, has the highest values. Conversely, higher values of I correspond to lower values for I_p . E.g., in the case of the data set 8 (Table 3) the lowest value was obtained for I , and the highest one for I_p ; in the case of sets 19 and 20 (Table 3) high values for I and, respectively, low for I_p have been obtained.

We may conclude by stating the adequacy and the univocal value of the performance index I_p . I_p can be successfully employed in the estimation of thin layer chromatography separations as well as in the optimization of some eluent systems.

REFERENCES

1. C. Shannon "The Mathematical Theory of Communication" *Bell Syst. Tech. J.*, **27**, 379 (1948).
2. H. Kaiser, *Analyt. Chem.*, **42**, (2) 24A (1970).
3. J. Simon, M. Lederer, *J. Chromatog.*, **63**, 448 (971).
4. D. L. Massart, *J. Chromatog.*, **79**, 157 (1973).
5. L. Krauss, D. Dupokova, *Pharmazie*, **19**, 41 (1964).

ELECTROSYNTHESIS OF PROPIONITRILE

IV. Effect of the cathode crystalline structure on the faradaic yield¹

LIVIU ONICIU*, DAN A. LÓWY**, MARIA JITARU** and BOGDAN C. TOMA**

Received: June 27, 1988

Literature data reveal the electrocatalytic influence of "d-type" and "sp-type" metals, respectively, upon the acrylonitrile electroreduction process. Our experiments demonstrate that the selectivity of the propionitrile formation is strongly influenced by the crystalline structure of the cathodic metal, regardless of whether it belongs to the main or to the transitional metal group. Thus, the b.c.c. — structure metals without deviation in the lattice from the ideal ($\Delta = 0$): Fe and Cr, gave poor faradaic yields (r_F) in the propionitrile electro-synthesis. H.c.p. metals: Cd ($\Delta = 0.16$), Zn ($\Delta = 0.14$) and Co ($\Delta = 0$) behaved better ($r_F = 22 - 54\%$). Ideal — lattice f.c.c. metals: Cu, Ni, Pb and Al had the best behaviour, ensuring current yields up to 90%. An electrocatalytic explanation of the phenomena is put forward.

Literature data reveal the electrocatalytic influence of "d-type" and "sp-type" metals, respectively, on the electroreduction of homogeneous double bonds. The particular example of the activated C=C bond of acrylonitrile is mentioned [1].

The electrocatalytic activity of the cathode material in the non-dimerizant electroreduction (NDE) of acrylonitrile (AcN) to propionitrile (PN) was pointed out in our previous papers [2, 3]. The plot of the faradaic yield of the process vs. the exchange current density of the hydrogen electrode reaction (i_0), revealed different behaviour of the metals (Fig. 1): the sp-metals, set on a "volcano-shaped" curve, were poor catalysts, while the d-metals generally showed a better activity. However, two significant exceptions were found: on iron and chromium, typical d-type metals, an intense hydrogen evolution occurred.

Taking into account the above mentioned exceptions, we realized that the selectivity of PN formation — under identical electrochemical conditions — is determined essentially by the crystalline structure of the cathodic metal, regardless of whether it belongs to the main or to the transitional group (see Fig. 2). The aim of our paper is to demonstrate this.

Abbreviations: AcN — acrylonitrile; PN or AcNH₂ — propionitrile; NDE — non-dimerizant electroreduction; b.c.c. — body-centred cubic structure; h.c.p. — hexagonal closed-packed; f.c.c. — face-centred cubic structure; i_0 — exchange current density of the hydrogen electrode reaction; i — current density; r_F — faradaic yield; t — temperature;

S_{PN} — selectivity of PN formation: $S_{PN} = \frac{[PN]}{[PN] + [AdN]} \cdot 100 (\%)$; AdN — adiponitrile; ads — adsorbed species.

* University of Cluj-Napoca, Department of Physical Chemistry, 3400 Cluj-Napoca, Romania

** ICECHIM — Institute of Chemical and Biochemical Energetics, Cluj-Napoca Research Group, 3400 Cluj-Napoca, Romania

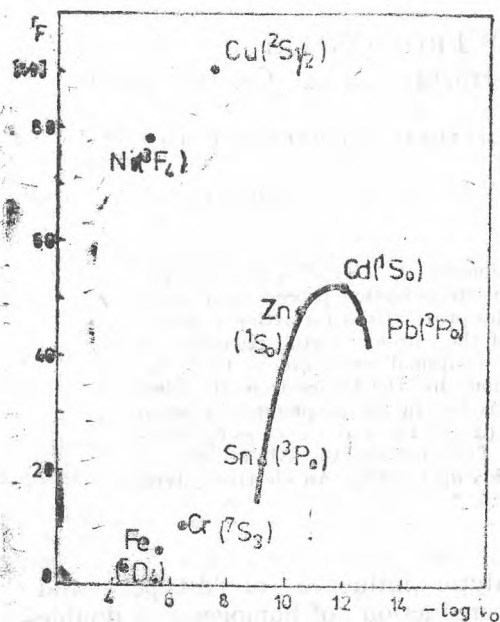


Fig. 1. Dependence of the faradaic yield (r_F) of propionitrile electroreduction on the exchange current density of the hydrogen electrode reaction (i_0)

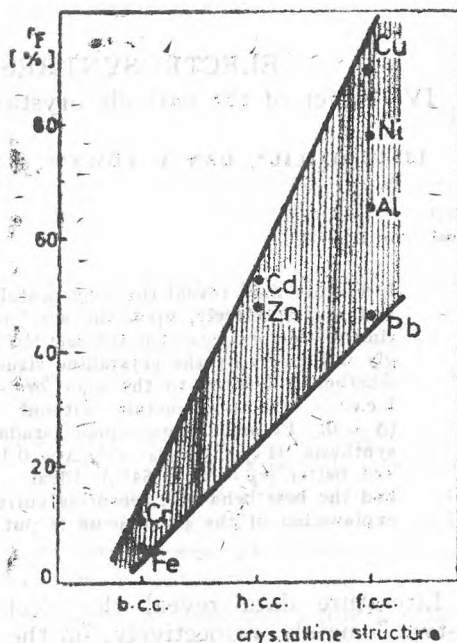


Fig. 2. Dependence of the faradaic yield (r_F) of propionitrile electroreduction on the crystalline structure of the cathode metal.

Experimental. All the experiments were carried out in neutral or slightly acid phosphate buffer supporting electrolyte ($\text{pH} = 5-7$), in the presence of approximately critical micellar concentrations of a trimethyl-alkylammonium salt (having a 12-14 carbon alkyl chain). Galvanostatic and quasi-isothermal conditions were ensured ($i = 70 \text{ mA}\cdot\text{cm}^{-2}$ and $t = 25 \pm 1^\circ\text{C}$). The experimental set-up and the operating parameters were detailed before [4].

Result and Discussion. The products of AcN electroreduction obtained under the above mentioned conditions were analyzed by gas-chromatography, on a conventional column, filled with SE-30 (10%), on Chromosorb GAWDMS (80/100 mesh). An M-9 type modular chromatograph (ITIM - Cluj-Napoca) was used; the method was previously described [5].

The experimental data thus obtained pointed out the dependence of the AcN electroreduction process on the crystalline structure of the cathode metal. Thus, Fe and Cr which had unsatisfactory compartment were of b.c.c. — structure metals without deviation in the lattice from the ideal ($\Delta = 0$). H.c.p. metals: Cd ($\Delta = 0.16$), Zn ($\Delta = 0.14$) and Co ($\Delta = 0$) ensured better yields ($r_F = 22-54\%$). The best results were obtained on ideal-lattice f.c.c. metals ($\Delta = 0$): on Cu, Ni and Pb current yields of up to 90% had been reached.

In order to verify [that f.c.c. metals are indeed the most proper for the NDE of AcN to PN, another typical f.c.c. lattice metal was tested as cathodic material: aluminium, which has a strongly different chemical character. The

experiments carried out with Al vs. stainless steel electrode couple, in neutral phosphate buffer electrolyte, led to a satisfactory r_F (up to 56.5%) and a very good selectivity of PN formation ($S_{PN} \geq 97\%$).

As shown in Fig. 2 these results are in agreement with those obtained on f.c.c. structure metals under similar conditions.

The resemblance in the comportment of the investigated metals can not be explained either with the similitude of their fundamental terms (as seen in Fig. 1, identical term metals can act in different ways and *vice versa*), or with a comparable value of their covalent radii, which vary from 1.18 (Al) to 1.48 Å (Cd).

The dependence of electrocatalytic effects on the structural properties of the electrode surface was investigated by Jüttner [6] for various electroreduction processes. His measurements were made exclusively by f.c.c. single crystal electrodes with defined structural properties. The catalytic response of gold and silver single crystal electrodes, previously modified by underpotential deposition of Pb, Tl or Bi on the (111) and (100) crystal planes, confirmed the importance of structural factors in heterogeneous catalysis. Thus, Jüttner's work generalized for the field electrocatalysis the wellknown theory of heterogeneous adatom catalysis.

In the case of PN electrosynthesis, a theoretical interpretation of the process seems to be possible by means of Balandin's multiplet theory [7], which stresses the importance of the geometrical harmony between the structures of the converting molecules and the catalyst. It has been stated that the distance between the two chemisorbing metal atoms on the catalyst surface (therefore on the electrode surface too) determines the distance between the two chemisorbed atoms of the substrate, and *vice versa* [8].

Concretely, due to the similitudes between heterogeneous catalysis and direct electrocatalysis, during the NDE of AcN, there must be a definite alignment between the geometry of C=C double bond participating in the reaction and the surface structure of the electrocatalyst.

The best geometrical correspondance between the cathode metal and the index group of AcN (C=C) was found in the case of aluminium. The value of the Al—Al active center distance ($d_{Al-Al} = 2.84$ Å) calculated from Al structure and AcN index group geometry [8] was very closed to the interatomic distance from X-ray diffraction data (Al . . . Al = 2.858 Å). In spite of the mentioned favourable structure and its good comportment in the NDE of AcN, the technological adoption of Al is improbable, because of its rapid deactivation by chemical corrosion.

One of the best geometrical correspondances was discovered investigating the iron: $d_{Fe-Fe} = 2.89$ Å and Fe . . . Fe = 2,866 Å. Such closed values were surprising, because in all our experiments carried out in the presence of cationic surfactants, Fe had a poor comportment. Acting in this way, in neutral and acid media the faradaic yield (r_F) attained was below 10% and the selectivity of PN synthesis was diminished by the trimerization process (up to 10% trimers were formed), while in basic medium, at 25°C, the chemical cyanoethylation process leading to bis (cyanoethyl)ether (bCEE) and β -cyanoethanol could not be avoided (up to 45% bCEE was formed).

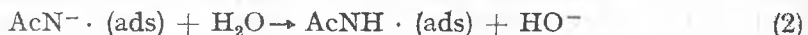
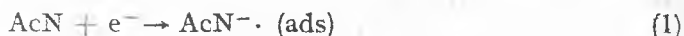
According to the literature data, in the early experiments of Knunyants *et. al.* [9,10], carried out at low temperatures (between - 2 and 0°C), in 0.7

N KOH electrolyte without adding any surfactant, good yields of PN synthesis were obtained ($\eta_F \leq 80\%$).

This behaviour indicates that in the absence of tensides, the PN formation takes place *via* catalytic electrohydrogeneration, having as reaction intermediate the adsorbed hydrogen atoms [1, 11]:



In the presence of quaternary ammonium salts, which are preponderantly adsorbed on the cathode surface, an electrochemical mechanism can be assumed [2, 3]:



Since the radicals are characterized by a strong electrophilicity, we can consider that in the electrochemical mechanism the first three steps take place in the adsorbed state and only carbanions are rejected by the cathode. Thus, the last protonation step (4) occurs in the bulk phase [2, 3].

In spite of the more sophisticated metal-electrolyte interface in the presence of surfactants, the catalytic activity changes depending on the lattice constant.

Thus, the worse compartment of lead compared with the other f.c.c. metals has its origine in the rather large interatomic distances in Pb. This is the reason why Hume-Rothery and Raynor had included lead among the elements of structural class II, together with Zn and Cd (distorted h.c.p. structures) and Hg (rhomboedral structure) [12]. As seen in Fig 2, during PN electrosynthesis Pb ensures comparable faradaic yields with Zn and Cd.

The very different behaviour of Pb and Sn, metals having the same fundamental term and a closed chemical character, can be explained on the basis of their crystalline structure. Opposed to the Pb f.c.c. lattice, in metallic tin each atom has 4 nearest neighbours which form a very flattened tetrahedron around it; therefore, following Hume-Rothery and Raynor, Sn forms a special structural class by its own [12, 13].

As a conclusion, it may be said that appropriate geometrical factors of the cathode metal are necessary, but no sufficient conditions for electrocatalytic activity in the non-dimerizant electroreduction of acrylonitrile to propionitrile. A more complete treatment has to take into account the energy states of the electrocatalytic surface, indicated by the applied overpotentials, which are accompanied by changes of the atomic distances in the lattice.

REFERENCES

1. H. Kita, in: "Electrochemistry" (H. Bloom, F. Gutmann, Eds.), Plenum Press, New York, 1975, p. 131.
2. L. Oniciu, M. Jitaru, D. A. Lówy, I. A. Silberg, B. C. Toma, I. Báldea, "Kinetics and Mechanism of the Nondimerizant Electroreduction of Acrylonitrile to Propionitrile", in: *Extended Abstracts of the 38th Meeting of ISE*, Maastricht, 1987, p. 285-287.
3. L. Oniciu, D. A. Lówy, M. Jitaru, I. A. Silberg, B. C. Toma, I. Báldea, *Rev. Chim. (București)*, **39**, 219 (1988).
4. L. Oniciu, I. A. Silberg, D. A. Lówy, M. Jitaru, F. Ciomoș, *Stud. Univ. Babeș-Bolyai, Chem.*, **31** (1), 80 (1986).
5. D. A. Lówy, I. A. Silberg, L. Oniciu, *Rev. Chim. (București)*, **36**, 354 (1985).
6. K. Jüttner, *Electrochim. Acta*, **31**, 917 (1986).
7. A. A. Balandin, "Multipletnaia teoria kataliza", Moscow, 1963.
8. D. Kalló, in: "Contact Catalysis" (Z. G. Szabó, Ed.), Akadémiai Kiadó, Budapest, 1976, Vol. 1, p. 317-334.
9. I. L. Knunyants, S. L. Varshavskii, A. P. Tomilov, L. V. Kabak, *Fr. Pat. 1401775*, 1965; *Chem. Abstr.*, **64**, 1660c (1966) and *G. Brit. Pat. 1014428*, 1965; *Chem. Abstr.*, **64**, 7683c (1966).
10. A. P. Tomilov, S. L. Varshavskii, I. L. Knunyants, *G. Brit. Pat. 1089707*, 1971.
11. L. Oniciu, M. Jitaru, D. A. Lówy, B. C. Toma, "Propionitrile electroynthesis on F.c.c. Crystalline structure Metals", in: *Extended Abstracts of the 39 Meeting of ISE*, Glasgow, 1988.
12. C. S. G. Phillips, R. J. P. Williams, "Inorganic Chemistry. II. Metals", Oxford University Press, New York and Oxford, 1966, p. 33.
13. N. S. Akhmetov, "General and Inorganic Chemistry", 3rd Edition, Mir Publishers, Moscow, 1987, p. 270, 504.

SEMICONDUCTOR GAS SENSORS I. INSTALLATION FOR OBTAINING GAS STANDARDS IN THE AIR

M. ANTON*, I. LEOCA*, D. GHETE*, F. PUSKAS*, C. ROMAN*, N. PRODAN*, I. C. POPESCU**
and E. CORDOȘ**

Received: July 6, 1988

To test semiconductor gas sensors, an installation for obtaining gas standards in the air has been worked out. The installation of static type runs on the basis of volumetric and manometric principles, in the concentration range 0.01–2%. For checking up the working accuracy of the installation, we resorted to the statistic analysis of the hypothesis of identity of the chromatograph calibration line with the installation sampling line.

Introduction. One of the actual studies concerning the environmental quality control is the detection of gaseous pollutants from the atmosphere.

Among various methods used for this purpose, solid state gas sensors have been given a great importance in recent years [1]. Semiconductor gas sensors respond to a large extent to the requirements an ideal gas sensor has to fulfil: high sensitivity, great speed of response, reduced dimensions, simplicity, durability and low cost [2–3]. Naturally, testing a sensor capable of detecting the presence of inflammable and toxic gases in the air requires an installation for obtaining standards of such gases in the air. Therefore, the present paper deals with an installation for preparation gas standards in the air. Considering the known static methods for the generation of gas standards [4–5], a manometric method (MM) and a volumetric method (VM) were chosen. The installation supplies enough amount of gaseous mixture for testing or calibrating the sensors under atmospheric pressure and conditions of controlled temperature and moisture. Experimental control of the preparation of gas standards has been performed with the help of gas chromatography.

Experimental. The schematic diagram of the installation is shown in Fig. 1. The main part of the installation is a glass flask (1) with four necks. The central neck (2) is useful for obtaining vacuum in the flask or introducing the gas, respectively the air.

Through the lateral necks (3) a thermometer is inserted, respectively, an evaporator with septum and the sensor to be studied. The volume of the flask, measured by filling it with water at 20°C, is of 4920 cm³. The flask is introduced into a thermostat (5). Homogenization of the mixture is carried out by a magnetic stirrer (4). The vacuum in the flask is obtained by means of a preliminary vacuum pump (PVP–10, FAN Bucharest). The pressure in the glass flask is measured utilizing a mercury manometer (6).

Manometric method (MM) consists in introducing the gas of known concentration (c_0 ; %vol) from a tank under pressure (7) into a thermostated and preliminary vacuumed flask to the desired pressure (p), read on the mercury manometer (6). Then, the air filtered (sintered glass filter G₃) and

* IAUC – Cluj-Napoca, 3400 Cluj-Napoca, Romania

** University of Cluj-Napoca, Department of Chemistry, 3400 Cluj-Napoca, Romania

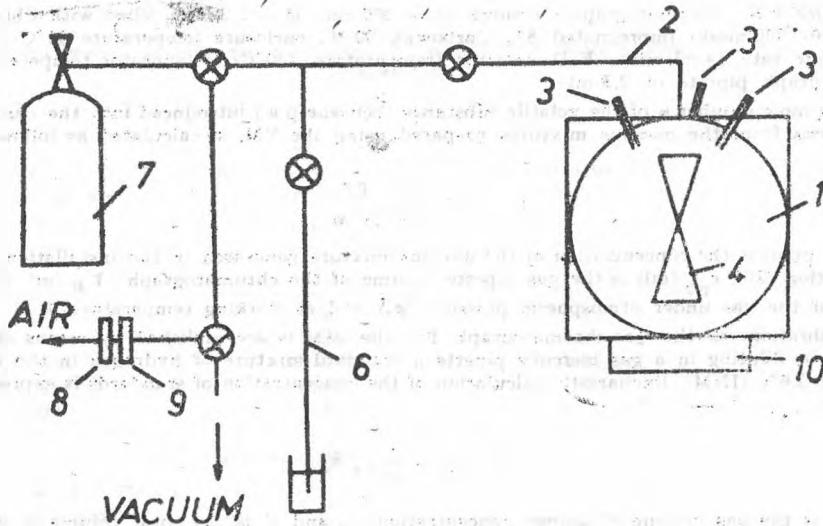


Fig. 1. Schematic diagram of the installation for obtaining gas standards in the air. 1 — flask; 2 — central flask neck; 3 — lateral flask necks; 4 — stirrer; 5 — thermostat; 6 — mercury manometer; 7 — gas tank; 8 — filter; 9 — dryer; 10 — magnetic stirrer.

dried (upon CaCl_2) under atmospheric pressure (p_a) is brought into the flask. The concentration of the gaseous mixture in the air can be calculated [5] from the equation:

$$c \text{ (ppm)} = \frac{p}{p_a} \cdot c_0 \cdot 10^4 \quad (1)$$

Volumetric method (VM) presumes the injection of a known volume (v_1) of the volatile liquid into the thermostated and vacuumed initial flask with a microlitre syringe, using an evaporator with septum. Then, like in case of MM, the air filtered and dried, under the atmospheric pressure (p_a), is introduced into the flask. The concentration of the mixture thus obtained is calculated [5] by the equation:

$$C \text{ (ppm, vol)} = \frac{RT \cdot \rho_1 \cdot v_1}{M p_a \cdot V} \cdot 10^6 \quad (2)$$

where, p_a is the atmospheric pressure (torr); V is the flask volume (ml); M is the molecular weight of the employed volatile substance (g/mol); v_1 is the volume of the injected volatile substance (ml); ρ_1 is the density of the volatile substance at working temperature (g/ml); $R = 8,314 \text{ J/(mol} \cdot \text{K)}$; T is working temperature (K).

In order to obtain gaseous mixtures with the desired moisture content, in both cases of MM and VM, before introducing the air into the flask, the necessary amount of water is injected into the evaporator. After homogenizing for about 5 minutes, the gaseous mixture thus prepared can be used.

To check the accuracy of the installation, gaseous mixtures are sampled with a gas mercury pipette (100 ml volume). These samples are analysed by a gas chromatograph (M-9, ITIM - Cluj-Napoca). Operating conditions of the chromatograph were the followings:

— for MM: chromatographic column ($L = 200 \text{ cm}$; $\varnothing = 2,2 \text{ mm}$) filled with molecular sieve 5 Å; enclosure temperature 80°C ; carrier gas argon (flow rate 15 ml/min); catarometer detector (temperature 100°C ; current intensity 50 mA); chromatograph pipette of $2,5 \text{ ml}$.

— for VM: chromatographic column ($L = 200$ cm; $\varnothing = 2,2$ mm) filled with Chromosorb G (AW; 100–200 mesh) impregnated 5% Carbowax 20 M; enclosure temperature 80°C ; carrier gas argon (flow rate 14 ml/min); FID detector (temperature 150°C); evaporator temperature 150°C ; chromatograph pipette of 2,5 ml.

The mole number n of the volatile substance (benzene p.a.) introduced into the chromatograph for analysis from the gaseous mixtures prepared using the VM, is calculated as follows:

$$n = \frac{c \cdot v_{\text{pip}}}{10^6 \cdot V_M} \quad (3)$$

where, c (ppm) is the concentration of the gaseous mixture generated in the installation (calculated with relation (2)); v_{pip} (ml) is the gas pipette volume of the chromatograph; V_M (ml) is the molar volume of the gas under atmospheric pressure (p_0) and at working temperature T .

Calibration of the gas-chromatograph for the MM is accomplished by means of standards obtained by diluting in a gas mercury pipette a standard mixture of hydrogen in the air of concentration 2,6% (INM—Bucharest). Calculation of the concentration of standards is expressed by the equation:

$$C(\%) = \frac{v}{V} C_0(\%) \quad (4)$$

where, v is the gas volume of known concentration C_0 and V is the total volume of the mixture under atmospheric pressure.

Standards for VM consist in two solutions of benzene with isopropanol of $1^0/_{00}$ and $5^0/_{00}$ concentrations. The number of moles of benzene (n_E) injected into the chromatograph for calibration is calculated from:

$$n_E = \frac{\rho_B}{M_B} \cdot C_E \cdot V_E \quad (5)$$

where, ρ_B and M_B correspond to the density (g/cm^3) and molar weight (g/mol) of benzene, C_E and V_E are referring to the concentration ($^0/_{00}$ vol) and volume (ml) of the solution of benzene into isopropanol injected into the chromatograph.

Results and discussions. For checking up the accuracy of the installation described in this paper, we have resorted to the statistic analysis of the hypothesis of identity of the chromatograph calibration line, using proper standards (hydrogen for MM and benzene for VM), with the line of samples, measured on the same chromatograph, using gaseous mixtures (hydrogen for MM, respectively benzene for VM) generated in the installation. Thus, it can be stated that, for a meaning level (α) conveniently chosen, the difference between the proper parameters of the two lines is, statistically, nonsignificantly non-zero [6].

The results corresponding to the chromatograph calibration with hydrogen standards in the air of concentration range 0,1–2,6% (vol), as well as with isopropanol benzene standards, covering the range 10^{-8} to 10^{-7} moles, are presented in Table 1. It also includes the equations of the regression lines, corresponding to the two calibrations, equations using the least squares method.

Data obtained on the chromatograph, employing the samples prepared in the installation through MM and VM, and the equations of the two regression lines calculated through the least squares method are shown in Table 2.

Table 1

Data used for gas-chromatograph calibration with standards of hydrogen in the air (I) and benzene in isopropanol (II)

I		II	
Concentration of H ₂ standard in the air (ppm)	Chromatographic peak area (mm ²)	C ₆ H ₆ moles into the standard ($\cdot 10^7$)	Chromatographic peak area (mm ²)
Relation	4	5	
	1354	1.12	212
	4658	3.36	612
	7952	4.70	881
	18236	6.72	1532
	26000	10.08	2300

Equation of "standards" lines

$y = 3.85 + 0.035 \cdot x$	$y = -136.2 + 239.7 \cdot 10^{-8} x$
COR = 0.9998	COR = 0.9955

Table 2

Results of gas-chromatograph calibration using samples of hydrogen in the air mixtures (I), respectively benzene in the air (II), prepared in the installation through MM (I), respectively VM (II)

I		II		
Concentration of sample of hydrogen in the air (ppm)	Chromatographic peak area (mm ²)	Concentration of C ₆ H ₆ sample in the air (ppm)	C ₆ H ₆ moles introduced into the chromatograph ($\cdot 10^8$)	Chromatographic peak area (mm ²)
Relation	1	2	3	5
	1771	169	1.70	375.0
	3578	282	2.85	623.1
	5278	395	3.98	914.3
	7403	621	6.26	1291.9
	8783	847	8.54	1840.0
	10732	362.2		
	12900	465.5		

Equation of "samples" lines

$y' = -10.25 + 0.036x'$	$y' = 30.2 + 209.7x'$
COR = 0.9977	COR = 0.9979

Statistic analysis of the identity of "standards" line ($y = A + Bx$) with "samples" line ($y' = A' + B'x'$) has been performed, for both MM and VM, using the data from Tables 1 and 2 and covering the following stages:

a) The general dispersions (s_0^2) [7] corresponding to the two lines are compared using the "F" criterion [8];

b) The hypothesis of the parallelism of the two lines is verified by the Student test [9], calculating t_{exp} from (6):

$$t_{\text{exp}} = \frac{|B - B'|}{s_{B-B'}} \quad (6)$$

where:

$$s_{B-B'} = \sqrt{s_0^2 \left(\frac{1}{D} + \frac{1}{D'} \right)} \quad (7)$$

$$s_0^2 = \frac{(n-2)s_0^2 + (n'-2)s_0'^2}{n+n'-4} \quad (8)$$

$$D = \sum_{i=1}^n x_i^2 - \frac{(\sum x_i)^2}{n} \quad (9)$$

$$D' = \sum_{i=1}^{n'} x_i'^2 - \frac{(\sum x_i')^2}{n'} \quad (10)$$

n and n' being the number of the pairs of values (x, y) , respectively (x', y') , which lied at the basis of plotting the "standards" line, respectively the "samples" line.

c) The hypothesis of the identity of the two lines is verified using the Student test [9], t_{exp} being calculated from the equation (6):

$$t_{\text{exp}} = \frac{|\hat{B} - \bar{B}|}{s_{\hat{B}-\bar{B}}} \quad (11)$$

where \bar{B} results from the hypothesis of the identity of the two lines:

$$\bar{B} = \frac{\frac{B \cdot D}{s_0^2} + \frac{B' \cdot D'}{s_0'^2}}{\frac{D}{s_0^2} + \frac{D'}{s_0'^2}} \quad (12)$$

\hat{B} follows from the hypothesis of the parallelism of the two lines:

$$\hat{B} = \frac{\frac{\sum y}{n} - \frac{\sum y'}{n'}}{\frac{\sum x}{n} - \frac{\sum x'}{n'}} \quad (13)$$

and $s_{\hat{B}-\bar{B}}$ is calculated from the equation:

$$s_{\hat{B}-\bar{B}} = \sqrt{s_0^2 \left(\frac{1}{(\bar{x} - \bar{x}')^2} \left(\frac{1}{n} + \frac{1}{n'} \right) + \frac{1}{D + D'} \right)} \quad (14)$$

The results of the calculations, shown in Table 3, lead to the following conclusions, applicable to MM and VM:

Table 3

Verification results of the hypothesis of the statistically identity of "standards" line ($y = A + Bx$) with "samples" line ($y' = A' + B'x$)

Stage	Manometric method	Volumetric method
a)	$F_{exp} = 2.54 < F^{tab} = 5.41$ $\alpha = 0.05 (n - 2; n - 2)$	$F_{exp} = 4.34 < F^{tab} = 9.28$ $\alpha = 0.05 (n - 2; n - 2)$
b)	$t_{exp} = 0.84 < t^{tab} = 2.306$ $\alpha = 0.05 (n + n' - 4)$	$t_{exp} = 1.82 < t^{tab} = 2.45$ $\alpha = 0.05 (n + n' - 4)$
c)	$t_{exp} = 0.387 < t^{tab} = 2.306$ $\alpha = 0.05 (n + n' - 4)$	$t_{exp} = 0.33 < t^{tab} = 2.45$ $\alpha = 0.05 (n + n' - 4)$

- a) Statistically general dispersions of the lines do not differ ($F_{exp} < F_{tab}$).
 b) "Standards" line is, at least statistically, parallel to "samples" line ($t_{exp} < t_{tab}$).
 c) The compared lines are, statistically, identical ($t_{exp} < t_{tab}$).

Taking into account the statistic analysis, one can consider that the installation for preparation standard gaseous mixtures in the air works with the acquired degree of accuracy.

For estimating the relative error of the installation, using the equations from Table 1 and the values of the pick areas from Table 2 (columns 2 and 5), the concentrations of the mixtures prepared in the installation through MM, respectively VM have been estimated. The results are shown in Table 4. For MM it has been established that the relative error does not exceed 5% for concentrations of hydrogen in the air higher than 5000 ppm. In VM case, the rela-

Table 4

Chromatographic determination results of the concentrations of mixtures prepared in the installation through MM (I) and VM (II)

I			II			
Calculated concentration of H_2 (ppm)	Determined concentration of H_2 (ppm)	Relative error (%)	Calculated concentration of C_2H_6 in the air	Moles of calculated C_2H_6 (10^6)	Moles determined C_2H_6 (10^6)	Relative error (%)
1771	1489	15.9	169	1.70	2.13	25
3578	3142	12.2	282	2.85	3.16	10.8
5278	4992	5.4	395	3.98	4.38	10.0
7403	7572	2.3	621	6.26	5.95	4.9
8783	8895	1.3	847	8.54	8.23	3.6
10732	10196	5.0				
12900	13135	1.8				

tive error does not exceed 10% for concentrations of benzene in the air higher than 300 ppm.

Conclusions. The described installation permits to obtain gas standards at atmospheric pressure of concentration range between 0,01–2%, with a relative error better than 10%, at controlled temperature and moisture content. Installation can be operated manometrically, for gaseous substances at room temperature, or volumetrically, for volatile liquids. The possibility of obtaining vacuum in the flask eliminates sample contamination. For these reasons we can say that the installation is well suited for testing and calibrating gas sensors.

REFERENCES

1. D. Williams and B. McGeehen, "Review of Solid State Gas Sensors and Monitors" Harwell, AERE-R-11022 (1983).
2. D. K. Burns, P. N. Kember, S. Taylor and E. Williams, "Air Pollution Monitoring and the Role of Semiconductor Sensors", *Environ. Technol. Lett.*, **1**, 259 (1980).
3. G. Heiland, "Homogenous Semiconducting Gas Sensors" — *Sensors and Actuators*, **2**, 343 (1982).
4. J. Namiesnik, "Generation of Standard Gaseous Mixtures", *J. Chromatog.*, **300**, 79 (1984).
5. G. O. Nelson, *Controlled Test Atmospheres*, Ann Arbor Science Publishers, Inc. 1972, p. 59.
6. V. V. Nalimov, "Primenenie matematicheskoi statistiki pri analize veshchestva", Gos. izd., fiz-mat. lit. Moscou, 1960.
7. C. Liteanu and I. Răcă, „Teoria și metodologia statistică a analizei urmelor”, Ed. Scrisul Românesc, Craiova, 1979, p. 70.
8. *Idem*, p. 46.
9. *Idem*, p. 30.

NOTE DE LABORATORCONDENSATION OF 2,4-DINITROBENZALDEHYDE WITH
NAPHTHALINE UNDER THE ACTION OF CONCENTRATED
SULPHURIC ACID

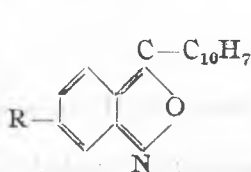
I. TĂNĂSESCU and E. RAMONȚIAN*

Received: October 8, 1988

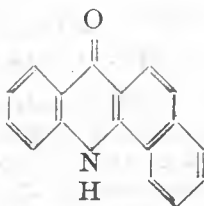
The 2,4 dinitrobenzaldehyde by condensation with naphthaline under the action of concentrated sulphuric acid yields 3-nitro-C- α -naphtylantranil and 3-nitro-N-oxo-C-oxybenzoacridine.

It was shown elsewhere [1] that upon condensation of orthonitro-benzaldehyde with naphthaline, under the action of concentrated sulphuric acid, a black mass is yielded, but no pure substance has been possible to isolate out of this.

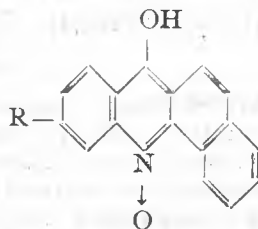
Upon the condensation of 2,4-dinitrobenzaldehyde with naphthaline [2], under the action of concentrated sulphuric acid, 3-nitro-C- α -naphtylantranil (I) with melting point of 186°C and 3-nitro-N-oxo-C-oxybenzoacridine (IIa) with a melting point of 360°C can be isolated in pure state.



I, R = -NO₂
III, R = H



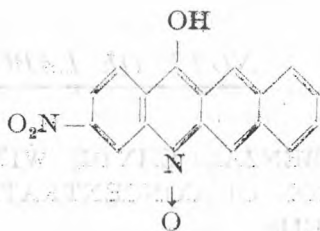
IV



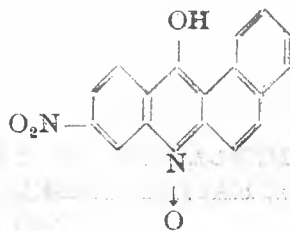
II a, R = -NO₂
V, R = H

Within naphthaline, the α -position is most reactive, and consequently the yielded antranil is α -naphtyl. In the case of 3-nitro-N-oxo-C-oxybenzoacridine three isomers are possible: (IIa, IIb, IIc). The IIa isomer is probably obtained as the $\alpha\beta$ -position is attacked more easily than the $\beta\beta$ -position (IIb), and because of steric considerations, the benzo group is more remote from the oxidril than it is in (IIc).

* University of Cluj-Napoca, Faculty of Chemical Technology, 3400 Cluj-Napoca, Romania



II b



II c

In [1] the authors show that upon condensation of orthonitrobenzaldehyde with naphthaline under the action of polyphosphoric acid in a warm place, C-naphthylanthranyl (II) is isolated and directly acridone (IV). The direct formation of acridone (IV) instead of N-oxo-C-oxy-acridine (V) is explainable in that the condensation in the case of polyphosphoric acid takes place at temperatures between 96–100°C, when N-oxo-C-oxyacridine (V), which is certainly formed intermediately by loss of oxygen, is isomerized in acridone (IV), as shown previously [3].

Experimental. 3-Nitro-C- α -naphthylanthranyl (I). 2 g of 2,4-dinitrobenzaldehyde and 1.3 g of naphthaline are dissolved in 20 ml of chloroform, to which 10 ml of concentrated sulphuric acid is added. The solution is kept for 3–4 days at room temperature, being stirred from time to time. Then, the chloroform is decanted, and the remained sulphuric solution is washed 5 times with 20 ml chloroform, and subsequently is poured in half-litre of water, under continuous stirring. A black mass precipitates, which is filtered. This mass is extracted with 50 ml of chloroform. Impure 3-nitro-C- α -naphthylanthranyl is yielded from the reunited chloroform solutions, after the distillation of chlorophorm. In view of purification, this is recrystallized — once from benzene (100–120°C) and then from ethonol. In its pure state, the substance is yellowish-lemon, with melting point of 186°C, slightly soluble in benzene, chloroform, acetic ester, but hardly soluble in benzene and alcohol, particularly at cool.

$C_{17}H_{10}O_3N_2$ (290.4) calc. C 70.3; H 3.5; N 9.7

found C: 70.3; H: 3.8; N: 9.3

A yellowish-orange compound is yielded with mercuric chloride (II) in acetic ester solution, with the melting point of 214°C.

3-Nitro-N-oxo-C-oxybenzoacridine (IIa). The remaining amount resulted from the chlorophormic extraction is dissolved in 2N sodium hydroxide solution and filtered of impurities. The alkaline solution is precipitated with hydrochloric acid, 3-nitro-N-oxo-C-oxybenzoacridine. This is recrystallized from pyridine. In its pure state, it is a reddish substance with the melting point of over 360°C, very hardly soluble in current solvents at warm. It is however soluble in pyridine and nitrobenzene, especially at warm.

$C_{17}H_{10}O_4N_2$ (306.4) calc. ed C: 66.6; H: 3.3; N: 9.2

found C: 66.2; H: 3.2; N: 9.4

BIBLIOGRAFIE

1. I. Tănăsescu, M. Ionescu, I. Goia, H. Mantsch, *Bull. Soc. Chim. France*, **1960** 698.
2. E. Ramonțian, *Teză de doctorat* 1934, p. 48, 77.
3. I. Tănăsescu, E. Ramonțian, *Bull. Soc. Chim. France*, (5) **1**, 549 (1934).

RECENZII

Sydney Ross, Ian Douglas Morrison, *Colloidal Systems and Interfaces*, Wiley-Interscience, New York, 1988, 422 pp.

The nature of dispersed systems (suspensions, emulsions and foams) is determined not only by their specific chemical composition but also by particulate and interfacial properties. These properties are the subject matter of colloid and interface science.

After a short *Introduction* where the object of study of the science is defined, the book treats *particulate properties* — optical, rheological (pertaining to flow) and statistical —, as well as new investigation techniques, in *Part I* consisting of five chapters. *Interfacial properties* — capillarity, (insoluble) spreading monolayers and adsorption from solutions — form the topics of the seven chapters distributed in *Part II*. The other two parts of the book deal with: *stability of dispersions* — attraction and repulsion forces, colloidal stability, kinetics of coagulation — (the four chapters of *Part III*), and *dispersed-phase systems* — particulars of the behavior of suspensions, emulsions and foams — (the three chapters of *Part IV*). Each part is provided at the end with pertinent references, where suggestions are made for most suited papers, reviews and books in the current literature. Moreover, the book ends up with a general *Bibliography* — in which recommended general texts are marked with an asterisk —, ten *Appendices*, very useful to the detailed understanding of the issues discussed in the four parts of the book, and an *Index* meant for rapid reference to the items of interest. It is noteworthy to underline that beside data on physical constants, units, mathematical formulas etc., the *Appendices* also provide useful information in that contributors to colloid and interface science and

their lifetimes, Kendall Awardees — granted in recognition for and to encourage outstanding contributions to this domain —, and manufacturers of instruments and processing equipment are recorded.

Colloidal Systems and Interfaces is an easy to read book: the style is clear, concise and straightforward; the text is rich in formulas, and just the right amount of tables and well reproduced diagrams are provided for a synthetic presentation of the aspects discussed. The concepts and techniques specific to colloid and interface science are harmoniously presented, so as researchers may avail themselves of the experience of previous contributors to this field of science. The *Parts-end-references* and those at the end of the book direct the reader to bibliographical sources of a more detailed availability in respect of the 'problematique' presented. The book also stands out in that it describes new techniques to investigate the properties of colloidal systems — to cite only a few would suffice, we believe, namely: particle size distribution by quasi-elastic light scattering and laser light scattering; dilatational surface elasticity from the damping of ripples; foams stability by the automatic recording of small pressure differences etc.

The book turns up excellent text for an introductory course on colloid and interface chemistry. It is intended for student environment, as well as for the industrial milieu — chemists or chemical engineers who may not have had a formal university course in colloid and interface chemistry but find that the nature of the problems that must be solved necessitates the rapid acquisition of some knowledge of that subject.

MARIA TOMOAI-COTIȘEL

Participări la manifestări științifice internaționale

● La Congresul Internațional de „Membrane și Procese de Membrană”, organizat de Societatea de Membrane din Japonia și Societatea Europeană de Membranologie și Tehnologie în cooperare cu Fundația Kidney din Japonia, în perioada 8—12 iunie 1987 la Tokio în Japonia, lucrarea *Specific Interactions in Lipid-Carotenoid Monolayers*, Maria Tomoaia-Cotișel, János Zsakó, Emil Chifu și Peter J. Quinn, a fost prezentată de Dr. Peter J. Quinn de la Universitatea din Londra, King's College, U.K.; lucrarea *Molecular Structure and Monolayer Properties of some Carotenoids*, János Zsakó, Maria Tomoaia-Cotișel, Emil Chifu și Eiji Osawa, a fost prezentată de Dr. Eiji Osawa de la Universitatea Hokkaido din Sapporo, Japonia.

● La Conferința Internațională de Apă și Ioni în Sisteme biologice organizată la București în perioada 24—28 mai 1987, Csaba Muzsnay a prezentat lucrarea *Some Molar Properties of Associated H₂O and D₂O (II). Treatment by means of Three Elementary Equilibrium Constants*, Csaba Muzsnay, Mark P. Gáspár și L. Benke.

Participări la manifestări științifice naționale

● La cea de a III-a Consfătuire de lucru privind „Metode biofizice utilizate în investigarea interacțiunii medicamentului cu membranele celulare” organizată la Universitatea „Al. I. Cuza” din Iași în perioada 15—17 octombrie 1987, lucrarea *Filme monomoleculare de acid stearic pe suport de procaină*, Maria Tomoaia-Cotișel, Emil Chifu, Aurora Mocanu, János Zsakó, Marius Sălăjean a fost prezentată de Maria Tomoaia-Cotișel.

Vizite din străinătate

Între 2 oct.—7. oct. 1987 prof. Eric Brown de la Facultatea de Științe Le Mans (Franța) a făcut o vizită la Facultatea de Tehnologie Chimică și a prezentat o conferință cu titlul: *Sinteze asimetrice totale de lignani biologic activi*.

Publicări de tratate, cărți și cursuri universitare

I. Haiduc and D. B. Sowerby (Editors), *The Chemistry of Inorganic Homo- and Heterocycles*, Vol. 1 și 2, Academic Press, London, 1987.
L. Kékedy, *Sensori electrochimici metalici și ion-selectivi*, Ed. Academiei RSR, București, 1987, 230 p.
Adriana Donea, *Chimie organică*, vol. 2, Lito Univ. Cluj-Napoca, 1987, 153 pag.
I. Hopârtean, *Chimie Organică*, partea a 2-a, Lito. Univ. Cluj-Napoca, 1987, 287 pag.
F. Jugrestan, *Tehnologia produselor farmaceutice*, partea I-a, Lito. Univ. Cluj-Napoca, 1987, 315 pag.
I. Panea, *Fotochimie organică. Aplicații tehnologice*, Lito. Univ. Cluj-Napoca, 1987, 303 pag.

Lucrări științifice apărute în reviste de specialitate din țară și străinătate

E. Chifu, A. Chifu, M. Tomoaia-Cotișel, J. Zsakó, „Specific Interaction in Monomolecular Membranes of Biological Interest”, *Rev. Roumaine Chim.*, **32**, (7), 627 (1987).
E. Chifu, M. Sălăjean, M. Tomoaia-Cotișel, “Fatty Acid Films at the Benzene/Water Interface”, *Rev. Roumaine Chim.*, **32**, (7), 683 (1987).
E. Chifu, M. Tomoaia-Cotișel, “Thin Liquid Layers”, *Seminars in Biophysics*, vol. 4, P.T. Frangopol, V. V. Morariu Eds., CIP Press, Bucharest, 1987, p. 163.
E. Chifu, C. I. Gheorghiu, “Surface Mobility of Surfactant Solutions. XII. Remarks Concerning the Marangoni Flow through an Inclined Canal”, *Rev. Roumaine Chim.*, **32**, (9/10), 945 (1987).
I. Cristea, V. Fărcășan, „Sinteza unor derivați de 1-(pirimidinil)-5-pirazolonă”, *Rev. Chim. (București)*, **38**, (8), 674 (1987).
I. Cristea, V. Fărcășan, „Compuși biologic activi din clasa pirimidil-pirazolonelor”, în *Realizări biochimice și dezvoltarea civilizației contemporane*, Academia R.S.R. — Filiala Cluj-Napoca, 1987 p. 112.
M. Sălăjean, E. Gavrilă, E. Chifu, „Studiul coalescenței unei picături la o interfață lichid-lichid plană. I. Timpuri de coalescență”, *Rev. Chim. (București)*, **38**, (10), 882 (1987).
M. J. Begley, D. B. Sowerby, I. Haiduc, “The Crystal Structures of the Diphenyldithiophosphinates of Antimony (III) and Bismuth (III):

- $M(S_2PPh_2)_3$ ($M = Sb$ or Bi)", *J. Chem. Soc. Dalton Trans.*, **1987**, 145.
- D. B. Sowerby, I. Haiduc, "The crystal structure of bismuth diethyldithiophosphate-benzene, $Bi(S_2PET_2)_3 \cdot C_6H_6$ ", *J. Chem. Soc. Dalton Trans.*, **1987**, 1257.
- C. Silvestru, I. Haiduc, S. Klima, U. Thewalt, M. Gielen, J. J. Zuckerman, "Synthesis and characterization of di- and triorganotin (IV) diethyldithiophosphinates. The crystal and molecular structure of bis (diethyldithiophosphinato) dimethyltin(IV), $Me_2Sn(S_2PET_2)_2$ ", *J. Organometal. Chem.*, **327**, 181 (1987).
- C. Silvestru, F. Ilies, I. Haiduc, M. Gielen, J. J. Zuckerman, "Di- and triorganotin (IV) diphenyldithiophosphinates", *J. Organomet. Chem.* **330**, 315 (1987).
- L. Kékedy, D. Dumitrescu, "Recunoașterea formelor, o metodă modernă de prelucrare a datelor analitice. I. Principii generale", *Rev. Chim. (București)*, **38**, 339 (1987).
- D. Dumitrescu, L. Kékedy, "Recunoașterea formelor, o metodă modernă de prelucrare a datelor analitice. II. Clasificarea unor ape minerale indigene pe baza datelor de analiză chimică", *Rev. Chim. (București)*, **38**, 417 (1987).
- L. Kékedy, S. Varga, "Determinarea urmelor de oxigen dizolvat pe cale spectrofotometrică prin complexarea Mn(III) cu acid fosforic concentrat", *Rev. Chim. (București)*, **38**, 169 (1987).
- S. Mager, M. Horn, I. Grosu, "Derivați din clasa 1,3-dioxanului cu activitate biologică", în *Realizări biochimice și dezvoltarea civilizației contemporane*, Academia R.S.R. — Filiala Cluj-Napoca, 1987, p. 119.
- I. Simiti, A. Marie, M. Coman, R. D. Pop, H. Demian, S. Mager, "Kondensation von 3-Mercapto-5-Phenyl-1,2,4-Thiazol mit Monochloracetaldehyd", *Arch. Pharm.*, **320**, 528 (1987).
- V. Andreica, Gh. Marcu, N. Triș, A. Tibad, "Sticle colorate pentru suprapunere pe bază de cupru", *Materiale de Construcții (București)*, **17**, (2), 141 (1987).
- L. Oniciu, D. A. Löwy, Maria Jitaru, I. A. Silberg, B. C. Toma, "Electrosynthesis of Propionitrile. II. Phase Equilibria in the Acrylonitrile—Water system in the Presence of Cationic Surfactants and Electrolyte", *Rev. Roumaine Chim.*, **32**, (7), 701 (1987).
- L. Oniciu, D. A. Löwy, I. A. Silberg, C. E. Florea, "A New Multipurpose Reference Electrode", *Analisis*, **15**, (4), 197 (1987).
- L. Oniciu, Maria Jitaru, D. A. Löwy, I. A. Silberg, B. C. Toma, I. Bâldea, Kinetics and Mechanism of the Non-Dimerizing Electroreduction of Acrylonitrile to Propionitrile", *Extended Abstracts of the 38th Meeting of ISE, Maastricht, the Netherlands*, Sept. 13—18, 1987, p. 285.
- L. Oniciu, Pântea, L. Mureșan, V. A. Topan, D. Gherțoiu, "Caracterizarea unor membrane schimbătoare de ioni", *Rev. Chim. (București)*, **38**, (2), 109 (1987).
- L. Oniciu, S. Agachi, L. Fischer, "Dimensiunarea tehnologică a unei baterii de pile de combustie metanol- H_2O_2 cu puterea de 10 kW", *Rev. Chim. (București)*, **38**, (1), 73 (1987).
- D. A. Löwy, I. A. Silberg, L. Oniciu, O. H. Oprea, A. Horváth, "Modificarea chimică a poli- etilenei. II. Studiul produselor de condensare a polimerului funcționalizat prin spectrometrie în IR", *Materiale plastice (București)*, **24**, (1), 8 (1987).
- L. Oniciu, D. A. Löwy, A. Horváth, "Modificarea chimică a polietilenei, III., Studii fizicochimice și electrochimice asupra polimerului funcționalizat", *Materiale plastice (București)*, **24**, (4), 218 (1987).
- I. Panea, V. Fărcășan, F. Paiu, I. Bâldea, V. Chiorean, "Coloranți polimetinici biologic activi", *Progrese în Cercetarea Biochimică*, Academia R.S.R., Filiala Cluj-Napoca, 1986, p. 73.
- I. Panea, V. Chiorean, I. Bâldea, "1-H-Indolo-3-dimetincianine cu acțiune microbiostatică", *Ibid.*, p. 128.
- M. Tomoaia-Cotișel, J. Zsakó, E. Chifu, P. J. Quinn, "Intermolecular Interactions in Lipid-Carotenoid Monolayers", *Biochem. J.*, **248**, (3), 877 (1987).
- M. Tomoaia-Cotișel, J. Zsakó, A. Mocanu, M. Lupea, E. Chifu, "Insoluble Mixed Monolayers. III. Ionization Characteristics of some Fatty Acids at the Air/Water Interface", *J. Colloid Interface Sci.*, **117** (2), 464 (1987).
- M. Tomoaia-Cotișel, J. Zsakó, E. Chifu, P. J. Quinn, "Molecular Association in Lipid-Carotenoid Monolayers", *The Metabolism, Structure and Function of Plant Lipids* P. K. Stumpf, J. B. Mudd, W. D. Ness, Eds, Plenum Press, New-York, 1987, p. 131.
- M. Tomoaia-Cotișel, J. Zsakó, E. Chifu, D. A. Cadenhead, H. E. Ries Jr., "Collapse Mechanism of Some Carotenoid Monomolecular Films-Membrane Model", *Progress in Photosynthesis Research*, J. Biggins, Ed., Vol. II, 4, Martinus Nijhoff Publ., Dordrecht (The Netherlands), 1987, p. 333.
- M. Tomoaia-Cotișel, J. Zsakó, E. Chifu, "Ejection Curves and Miscibility of Egg Lecithin with Some Carotenoid Derivatives", *Rev. Roumaine Chim.*, **32**, (7), 663 (1987).
- E. Vargha, D. Breazu, F. Gönczy, F. Muzsnay, É. Pöllnitz, "Educoranți de natură peptidică", *Realizări biochimice și dezvoltarea civilizației contemporane*, Academia R.S.R. — Filiala Cluj-Napoca, 1987, p. 135.
- I. Gănescu, Cs. Várhelyi, "Metal— and Metal (III)—amine salts of the $H_4Pt(SCN)_4$ and $H_2Pt(SCN)_6$ acids", *Rev. Roumaine Chim.*, **32**, (3), 255 (1987).

- E. Grünwald, H. Trif, M. Harsányi, J. Harsányi, Cs. Juhos, Cs. Várhelyi, „Electrodepunerea lucioasă a aliajului de zinc-cobalt din electroliți slab acizi”, *Industria ușoară (București)*, **34**, (2), 77 (1987).
- T. Takácsik, E. Grünwald, Cs. Juhos, M. Harsányi, J. Harsányi, Cs. Várhelyi, „Influența și dozarea unor impurități din electroliți de cromare neagră”, *Industria ușoară (București)*, **34**, (3), 125 (1987).
- E. Grünwald, H. Trif, M. Harsányi, J. Harsányi, Cs. Juhos, Cs. Várhelyi, „Die galvanische Abscheidung von glänzenden Zink-Kobalt-Legierungsschichten aus schwachsauren Elektrolyten”, *Galvanotechnik*, **78**, (6), 1610 (1987).
- Cs. Várhelyi, J. Zsakó, G. Liptay, Z. Finta, „On the dioximine complexes of transition metals, LXXXVIII. TG and DTA study of the thermal decomposition of some complexes $MCo(DH)_2XY$ and $Co(DH)_2(H_2O)_X$ ”, *J. Thermal Anal.*, **32**, 785 (1987).
- J. Zsakó, V. Neagu, M. Tomoaia-Cotișel, E. Chifu, „Molecular Structure and Monolayer Properties”, *Rev. Roumaine Chim.*, **32**, (8), 739 (1987).
- J. Zsakó, J. Sztatisz, Á. Czégeni, G. Liptay, Cs. Várhelyi, „Kinetic analysis of thermogravimetric data, XXVI. DSC study on the thermal decomposition of some metal and ammonium salts of the hydrogen hexachlororhenate (IV) acid”, *J. Thermal Anal.*, **32**, 463 (1987).
- J. Zsakó, M. Tomoaia-Cotișel, V. Tâmaș, V. Coman, E. Chifu, „Monomolecular Films of Some Apocarotenoid Derivatives”, *Rev. Roumaine Chim.*, **32**, (11/12), 1193 (1987).
- K. Makkay, C. Constantin, N. Mihail, Procedeu pentru prepararea lactatului de colină, Brevet R.S.R. nr. 87 794 din 1985.
- N. Mihail, C. Nistor, K. Makkay, V. Nistor, C. C. Nistor, Preparat medicamentos cu efect hepatoprotector și energizant, Brevet R.S.R. nr. 88 870 din 1985.
- N. Mihail, C. Nistor, K. Makkay, V. Nistor, Preparat hepatotrofic Brevet R.S.R. nr. 88 869 din 1985.
- K. Makkay, C. Nistor, N. Mihail, Preparat medicamentos cu efect hepatoprotector, Brevet R.S.R. nr. 88/869 din 1985.
- N. Mihail, C. Nistor, K. Makkay, V. Nistor, M. Onișor, Preparat medicamentos cu efect hepatoprotector, Brevet R.S.R. nr. 88 868 din 1985.
- Gh. Marcu, M. Bădescu, Al. Botar, Procedeu de depunere a unor săruri de tetraalchilamoniu ale unor heteropolianioni pe diferite suporturi cromatografice, Brevet R.S.R. nr. 34 512 din 25 noiembrie 1987.
- E. Vargha, D. Breazu, F. Gönczi, É. Muzsnay, É. Pollnitz, Procedeu de obținere a Laspartil-L-fenilalaninatului de metil, Brevet R.S.R. nr. 88 701 din 28 iunie 1985.

Susțineri de teze de doctorat

Popa Traian-Viorel, *Complecși π -metalorganici cu aplicații ca aditivi antidetonanți*, conducător științific: prof. dr. Ionel Haiduc (21 februarie 1987).

Sârbu Costel, *Cromatografie pe strat subțire cu detecție prin fluorescență*, conducător științific: prof. dr. doc. Liviu Oniciu (3 iunie 1987).

Jitian Simion, *Studiul fizico-chimic al placării metalelor cu pelicule de polimeri*, conducător științific: prof. dr. Emil Chifu (7 iulie 1987).

Brevete

I. Panea, V. Săndulescu, R. Cârstoiu, N. Popovici, Derivat de hidrazonoisatină și procedeu de preparare a acestuia, Brevet R.S.R. nr. 93 178 din 9. 04. 1987.



În cel de al XXXIII-lea an (1988) *Studia Universitatis Babeş-Bolyai* apare în specialitățile :

matematică
fizică
chimie
geologie-geografie
biologie
filosofie
științe economice
științe juridice
istorie
filologie

In the XXXIII-rd year of its publications (1988), *Studia Universitatis Babeş-Bolyai* is issued as follows :

mathematics
physics
chemistry
geology-geography
biology
philosophy
economic sciences
juridical sciences
history
philology

Dans sa XXXIII-e année (1988), *Studia Universitatis Babeş-Bolyai* paraît dans les spécialités :

mathématiques
physique
chimie
géologie-géographie
biologie
philosophie
sciences économiques
sciences juridiques
histoire
philologie